Republic of Iraq

Ministry of Higher Education

and Scientific Research

University of Babylon

College of Engineering

Civil Engineering Department

# Structural Behavior of Slurry Infiltrated Fibrous Reinforced Concrete Vierendeel System

A Thesis

Submitted to the College of Engineering at University of Babylon in Partial Fulfillment of the Requirements for the Degree of Master in Engineering / Civil Engineering /Structures

By

**Raghda Ali Naser Abdulhussein**

Supervised by

**Assis. Prof. Dr. Khalid K. Shadhan**

**1444 A.H** **2023 A.D**

بسم الله الرحمن الرحيم

" وَلَقَدْ آتَيْنَا دَاوُودَ وَسُلَيْمَانَ عِلْمًا وَقَالَا الْحَمْدُ لِلَّهِ

الَّذِي فَضَّلَنَا عَلَى كَثِيرٍ مِنْ عِبَادِهِ الْمُؤْمِنِينَ "

صدق الله العظيم

سورة النمل الآية (15)

## Supervisor's certification

I certify that this thesis (**Structural Behavior of Slurry Infiltrated Fibrous Reinforced Concrete Vierendeel System**) and submitted by the student (**Raghda Ali Naser**) was prepared under my supervision at a part of requirements for a master degree of science in Civil Engineering

Signature:

Name: Asst. Prof. Dr. Khalid K. Shadhan

Date: 25/10/2023

I certify that this thesis mentioned above has been completed in Civil Engineering in the college of Engineering / University of Babylon

Signature: 25/10

Head of Department: Asst. Prof. Dr. Zaid H. Majeed AL-Hasoon

Date: 25/10/2023

# Examining Committee Certificate

We certify that we have read this thesis entitled "**Structural Behavior of Slurry Infiltrated Fibrous Reinforced Concrete Vierendeel System**" and as an examining committee Examined that student" **Raghda Ali Naser Abdulhussein**" in its content and that in our opinion it meets standard of a thesis for the degree of Master in engineering / Civil Engineering / Structures Engineering.

Signature:

Name: **Prof.**

**Dr. Nameer A. Alwash**

(Chairman)

Date: 25/10/ 2023

Signature:

Name: **Prof.**

**Dr. Nabeel Hasan Ali Al-Salim**

(Member)

Date: 25/10/ 2023

Signature:

Name: **Prof.**

**Dr. Sadjad A. Hemzah**

(Member)

Date: 25/10/ 2023

Signature:

Name: **Asst. Prof.**

**Dr. Khalid K. Shadhan**

(Supervisor)

Date: 25/10/ 2023

**Approved of Head of Department**

Signature:

Name: **Asst. Prof. Dr. Zaid H. Majeed AL-Hasoon**

Date: 5/12/2023

**Approved of The Dean of College**

Signature:

Name: **Prof. Dr. Laith Ali Abdul- Rahaim**

Date: / /2023

## ACKNOWLEDGMENTS

In the name of ALLAH, the most compassionate, the most merciful. Praise be to ALLAH, and pray and peace be on his prophet Mohammed and his family.

First, I would like to express my appreciation and gratitude to my supervisor Dr. Khalid Karim Shadhan for his remarkable suggestions and guidance. I am really indebted to him.

I would like to express my deepest feelings of my family for their endless love, care, patience and great support throughout my pursuit for education. I hope this achievement will fulfill the dream they envisioned for me.

Special thanks to my aunt. Without her help and support, the completion of this work would not have been possible.

Thanks to all the staff of Civil Engineering Department/College of Engineering / University of Babylon for their appreciable support.

Thanks also extended to all friends for their help and useful discussion.

**Great Thanks for All**

**Raghda**

**2023**

# Abstract

This research presents an experimental and numerical investigation of structural behavior of SIFCON Vierendeel system. The experimental program contains casting and testing eight SIFCON Vierendeel specimens. The dimensions of the specimens were (1350*250)mm which they are length and height respectively. In this study, the main variables were the void shape, void ratio and width of the specimen. All the specimens are cast of slurry infiltrated fiber concrete with 7% steel fiber.

The control specimen has square voids, void ratio (0.4), width (60 mm). The specimens were divided into three groups, the first group variable is the void shape (circle, triangle), the second one variable is the void ratio (0, 0.2, 0.6), while the third group variable is the width (40, 80) mm.

The experimental results have showed that the ultimate load decreases with the increase of the void ratio, for specimen with 0.6 void ratio the reduction in the load carrying capacity is 60.5% compared with control specimen, while the increasing in the load capacity for solid specimen is 146.7% and 37.1% for specimen with 0.2 void ratio.

On the other hand, it was found that the ultimate load of the specimen with circular openings higher than the ultimate load of the specimen with square openings by about 8%, while the load carrying capacity of the specimen with triangular openings decrease in about 10.9% compared with the specimen with square openings.

With regard to the width, the results have shown that the ultimate load increases with the increase of width of the specimens, when the width increases to 80 mm, the increasing in the ultimate load is about 27%, while when the width reduces to 40 mm, the reduction in the ultimate load is about 46.4% compared with control specimen.

In the second part of this study, a three-dimensional finite element model, using the concrete damaged plasticity model and material properties obtained from laboratory tests was conducted to simulate SIFCON Vierendeel specimens within a commercial finite element software package ABAQUS/standard 2017. This study included the effects of various parameters; openings size, openings shape, and width of the specimen. Numerical results are compared with the obtained experimental results in terms of load–mid span deflection curves and cracking-propagation behavior. The results have shown that finite element analysis predicted the behavior of Vierendeel specimens in good agreement with the experimental data and predicted the response of the specimens with variation in various parameters with good accuracy.

# List of Content

# List of Tables

# List of Figures

# List of Plates

## Abbreviations and Notation

ACI American Concrete Institute

ASTM American Society for Testing and Material

BS British Standards

EC Euro code

CDP Concrete Damaged Plasticity

C3D8R 8-Node Linear Brick Element, with Reduced Integration

CFRP Carbon Fiber Reinforced Polymer

et al. And others

EXP. Experimental

Eq. Equation

Ec Concrete initial tangent modulus

FRP Fiber Reinforced Polymer

FE Finite Element

FEA Finite Element Analysis

FEM Finite Element Method

fcu Concrete cubic strength

fc' Concrete cylinder strength

ft Concrete tensile strength

fc Stress of concrete

HSC High strength concrete

IQS Iraqi Specification

MIFC Mortar Infiltrated Fiber Concrete

SIFCON Slurry Infiltrated Fiber Concrete

T3D2 2-Node, 3D Truss Element

w/c Water to Cement ratio

3D Three-Dimensional

$\delta u$ Deflection of member at ultimate load

$\delta s$ Deflection of member at service load

# 1 CHAPTER ONE: INTRODUCTION

## 1.1 Overview

A Vierendeel (girder) truss composed of a series of rectangular or trapezoidal panels without diagonal members and it depends on the rigidity of joints for its stability. This type of trusses do not have the usual triangular voids which are used in pin joint, rather employing rectangular opening with rigid connection in the elements.

The Vierendeel truss, in spite of its designation, is not a truss in the conventional sense, where the conventional truss is designed to carry and resist axial forces, but in the other hand (and because of the omitted) new forces are imposed on it, like shear forces and flexural forces.

Vierendeel truss offers some esthetic qualities, has simple details because of the limited number of members at a joint, is easier to form and place and can be pre-cast or cast in place.

The Vierendeel's popularity today is not attributable to engineering assets, but to the architectural and mechanical integration possible, where expression requires a rectangular grid of openings, be it for doors, windows, or corridors, the Vierendeel is preferred. Where large open spaces occur below such rectangular grids, the Vierendeel excels again. The height can be as small as the structural depth between the ceiling of the story below to the floor of the story above, and therefore invisible to the layman's eye. Such a floor system resembles a castellated beam, but with much larger web openings. Wherever mechanical requirements are extensive and require room to accommodate large duct work or elbow room to change directions, the Vierendeel appears highly advantageous. As in most structural systems, the Vierendeel gains tremendous rigidity with increased depth. In addition, several stories of a Vierendeel grid linked

together can open extremely large areas of space below the framework and still permit rectangular openings through the system. These unique architectural opportunities have kept the Vierendeel current.[1]

The various types of Vierendeel trusses used in practice are shown in Figure 1-1

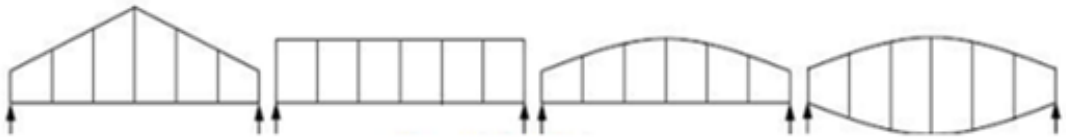

**Figure 1-1: Types of Vierendeel trusses[2]**

## 1.2 Applications of Vierendeel trusses

Vierenedeel trusses used in structural when the free space between top and bottom chord is required such as in clerestory lighting in churches and also for main girders in factories, bridges and ware house sheds. Both steel and reinforced concrete have been used as material construction. Vierendeel girders have widely used in Europe and particularly in Belgium where pioneering work on this type of girders were made [2].

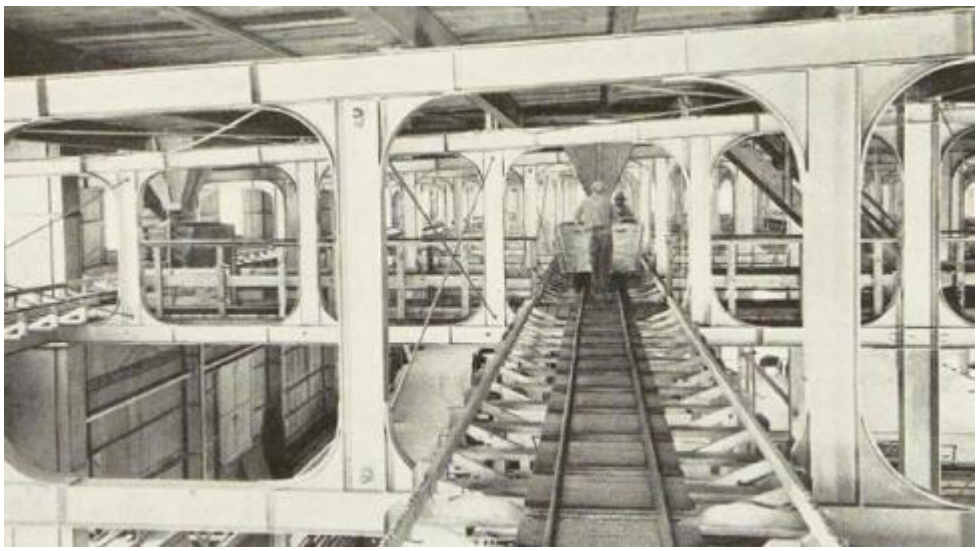

**Figure 1-2: Vierendeel truss in international agricultural corporation plant in Chicago[3]**

**Figure 1-3: Vierendeel truss in Sarah Brasilia hospital, Brazil[4]**

## 1.3 Slurry Infiltrated Fibers Concrete

(SIFCON) can be described as a special type of fiber reinforced concrete (FRC) [5] , and it is a relatively new material that differs from fiber-reinforced concrete in two aspects; fiber content and methodology of production [6]. In the normal FRC, fiber content usually varies from (1 to 3%) by volume whereas in SIFCON fiber contents vary in the range (4 to 20%). It is a function of several parameters, such as the shape, diameter, and aspect ratio of fibers; their orientation; the method used in packing; mold size; and the extent of vibration. SIFCON exhibits good strength and ductility compared to traditional FRC with a high volume fraction of steel fibers[7, 8].

SIFCON is characterized as extremely ductile material and high absorb energy. It additionally possesses high resistance to impact and explosive loading. SIFCON has an economical material if it is notably employed in the regions wherever it is fascinating properties are consumed such as beam-column joints and base of shear walls in structures to resist blast and earthquake loads [9].

Due to the small size of the materials that are used in mortar infiltrated fibers concrete, gaps are filled to maximum level so that

resulting in concrete contains gaps at minimum level. Furthermore; due to the rich fiber content, high-performance concretes are produced concerning flexural and toughness strengths[10].

### 1.3.1 Advantages of Mortar Infiltrated Fibers Concrete

In general, mortar infiltrated fibers concrete is very ductile and particularly well suited for structures which require higher ductility. Many advantages for using SIFCON can be shown below [11] :

- Slurry infiltrated fibers concrete possess excellent durability, energy absorption capacity, impact and abrasion resistance and toughness.

- The balling problem of fibers with increase in fiber volume in (FRC) can be resolved by slurry infiltrated fibers concrete, because of its fiber alignment.

- Modulus of elasticity (Ec) values for mortar infiltrated fibers concrete specimens is higher when compared with FRC.

- Deflection for mortar infiltrated fibers concrete will be very less compared to conventional concrete structural components (i.e.higher stiffness).

- SIFCON has high strength and ductility. It also reveals a very high degree of ductility as a result of which it has superior stability under dynamic, fatigue and repeated loading [11].

### 1.3.2 Disadvantages of Mortar Infiltrated Fibers Concrete

In spite of unique properties of mortar infiltrated fibers concrete, it doesn’t have many limitations. Uniformity and quality control of fiber distribution in addition to high placement cost associated with manual addition of fibers, restricted wide applications of these composites [12].

## • Steel Fiber

Cementitious matrices such as concrete have low tensile strength and fail in a brittle manner. Adding short needle-like fibers to such matrices enhances their mechanical properties, particularly their toughness, ductility, energy absorbing capacity and damage tolerance in members subjected to reverse cyclic loading. Thus fibers can smooth, indented, coiled, crimped, twisted, with end hooks, paddles, buttons, deformed with typical lengths of 6 mm to 150 mm and widthes ranging from 0.005 mm to 0.75 mm. In some fibers the surface is etched or plasma treated to improve bond at the microscopic level. The main factors that control the performance of the composite material are: physical properties of fibers and matrix and the strength of bond between fibers and matrix[13-15]**.**There are many types of steel fiber used to produce SIFCON as shown in Figure 1-. The most widely used types are hooked and crimped fibers. Straight and deformed fibers are used also, but they are less popular. Smaller or shorter fibers may pack denser than longer fibers and higher fiber volumes can be achieved with careful and sufficient vibration[6].

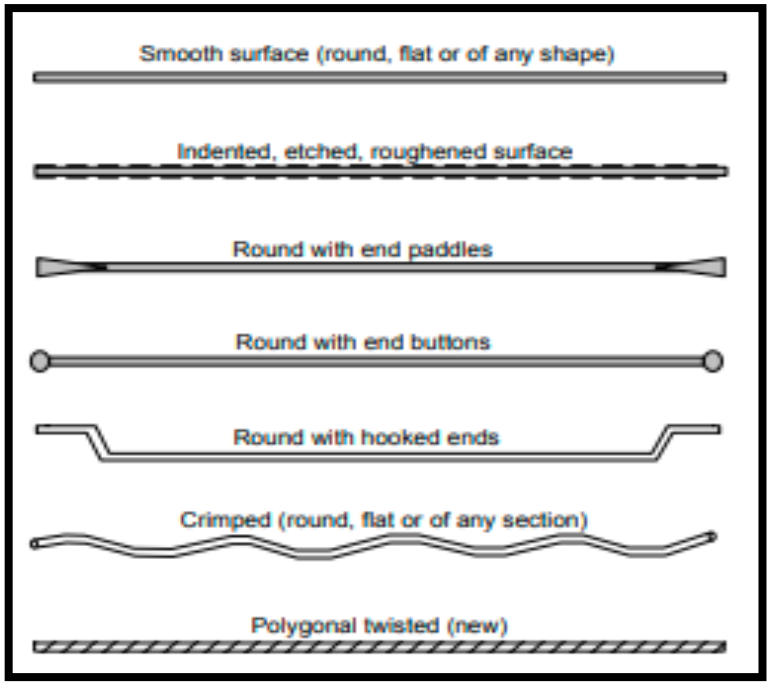


**Figure 1-4: Steel fibers commonly used in SIFCON[13].**

## 1.4 Scope of the Work and Objectives

This experimental study focused on studying the structural behavior of slurry Infiltrated fibrous reinforced concrete Vierendeel system .

The tested specimens have same dimensions (1350*250 mm) which they are length and height respectively .

The specific objectives of the experimental study are to investigate the effect of the following main variables on the specimens :

1. Investigating the effect of changing the void shape (square, circle and triangle).

2. Investigating the effect of changing the void ratio.

3. Investigating the effect of changing width of the specimens.

4. Evaluating the validity and accuracy of using finite element method utilizing computer program (ABAQUS) and comparing with the experimental results.

## 1.5 Thesis Organization

The thesis is divided into six chapters. This chapter includes background information on the Vierendeel truss and mortar infiltrated fiber concrete and the objectives of the research followed by thesis organization, while **Chapter Two** describes literature review on Vierendeel truss and SIFCON.

In **Chapter Three** description for all steps of the experimental work, such as material characteristics, mixing, casting, curing and tests information, while **Chapter Four** presents and discusses the experimental results.

**Chapter Five** describes the numerical results and also a comparison with the experimental results.

Finally, **Chapter Six** summarizes the main conclusions obtained from the present research in addition to several suggestions for future work.

# 2 CHAPTER TWO: LITEREATURE REVIEW

## 2.1 Introduction

In this chapter, the literature review of Vierendeel truss and slurry infiltrated fiber concrete is presented.

## 2.2 Experimental and Analytical Work on Vierendeel Truss

**In 1896 Professor Arthur Vierendeel**, has developed a rigid frame with open-web girders having rigid joints, consisting of top and bottom chords with vertical members between the top and bottom booms. This type of open frames is popularly known as Vierendeel truss (girder). The prominent feature of the Vierendeel truss being the absence of the diagonal members and the frame depends on the rigidity of the joint for stability.

The analysis of Vierendeel type structures has been taken by researchers. In the following, reviews and discussions being carried out by some researchers, including experimental and theoretical studies, which they have been devoted to investigate the behavior and ultimate capacity of Vierendeel structures, and also include a brief review about the parameters of the study giving some useful conclusions.

**Chen (1962)** [16] described a method for analyzing Vierendeel truss, it consists of distributing arbitrary fixed-end moments assigned to the chord members at their ends. These fixed-end moments assigned to the chord members at their ends. These fixed-end moments are induced by an unknown sway in each panel of the girder, and are each proprtional to the respective values of K/L (where K: member stiffness, L:member length). Here, the distributed quantities at the end of the chord members are the influence moments induced by an independent sway in each panel of the

girder. Shear in any panel is obtained by dividing the sum of the influence moments in the divided panel by its panel length. At this stage, several equations are generated, and by the relaxation method one obtain the unknown values of the panels 'sway, after which the values of members' moment can be obtained. Chen compares his results with the slope-deflection method, and a negligible difference between them is found.

**P.C.Varghese et al.(1972)**[17], investigated the behavior of simple parallel chorded reinforced concrete Vierendeel girders. They made series of laboratory tests on thirty reinforced concrete Vierendeel girders with five loading case and six (depth/span) ratios for each loading case. It was found that the depth/span ratio has a considerable influence on the behavior of cracks and stiffness of the girders. They found that in the case of girders with low depth/span ratios, the cracks are spread over a greater portion of span and extend to the complete depth of bottom chords. On the contrary of girders with larger depth/span ratio, the cracks are limited to a few definite sections of the panel in shear span and other panels are almost free of cracks. Figure 2-1shows the types of loading.

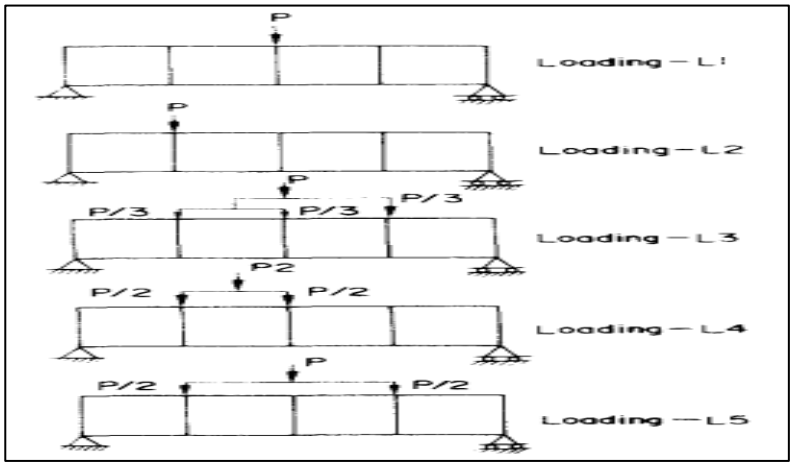


**Figure 2-1**: **Details of types of loading[17].**

**Korol(1977)**[18], made an extensive research program on Vierendeel joints in hollow structural section. A total (29) specimens

comprised of five distinct types were tested and their strength and stiffness properties were recorded. Design curves for prediction of joint strength have been proposed and design examples of Vierendeel trusses under panel joint loading were analyzed. It was found that unreinforced joint do not perform adequately, and hence necessitate some form of reinforcement. Also, they recommended using two types of connection in steel Vierendeel truss. These are haunch type and chord flange stiffeners due to their adequate strength and stiffness characteristics.

**Zhilin(1980)**[19], discussed the shear strength of the lower chord of the reinforced concrete and pre-stressed concrete Vierendeel truss. It was found that, the lower chord of a Vierendeel truss, when loaded, is subjected to the combined action of pre-stressed compression, large axial load, moment and shear. On the basis of these experimental data, Zhilin derived the practical formula for calculation of shear of the lower chord of the truss, taking into account the influence of the pre-stressed compression and longitudinal tension. The calculated results were in good agreement with the test results.

**Pararmasiveam(1980)**[20], studied the analysis of single bay symmetrical frames or Vierendeel frames under anti symmetrical loading by reducing them to that of open frames. The concept of slope-shear equation was presented. This concept leads to simpler solution, because of one important characteristic that the shear force in the chord members is statically determinant. The shear at any section of a column is equal to the sum of external loads above the section. In such a case it is more expedient to express the end moment of the member in term of the end slop and shear in member, thus formulating what are termed slope-shear equations. These procedures are preferred over the slope deflection equation since the deflection is unknown.

**Nameer A. Alwash (1995)**[21] , proposed a general non-linear method for the analysis of reinforced concrete frames. Then, this method was ultilized for the analysis of reinforced concrete Vierendeel trusses, where different parameters were included which where: combined effects of geometric non-linearity and shear deformations, material non-linearity, moment-axial interaction, possibility of local stress unloading and the effect of the elements ends rigidity. Experimentally, three models of reinforced concrete Vierendeel trusses of different shapes and dimensions were casted and tested up to failure as shown in Figure 2-2. The results were compared with those obtained theoretically by the proposed method. It was found that the proposed methods were efficient for modeling such structures and it was concluded that the prismatic members may be adopted in reinforced concrete Vierendeel trusses neglecting the end rigidity and cracked section is more representative than gross section in describing the section properties.

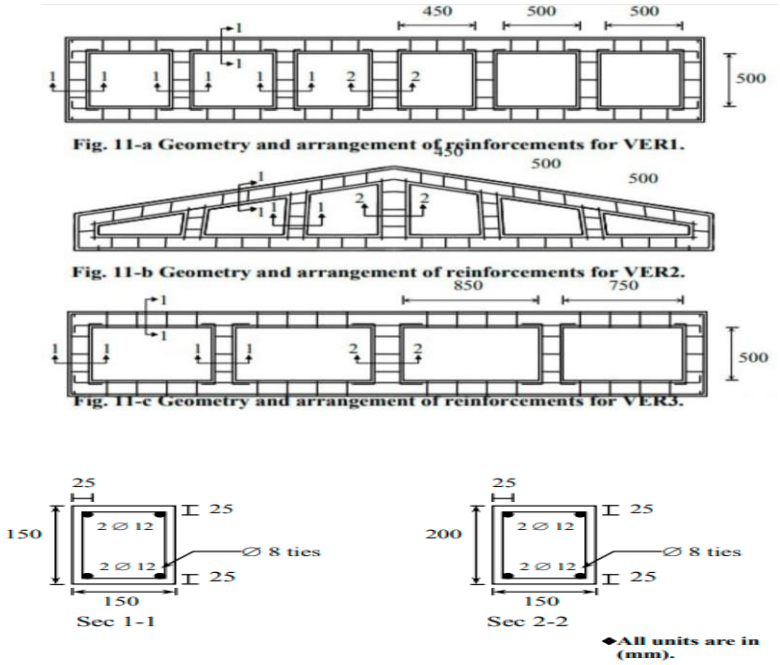


**Figure 2-2: Dimensions and details of reinforcement[21].**

**Shuber (1996)** [22], proposed a method for analysis of parallel chords Vierendeel trusses with rigid ended vertical members. This method included derivation of three general equations representing the relation between the redundant unknown (moment, shear and axial forces) at the center of the panel. The solution of the derived equations was accomplished by using successive approximations (Gauss Sedil). Several Vierendeel trusses were analyzed with varying number of panels, load case and member dimensions to show the accuracy of the proposed method.

**Kalid S.M., Aalaa W. H. (2008)**[23] developed a program named (P3DNFEA) to study the behavior of reinforced fibrous concrete vierendeel truss. Several parameters that affected the behavior of the structure like fiber volume fraction, aspect ratio, and the position of the portion in structure that uses fibrous concrete are studied in this work. The following conclusions were reached:

- The usage of inclined chords is recommended because this inclination greatly reduced the bending stress.
- The addition of steel fibers increases crack resistance, the tensile strength, crack control.
- Fiber diameter, fiber length and fiber volume fraction affect the mechanical properties of steel fiber reinforced concrete.
- The usage of steel fibers could be used in the shear and tension zones only for economical purposes.
- Tension zone is concentrated in the central bottom chord with some disconnected portions in structure, while shear zone is concerted in verticals and intermediate of external chords.

**Qassim M. S. et al.(2012)**[24] used ANSYS program to analyze the reinforced concrete Vierendeel trusses. From this study, the conclusions were:

- The first crack in the reinforced concrete Vierendeel trusses using inclined chord appears at higher load compared with structures having horizontal chord.
- The number of voids has an effect on ultimate strength of Vierendeel truss. It was found that the ultimate strength increases with increasing the number of voids in the structures having the same span.
- Good agreement with experimental test can be achieved if a good representation is made for the structure with appropriate selection for the coefficient of shear transfer.

## 2.3 Slurry Infiltrated Fibrous Concrete (SIFCON)

Steel fiber-reinforced composites, which use a considerable amount of steel fibers, were first propositioned by Lankard in 1979 at the Engineering Research Institute in Mexico[25].

SIFCON, as a special type of fiber reinforced concrete (FRC), has a discrete fiber matrix which lends significant tensile properties to the composite matrix and because of its high fiber content, SIFCON has also unique and superior properties in the area of both ductility and energy absorption[6].

SIFCON has been utilized as a pavement overlay material, and it has also been employed in real construction as a material for the repair and renovation of concrete bridge decks, among other things. Another practical application of this material was the connecting of seismic-resistant

reinforced concrete frames, which was another practical application of this material[7].

In spite of very high strength in compression for high or ultrahigh strength concrete, it considers essentially as a brittle material and both ductility and tensile strength for these concrete types can increase through inclusion of adequate fibers[26]. Therefore, concrete structures rely largely on the deformation and yield of their tensile reinforcement to achieve the ductility demand to prevent non ductile failures[27].

Slurry Infiltrated Fibrous Concrete (SIFCON) is an outstanding FRC form with high fiber material. Typically, the matrix contains slurry cement-sand or a fluent mortar. SIFCON boasts excellent energy absorption ability, higher ductility and high strength [28]. In any case, the improved material characteristic of SIFCON primarily their very high ductility and flexure resistances and the high tensile in addition to brilliant compressive strength lead to the conclusion that the use of this material in composite elements is promising. SIFCON has been commonly used for concrete overlays, refractory applications, and blast- and dynamic loading systems.

There is no coarse aggregates in SIFCON matrix. However, SIFCON matrix has high cementitious content where it is generally contented from cement or cement-sand. Also, silica fume and fly ash can be added[29]. Cement to sand proportions in SIFCON are usually 1:1, 1:1.5 or 1:2. where, maximum size of sand is most important parameter in SIFCON matrix. Several researchers recommended to use sand passing through 1.18 mm sieve or sand with maximum size 1, 0.6 or 0.5 mm to ensure complete penetration without honeycombing or clogging through the steel fibers network. For the matrix, the suggested water/cement ratio is 0.4 or less.

While, the required amount of (HRWR) to improve the slurry flow ability is varied from 2 to 5 percent by weight of cement[29, 30] When silica fume or fly ash is applied as a cement replacement additive, the recommended replacement between (20-60)% by weight of cement respectively. The most steel fiber widely used types to produce SIFCON are hooked end and crimped fibers. Straight, deformed fibers are also used, but are less common[29].

Due to the high steel fiber volume fraction that used in SIFCON processing, SIFCON density is higher than (FRC), and the rise in unit weight is approximately linearly proportional to the fiber content. However, for a matrix density of 1920 kg / $m^3$, the inclusion of steel fibers with a volume fraction in range (5 to 20) percent led to a rise in unit weight of between (2160 and 3130) kg / $m^3$[29, 31].

**(Parameswaran et al., 1993)**[32], produced slurry-infiltrated fibrous concrete (SIFCON) using three techniques for incorporating the steel fibers in the matrix. In the first one called (single-layer technique), the steel fiber is preplaced in the mold and the slurry is allowed to sequence through the fiber with the help of proper compaction by means of a table vibrator, as shown in Figure 2-3. The second technique concerned initial placing and packing of the fibers within the mold only up to one-third depth, followed by infiltration of the slurry up to the current level. The contents within the mold were then vibrated. The method was continual till the complete mold was filled and compacted. This technique known as (three-layer technique). The third technique called (immersion technique), consisted of filling the mold up to one-third depth by the slurry, implanting the fibers into it immediately thereafter, vibrating the contents, and continuance the method till the mold is full. The researchers found that these three methods proved to be effective during the deposition of the SIFCON samples. The three

layers and immersion techniques were found to be easier in actual practice than the single-layer technique [6].

**Figure 2-3:** casting procedure of SIFCON[5]

**Yazıcı et al. (2006)** [26] presented a study to investigate the influence of integrating high volume of Class C fly ash (FA) on autoclaved SIFCON mechanical properties. Cement was substituted in SIFCON compositions with up to 60 % FA and used three different volumes of steel fibers (2, 6 , and 10 )%. At almost every substitution of FA, the mechanical properties were positively affected. Moreover, flexural strength and durability were significantly improved by increasing the volume of fiber.

**Kim and Choi (2006)**[33] performed compressive and direct tensile tests to obtain SIFCON mechanical properties. Hooked-end steel fibers was used. Silica fume was used with amount 10% by cement weight while water/cement ratio was 0.4. Also, 0.5% water reducing agent was added to improve slurry workability. The test results in this study showed that SIFCON compressive strength is around 1.59 to 2.68 times that of cement paste while, tensile strength increased some 2.51 to 8.77 times. It is also observed that with the increasing fiber amount, SIFCON toughness and ductility are substantially improved. The stress-strain curves for tested

specimens in this paper are shown in Figure 2-4 and Figure 2-5 for compressive and tensile tests respectively.

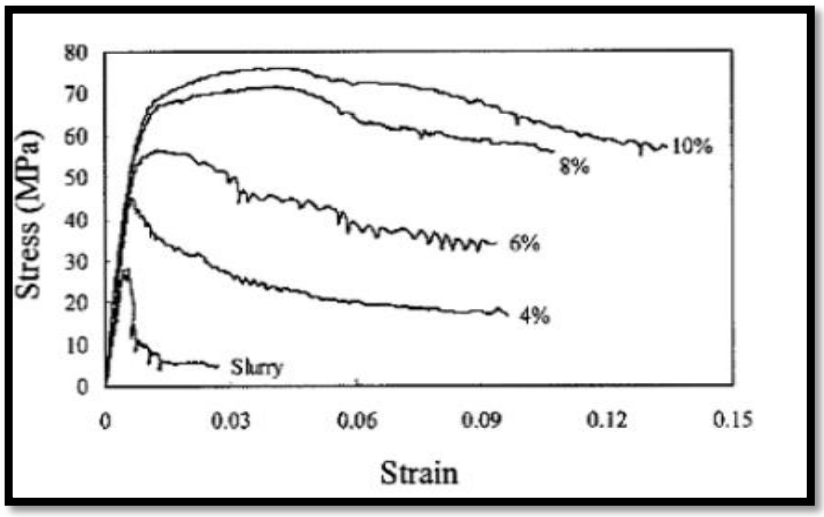


**Figure 2-4:** Stress-strain Curves of SIFCON in compression[33].

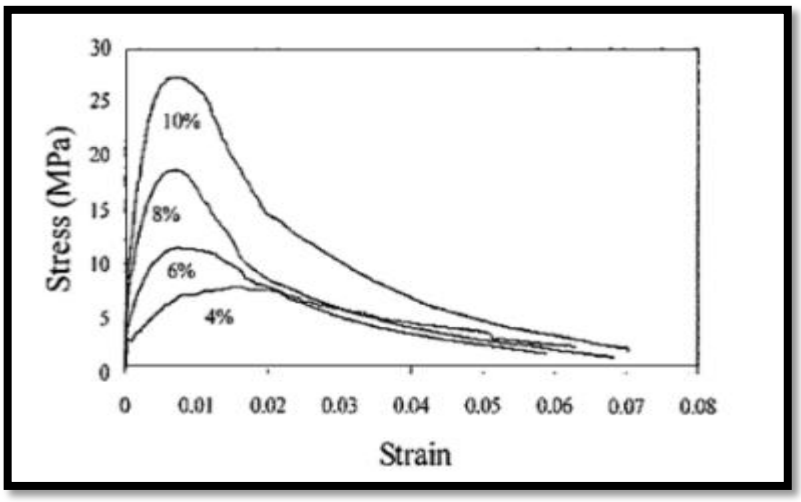


**Figure 2-5:**Stress-strain Curves for SIFCON samples in tension[33].

**(Abdul Rahim et al., 2014)**[34], used hooked-end fiber in prepare SIFCON. In order to determine the behavior of the steel fiber as reinforcement in concrete, three different percentage of steel fiber used, 3%, 4%, 5% and also the control sample without fiber. Sizes of prism used in this study are 100 x 100 x 500 mm. The behavior of steel fiber was investigated by using two point load test until failure. The area under load-

deflection curve shows the ductility of the specimen. Larger areas under the curve represent more ductile specimens. The control specimens have smallest area under the load deflection curve because there is no steel fiber to enhance the ductility of the specimens. The load-deflection data was recorded from the two-point load test. Based on the result, it was concluded that the optimum steel fiber content in this report was 5 % by volume friction which provided the highest flexural strength and deflection. Figure 2-6 shows load-deflection curve of SIFCON prism for different percentage of fiber.

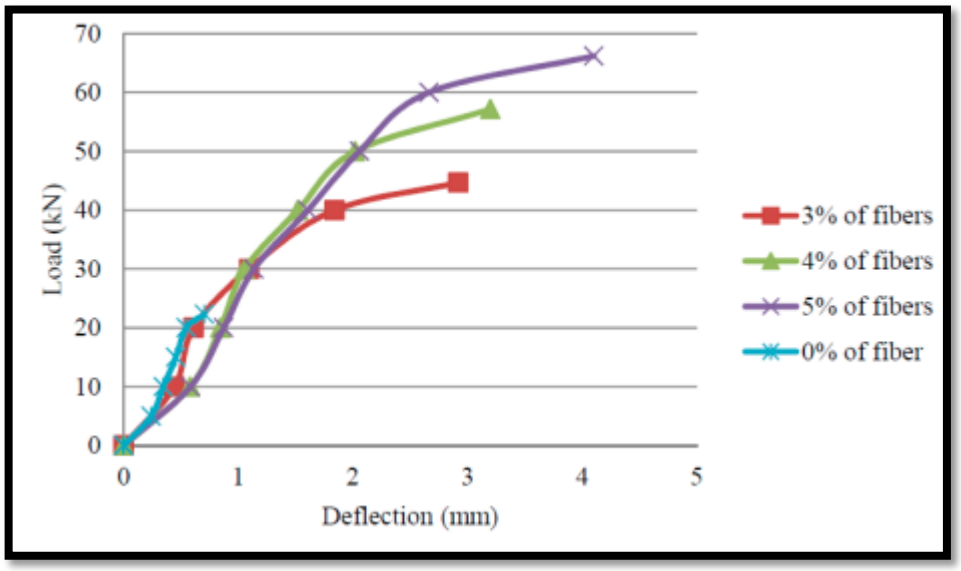


**Figure 2-6:**Load versus deflection curve of SIFCON [34]

**Giridhar et al. (2015)**[35] studied the effect of various volume fraction of steel fibers (4, 6, and 8%) on SIFCON mechanical properties. Two aspect ratios of hooked end steel fibers were utilized with lengths (50mm and 35 mm) and (1 and 0.55) mm diameter respectively. One of the concluded results was that the compressive strength for higher length fibers was less than that for smaller length.

## 2.4 Concluding Remarks

According to previous literatures, only few researchers provide the use of Vierendeel truss.

Therefore, the current experimental and numerical study will contribute in the recognition of the behavior of SIFCON Vierendeel truss. Several parameters will be considered such as: void ratio, void shape and the width of Vierendeel trusses.

# 3 CHAPTER THREE: EXPERIMENTAL WORK

## 3.1 Introduction

In this chapter, details of the experimental program are presented. A description of the raw materials used in casting of the specimen, and instrumentations used to obtain the different measurements. This chapter explains the research method only while **Chapter Four** will provide and discuss the results obtained from the tests mentioned. In the first part, all the raw materials properties and test procedure were explained. In the second part, the mix proportions of concrete, mixing procedure for fresh and hardened SIFCON were presented. Also, it includes a description, and identification of the tested Vierendeel specimens. Figure 3-1 presents a flowchart which shows the experimental program.

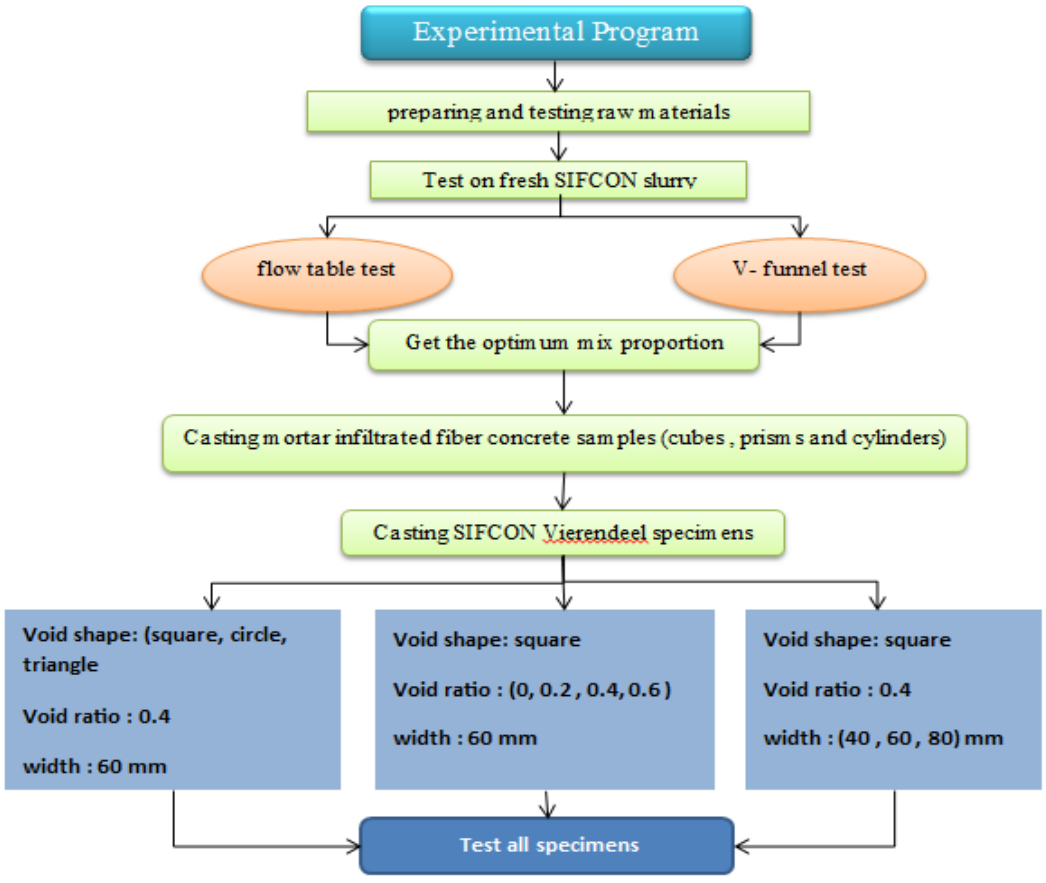


**Figure 3-1:Flow chart of the research plan.**

## 3.2 Description of The Specimens and Experimental Program

### 3.2.1 Description of Test Specimens

The experimental program consisted of testing eight Vierendeel specimens with five openings and dimensions 250 mm height , 1350 mm in length. The specimens are divided into three groups. All the specimens are cast of slurry infiltrated fiber concrete with 7% steel fiber.

The control specimen has square voids, void ratio (0.4), width (60mm).

The first group consisted of two specimens which have same void ratio (0.4), same width (60 mm) and different void shape (circle and triangle).

The second group consisted of three specimens which have same void shape (square ), same width (60 mm) and different void ratio (0, 0.2, 0.6).

The third group consisted of two specimens which have same void shape (square), same void ratio (0.4) and different width (40, 80 )mm.

Each group is presented in Table 3-1 with a simple diagram.

In fact, one additional specimen without openings was cast, as a trial specimen to check the devices and loading test system, which that used to test of all the other specimens.

### 3.2.2 Designation of Vierendeel Specimens

A symbol for each truss model has been set to distinguish it from the rest of the specimens, where each symbol in Table 3-1 is illustrated in Figure 3-2 .

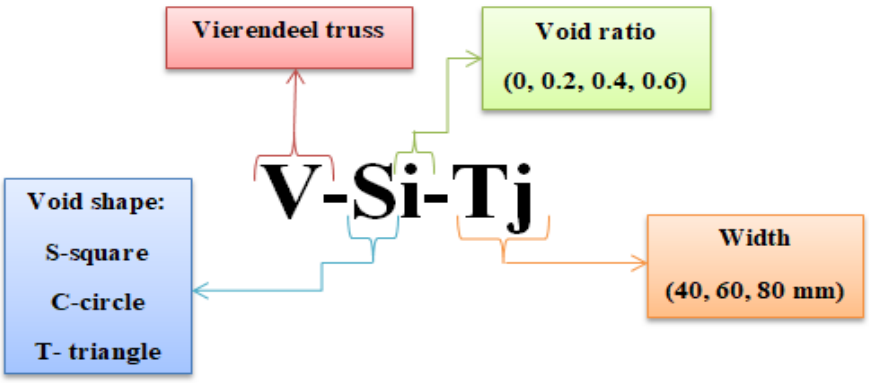


**Figure 3-2:Designation of Vierendeel truss specimen.**

**Table 3-1: Explain all specimens with notation**

| Group No. | Specimen designation | Void shape | Void ratio $\frac{V.voids}{V.total}$ | Width (mm) |
|---|---|---|---|---|
| **Control** | VS0.4T60 | Square | 0.4 | 60 |
| **I** | VC0.4T60 | Circle | 0.4 | 60 |
| | VT0.4T60 | Triangle | 0.4 | 60 |
| **II** | VS0.6T60 | Square | 0.6 | 60 |
| | VS0.2T60 | Square | 0.2 | 60 |
| | VS0T60 | Without openings | solid | 60 |
| **III** | VS0.4T40 | Square | 0.4 | 40 |
| | VS0.4T80 | Square | 0.4 | 80 |

The details of the specimems shown in Figure 3-3

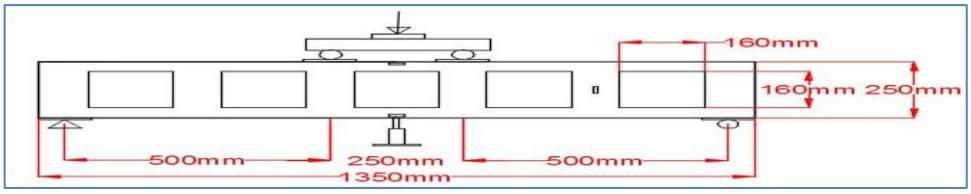


(a)VS0.4T60, VS0.4T40, VS0.4T80

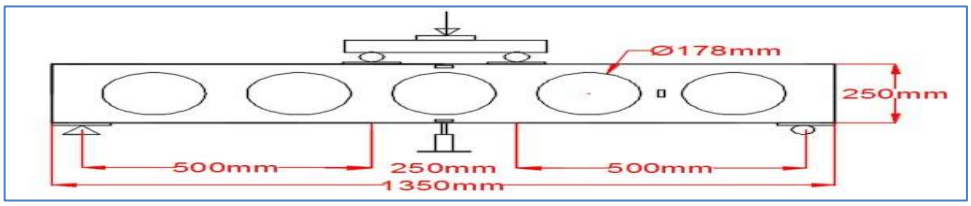


(b) VC0.4T60

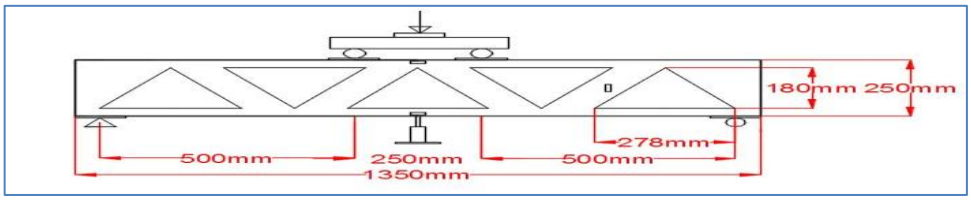


(c) VT0.4T60

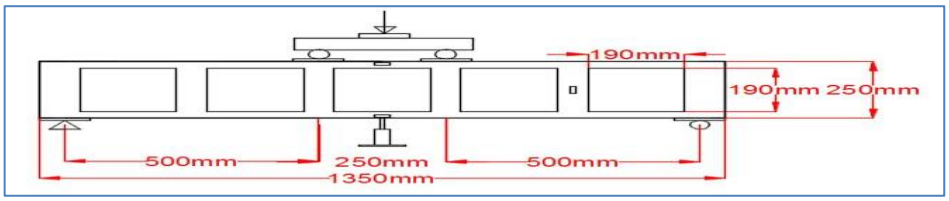


(d) VS0.6T60

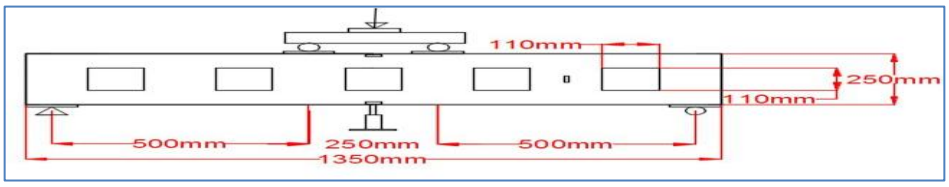


(e) VS0.2T60

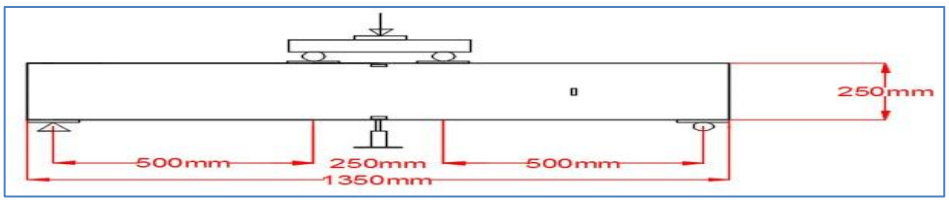


(f) VS0T60

**Figure 3-3: dimensions for Vierendeel specimens.**

## 3.3 Materials

### 3.3.3 Materials Used for Mortar Infiltrated Fiber Concrete

The materials used to cast the tested specimens include description of the cement, aggregate, mineral, chemical admixture, and fibers. The testing of each group of material is explained below.

#### 3.3.3.1 Portland Cement

Ordinary Portland cement (Type I) named Mass was used in casting all tested specimens. The physical and chemical properties of the used cement are given in Table 3-2 and

Table 3-3 respectively. These properties have been checked according to the Iraqi specification limits (IQS No.5/1984)[36] for ordinary Portland cement. The chemical and mechanical properties of the cement used have been tested in Construction Material and Environmental Laboratories at University of Babylon.

**Table 3-2: Physical Properties of Cement.**

| Physical Properties | Test results | Limits According to IQS |
|---|---|---|
| **Initial setting time (hour:min.)** | 02:23 | ≥ 00:45 (hour:min.) |
| **Final setting time (hour:min.)** | 03:25 | ≤ 10:00 (hour:min.) |
| **Fineness (Blaine) in ($m^2/kg$)** | 326 | ≥ 250 $m^2/kg$ |
| **Compressive strength, MPa** | | |
| **3 days** | 20 | ≥ 15 Mpa |
| **7 days** | 39 | ≥ 23 Mpa |

**Table 3-3: Chemical Analysis and Main Compounds of Cement.**

| Oxide | Test Result | Limit According to IQS |
|---|---|---|
| **CaO%** | 62.41 | ------ |
| **Si$O_2$%** | 20.88 | ------ |
| **$Al_2O_3$%** | 4.06 | ------ |
| **$Fe_2O_3$%** | 5.40 | ------ |
| **MgO%** | 1.60 | ≤ 5% |
| **S$O_3$%** | 1.19 | ≤ 2.5% if $C_3A$< 5% |
| **Loss on Ignition%** | 2.68 | ≤ 4% |
| **Total** | 98.22 | ------ |
| **Free lime** | 0.84 | ------ |
| **Insoluble Residue%** | 0.56 | ≤ 1.5% |
| **L.S.F** | 0.91 | 0.66-1.02 |
| **M.S.** | 2.21 | ------ |
| **M.A.** | 0.75 | |
| **$C_3S$%** | 53.57 | ------ |
| **$C_2S$%** | 19.45 | ------ |
| **$C_3A$%** | 1.62 | ≤ 3.5% |
| **$C_4AF$%** | 16.43 | ------ |

### 3.3.3.2 Fine Aggregate

Natural fine aggregate imparted from the region of (AL-NAJAF) was used as natural sand. This natural sand was too coarse to be used successfully in making mortar. Thus, just fine sand that was sieved by (600 μm sieve) to separate the coarser particles, is used for the preparation of mortar and using this size of sand proved to be successful for all mortar mixes during the experimental work. Table (3-4) shows the grading and

sieve analysis of fine aggregate. It conforms to the (IQS No.45/1984) limitation zone (4)[37]. The natural sand physical and chemical characteristics are listed in

Table 3-5. Fine aggregate has been tested at the University of Babylon in the Construction Material and Environmental Laboratories of Civil Engineering Department.

**Table 3-4: The sieve analysis of the sand used in mortar**

| Sieve size | Cumulative passing % | Limits of (IQS No. 45/1984) Zone (4) |
|---|---|---|
| **10 mm** | 100 | 100 |
| **4.75 mm** | 100 | 95-100 |
| **2.36 mm** | 100 | 95-100 |
| **1.18 mm** | 100 | 90-100 |
| **0.60 mm** | 100 | 80-100 |
| **0.30 mm** | 45 | 15-50 |
| **0.15 mm** | 10 | 0-15 |

**Table 3-5: Chemical and Mechanical Properties of the Used Sand**

| Main properties | Test results | Limits of IQS No.45/1984 |
|---|---|---|
| **Specific gravity** | 2.60 | - |
| **Fineness modulus** | 1.45 | - |
| **Sulfate content %** | 0.23 | $\leq 0.5\%$ |
| **Absorption %** | 2% | - |

### 3.3.3.3 Micro Silica Fume (S.F)

Silica fume is an ultra-fine material with spherical particles, the diameter of particles average being about 0.15 μm. This makes it

approximately 100 times smaller than the average cement particle. Silica fume improves the cement paste microstructure and making it more resistant to any form of external impact.

In this investigation, silica fume used which is commercially known as Master Ros MS 610 produced by (MASTER BUILDERS SOLUTIONS) company used by utilizing as a partial replacement (10%) by cement weight. The chemical analysis of SF used is shown in Table 3-6, whereas the physical requirement is shown in

Table 3-7. The results show that the (SF) used in present study conforms to the requirement of the (ASTM C1240-05, 2015)[38]. Appendix (B-1) shows all manufacturer properties.

**Table 3-6: The chemical analysis results of SF provided by manufacturer.**

| Oxide composition | | Oxide content % | ASTM C1240-05 |
|---|---|---|---|
| **Silicon dioxide** | $SiO_2$ | 89.41 | Minimum 85% |
| **Aluminum oxide** | $Al_2O_3$ | 0.63 | - |
| **Ferric oxide** | $Fe_2O_3$ | 0.45 | - |
| **Calcium oxide** | CaO | 0.82 | < 1 |
| **Sulfur trioxide** | $SO_3$ | 0.87 | < 2 |
| **Potassium oxide and Sodium oxide** | $K_2O + Na_2O$ | 1.35 | - |
| **Loss on ignition** | L.O.I | 4.10 | Maximum 6% |
| **Chloride content** | Cl | 0.18 | - |

| | | | |
|---|---|---|---|
| **Free calcium oxide** | CaO | 2.15 | - |

**Table 3-7: Physical properties silica fume used provided by manufacturer.**

| Main property | Result | ASTM C1240-05 limits |
|---|---|---|
| **Strength activity index** | 130 % | ≥ 105 |
| **Percent retained on 45µm (No.325) sieve max %** | 1.70 | ≤ 10 |
| **Specific surface, Min,( $m^2$ /g)** | 23 | ≥ 15 |

### 3.3.3.4 High Range Water Reducing Admixture (HRWR)

High-range water reduction admixture was used for mortar production to provide the mortar with higher workability and would be liquefied sufficiently to flow through the thick fiber without creating honeycombs. In this study, a high-performance concrete super plasticizer which is known commercially as (Master Glenium 54) from (MASTER BUILDERS SOLUTIONS) company was used as an HRWR. It is free from chlorides and complies with (ASTM C494 / C494M, 2017)[39]. Appendix (B-2) shows all manufacturer properties.

### 3.3.3.5 Water

The water used in concrete mix and curing was tap water.

### 3.3.3.6 Steel Fibers

The fiber is hooked end steel fibers with a length of (35mm) and a diameter of (0.55 mm). Plate 3-1 shows the hooked fibers used in the present work.

Table 3-8 indicates the technical properties of steel fibers used as provided by the manufacturer company.

**Table 3-8: The properties of used fibers according to the manufacturer**

| Property | Results of hooked end steel fiber |
|---|---|
| **Appearance** | Bright and clean wire |
| **Length (l), mm** | 35 |
| **Diameter (d), mm** | 0.55 |
| **Aspect ratio (l/d)** | 60 |
| **Density (kg/$m^3$)** | 7800 |
| **Tensile strength (MPa)** | 1100 |

**Plate 3-1: Used steel fibers (Hooked end)**

## 3.4 Mix Proportion of Slurry Infiltrated Fiber Concrete

Many trial mortar mixtures were produced in the experimental work to find the best mix proportion which has the best fresh properties to find a suitable mix that has the best properties. In the fresh state concerning fluidity, filling ability and viscosity without bleeding and separation or pockets in the dense fiber network causing a decrease in the mechanical properties of mortar infiltrated fiber concrete.

Since there are no standard guidelines yet for the design of the slurry infiltrated fiber concrete mix. The results of the literature review, as illustrated previously in Chapter two, helped to design mortar infiltrated fiber concrete mixes. For most situations, the proportions of (sand to cement) by weight is equivalent to (1:1) and this ratio has been adopted in this study. In addition, several researchers used the content of cement varying from 800 to1000 kg / m³ and suggested using a w/c ratio by weight below 0.4 to produce the mortar. Therefore, after many trials mixes using ordinary Portland cement of amount (969) kg/$m^3$ with replacement 10% of silica fume was used. While the water/binder (w/b) ratio was kept constant as (0.28) by weight of Cementous material. The approach used to calculate the amount of high range water reducing admixture (HRWR) required for mortar is by first testing the slump flow with different amounts of HRWR until achieved the target value of (240 to 260) mm. Then, viscosity of mortar is checked by the V-funnel test through determining the flow speed. This sequence in tests was because that slump flow test is the easiest and quickest. The tests were done according to the (EFNARC 2005)[40] that showed in Table 3-10, below.

The amount of water for each 1m³ equal to (271.32) kg/ m³, and using 7 % steel fiber(hooked end steel fiber) that the volume fraction of form concrete was improved as a minimum practical limit that could fill the

mold and produce mortar infiltrated fiber concrete with a different type of mortar without using vibration. Table 3-9 reveals the optimum mixes with the weight proportions used in this study for $1m^3$.

**Table 3-9: Mix proportions of the mortar infiltrated fiber concrete**

| Mix proportions for mortar infiltrated fiber concrete using steel fibers | | | | | |
|---|---|---|---|---|---|
| **Cement Kg/m3** | **Sand Kg/m3** | **SF Kg/m3 10% rep.** | **Hooked fiber Kg/m3** | **w/b** | **HRWR by wt. of Cementous (%)** |
| 872.10 | 969 | 96.90 | 546 | 0.28 | 2.40 |

## 3.4.3 Tests of Fresh Mortar

The testing of mortar in its fresh state has a significant importance in mortar infiltrated fiber concrete preparation. The mortar must have enough liquidity to flow through the thick fiber bed. According to the mortar, just two tests have been suggested by (EFNARC 2005) [40]which are the (V-funnel and mini-slump flow tests). These tests were used to evaluate the filling ability, flow ability, viscosity, and segregation resistance of mortar. The flow table test represents the flow ability, segregation resistance, and uniformity of the mortar, while the V- funnel test is provided to measure mortar viscosity (measure of the flow speed). The two tests conducted on mortar are briefly described below.

### 3.4.3.1 Flow Table Test

The workability of mortar mixtures evaluated using the flow table test according to (EFNARC 2005)[41], The device used for this test consists of the cone with an internal diameter for the base of 100 mm, and 70 mm for the top side with a height of 60 mm as appearing in Plate3-2. The steps of the test are described by preparing about (0.5) liter of mortar then moistening the base plate and inside of slump cone is necessary, followed by placing the base plate on a stable level table and the slumped cone was centrally located on the base plate. After that the cone was filled with mortar. The mold was removed by a steady upward pull. Then the table immediately was dropped (25) times in (15) seconds[42]. The final average diameter of the mortar in two perpendicular directions was calculated and represented the slump flow in millimeter. According to the (EFNARC 2005)[41] limits, the value should be between (240-260 mm) and the result was 249, which is within the range.


**Plate3-2: Flow table test.**

### 3.4.3.2 V-Funnel Test

Mortar viscosity can be determined using the flow time of the V-Funnel. The time value obtained does not calculate the mortar viscosity but represented the flow rate. The mortar displaying the higher flow duration obtained from the V-funnel test can be regarded as a comparatively high viscosity. The apparatus used for this test is composed of V-Funnel, bucket, scoop, trowel, and stopwatch, as shown in Plate 3-3. The required amount of mortar that is needed to carry out the test was about (1) liter. The V-funnel was placed on leveled firm ground. Then wetting the inner surfaces of the funnel and the bottom gate while the trap door was kept opening to let the excess water drain. After that closed the trap door and placing a suitable pan underneath. The funnel was filled by the mortar without any compacting, and the mortar reached the end of the funnel. Within (10) seconds from filling, the door was opened, and allowed the mortar to flow. When opening the trap door, the stopwatch was started, and the time was recorded when the discharge is complete. This was taken as the light was seen up through the funnel from above. According to the (EFNARC 2005)[41] limits, the time of flow between (7-11) seconds is considered acceptable for mortar. The result was within the range (10 second).

**Plate 3-3: V-funnel test apparatus**

## 3.4.4 Tests of Hardened SIFCON

The following tests were performed on the slurry infiltrated fiber concrete (compressive strength, modulus of rupture, modulus of elasticity, and splitting tensile strength). All the results will be tabulated and discussed in Chapter Four.

### 3.4.4.1 Compressive Strength

The compressive strength test was calculated depending on the (ASTM C39-86) [43] and (BS.1881: Paw 116:1989)[44]. Compressive strength represents one of the most important properties of concrete, that could give a general recognition of the quality of concrete. Tests of the compressive strength of mortar infiltrated fiber concrete were carried out by using cylinders with dimension of (100*200 mm) and cubes with a dimension of (100*100*100 mm) loaded uniaxial by the compressive machine type CONTROLS with (1900 kN) capacity as shown in Plate 3-4. The samples were tested at the ages of (7, 28 days) of curing. The average of three specimens was recorded in the test.

**Plate 3-4: The Compressive Strength Testing Machine**

### 3.4.4.2 Flexural Strength Test (Modulus of Rupture)

This test was carried out using prismatic beams with dimensions of (100*100*400 mm) tested as simply supported beams with two-point loading based on (ASTMC78-02) [45] as shown in Plate 3-5. The specimens were examined at 7 and 28 days after being cured in water, with an average of three specimens being recorded.

**Plate 3-5: Flexural strength test**

### 3.4.4.3 Splitting Tensile Strength

Tensile strength was carried out using cylindrical SIFCON specimens of 100 mm diameter and 200 mm height according to the procedure in ASTM C496[46]. The specimens were tested at(7, 28 days) age by using automatic compression testers with a capacity of 1900 kN. Plate 3-6 shows the splitting tensile test setup.

**Plate 3-6: Splitting tensile test**

## 3.5 Mixing Procedure of Slurry

A proper mix is required to achieve the desired efficiency and homogeneity of the mortar and significant is the increased mixing period. That is to allow the High Range Water Reducing Admixture (HRWR) to reach its maximum capacity and to obtain complete disposal of silica fume (SF) by breaking up any agglomerated particles.

All trials of specimen mixes were performed by electrical drill mixer with suitable pan about of ($0.02m^3$) capacity as in Plate 3-7. Any remaining concrete pieces from the previous batch must be washed with a damp cloth before using the concrete mixer. The method adopted in present work based on previous research and was confirmed to achieve optimal workability during trial mixes[30, 32, 47]. The steps of mixing can be summarized as follows:

1. The mixer was cleaned off any residual fresh or hardened materials from the older mixes before the mixing process.

2. The total quantity of HRWR (Master Glenium 54) was mixed separately for nearly 0.5 minute with one third of mixing water.

3. The binder material [cement with silica fume (SF)] were mixed together in the mixer for one minute to spread the (SF) particles within the particles of cement, after that sand was added and mixed for two minutes to obtain a uniform dry mixture.

4. After that, two third of mixing water was added to the mix and mixed for one minute. Then HRWR with one third of water was fed to the mixer and mixed for about three minutes.

5. The mixer is then stopped, and the mixing for the remainder not reached by the blades is done manually.

6. Finally, to get the necessary flow ability, slurry components are mixed for an additional one minute.

**Plate 3-7: Mixing Process**

## 3.6 Casting, Compaction and Curing Process of the Specimens

The first step was the selection of materials, prepared and weighed according to the required volume of the mix then the mold has been oiled.

The following stages are to describe the process of casting process:

1. Plywood molds was provided before each casting by properly cleaning and lubricating the interior surface by oil to prevent adhesion with hardened concrete and set on a leveled ground as shown in Plate 3-8.

2. After many trials of casting, mortar infiltrated fiber concrete technique in a multi-layer method was used to embed steel fiber into the matrix of mortar[48]. The multi-layer technique involved the initial placement and packing of the fibers in slices of Alcobond .These were randomly oriented, followed by the mortar filling up the mold to the level of fibers . The mortar has to be flow able enough to ensure infiltration through the fiber.

3. To prevent honeycombing or voids in the mortar infiltrated fiber concrete a steel rod with a diameter of (3 mm) used to compact each layer. This step was repeated until the whole mold was filled up to the required level as shown in Plate 3-9, Plate 3-10.

With each mix, cubes samples were cast to determine the compressive strength of concrete. Cubes are (100*100*100 mm)

The conventional method of curing was employed to simulate the site conditions. Subsequently, specimens were cured using saturated burlap coverings and polyethylene sheet covering to avoid the evaporation of curing water as seen in Plate 3-12.

**Plate 3-8: Preparing Formworks**

**Plate 3-9: Casting Vierendeel Trusses**

**Plate 3-10: Continued**

**Plate 3-11: Casting SIFCON Samples**

**Plate 3-12: Curing Process**

## 3.7 Installation of Strain Gauges

Strain gauge is a device used to measure strain on an object. The gauge is attached to the object by an adhesive. As the object is deformed, the gauge is deformed, causing its electrical resistance to change. To install a strain gauge on concrete, the surfaces were well smoothed with the help of electric grinding, then apply acetone for dry clean surface, special adhesive used for adhering strain gauge for concrete by applying it on the strain gauge then places the strain gauge on concrete and slight pressure by thumb for (30) second to insure good adhesion as shown in Plate 3-14. All the strain gauges were attached to data logger device. Three strain gauges were used for each specimen, one at mid-span section in the compression zone and the second at the tension zone and the third at a mid-height at a distance 250 mm of support. Plate 3-13 shows the Strain Gauge Used, while Table 3-10 shows Properties of the Strain Gauge.

**Plate 3-13: Strain Gauge Used Throughout the Tests**

**Table 3-10: Properties of the Strain Gauge as Provided by Manufacturer.**

| Property | Specifications |
|---|---|
| Type | PFL-30-11-3LJC-F |
| LOT NO. | A802611 |
| Gauge length | 30 mm |
| Gauge factor | 2.09±1% |
| Gauge resistance | 118.5±0.5Ω |
| Quantity | 10 |
| Temp. compensation for | $11*10^{-6}/℃$ |
| Test condition | 23 ℃<br>50%RH |
| Transverse sensitivity | -0.1% |
| Batch no. | TL04M |
| Lead wires | 10/0.12 2W 3m<br>r=0.32(Ω/m) |

**Plate 3-14: Installation of Strain Gauge**

## 3.8 Test Procedure

Eight simply supported specimens were tested under two equal concentrated loads until failure occurred by using 400 KN capacity hydraulic testing machine in Structures Laboratory of The Civil Engineering Department at University of Babylon. One trial specimen was tested to check the accuracy or validity of supports and the used instruments before starting in the test program of Vierendeel specimens. All specimens were placed from one end on a roller and the other on a hinge Plate 3-15shows the details of support conditions. Bearing plates were used as supports and at loading points to avoid local crushing in concrete. The load was applied in stages by a load control mode at a load rate of 0.1kN/sec, the deflection of the specimens at the mid span was measured using LVDT. The specimens were painted with a white color in order to improve the visibility of the cracks as shown in Plate 3-16. Observations of crack development on the specimens were marked with a

heavy felt pen to make easy the positioning and identification of cracks during the test. Plate 3-17 and Plate 3-18 show the details of the machine used for testing specimens.

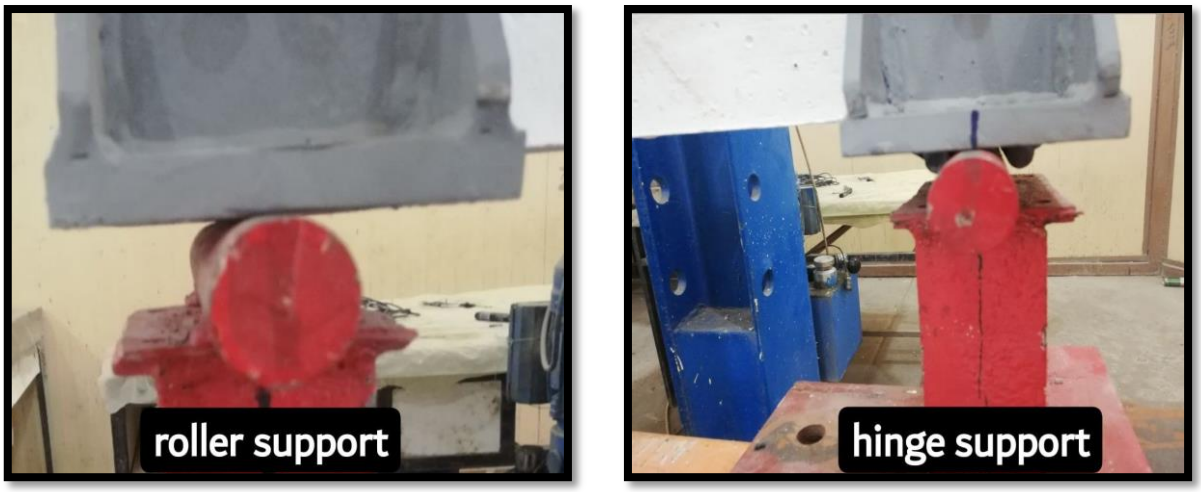


**Plate 3-15: Supports Used for all Specimens**


**Plate 3-16: Specimens after Painting**

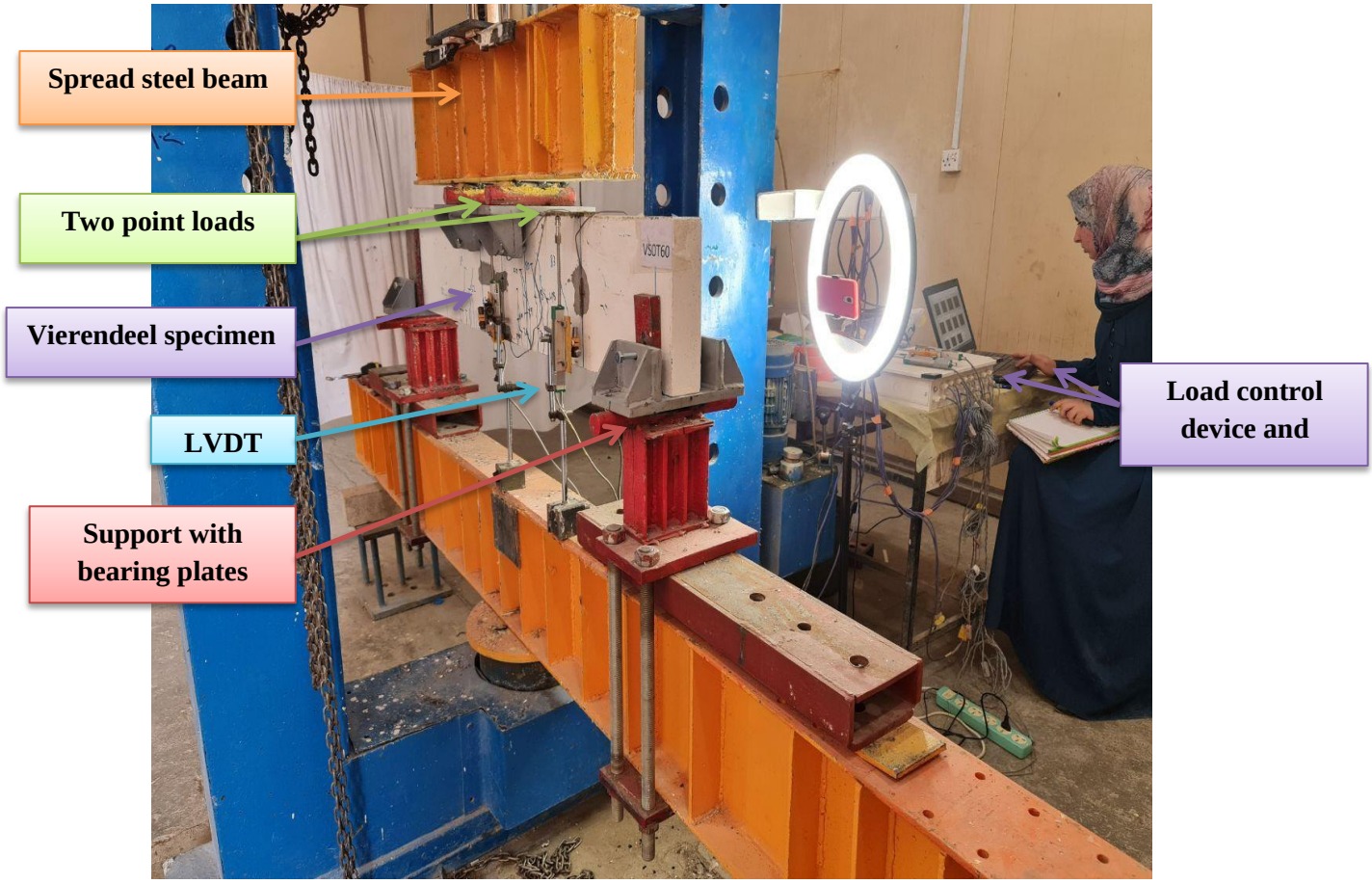


**Plate 3-17: testing machine in the laboratory of Babylon University**

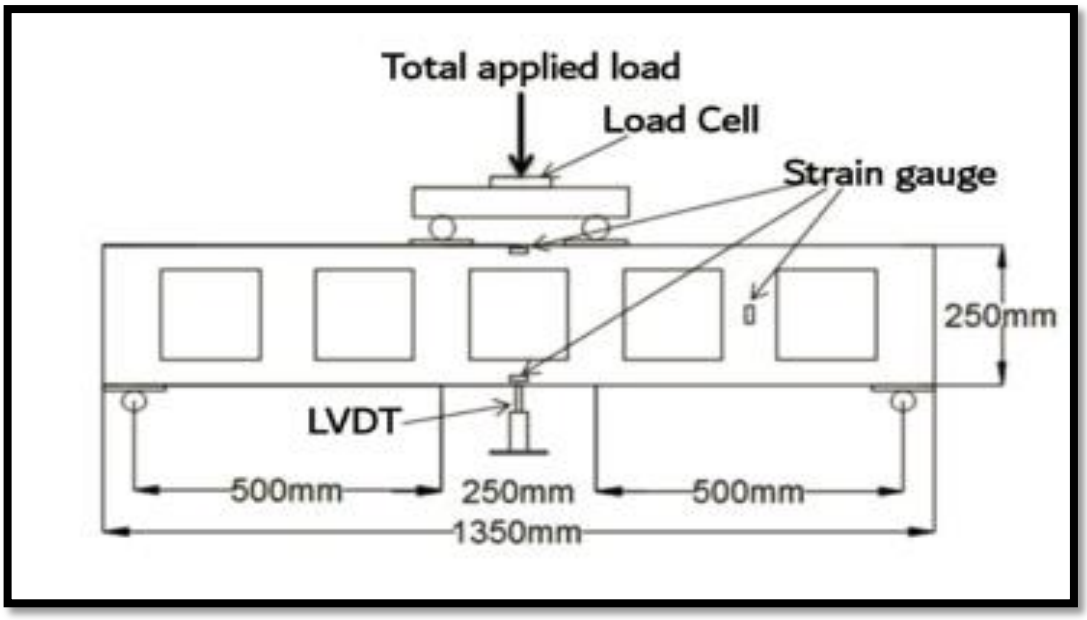


**Plate 3-18: Schematic test diagram**

# 4 CHAPTER FOUR: RESULTS AND DISCUSSION

## 4.1 Introduction

The most important findings from the experimental program mentioned in chapter three are explained in this chapter. First, the properties of hardened concrete obtained from tests of the control samples (cubes, cylinders, and prisms).

Then, test results obtained from specimens are represented and discussed including, ultimate load, load-deflection response, load strain curves, cracking behavior.

## 4.2 Mechanical Properties of Slurry Infiltrated Fiber Concrete

experimental test results of SIFCON mixes are presented, evaluated, and compared with previous literature in this chapter. Test results cover mechanical properties of hardened SIFCON (compression test, modulus of rupture test and splitting tensile strength ).

### 4.2.1 Compressive Strength

The most important characteristic of SIFCON is the compressive strength. Also, the common trend in the standard specifications depends mainly on concrete compressive strength for estimating the other mechanical properties[49, 50]. The test of compressive strength was carried out using three cubes (100×100×100) mm of SIFCON; cured at age of 7 and 28 days the results are shown in Table 4-1.

**Table 4-1**: **Compressive strength results**

| Avg. Compressive Strength (MPa) | |
|---|---|
| **7 days** | **28 days** |
| 68.99 | 92.85 |

### 4.2.2 Modulus of Rupture

Modulus of rupture values of Sifcon is carried out by testing three prisms with a dimensions of (100*100*400 mm) for (Vf) of fibers (7 %), at age of (7, 28) days, as presented in Table 4-2

**Table 4-2: Results and details of testing modulus of rupture**

| Avg. Modulus of rupture fr (MPa) | |
|---|---|
| **7 days** | 28 days |
| 33.87 | 38.74 |

### 4.2.3 Splitting Tensile Strength

In this study, splitting tensile test was carried out at age (7, 28) days to investigate the tensile strength for SIFCON with volumetric steel fiber ratio (7)%. The results of the test for cylindrical samples of (100×200 mm) are presented in Table 4-3. The considerable growth for SIFCON in tensile strength is resulted from binding fiber where the mechanism of bridging of fiber led to control the micro-cracks. In other hand, the using of hooked end type of steel fiber produces increasing in the bond between mortar and fiber, hence an enhancement in SIFCON mechanical properties. The test was performed in accordance with ASTM C496[51].

**Table 4-3: Result of splitting test**

| Avg. splitting test ( MPa ) | |
|---|---|
| **7 days** | **28 days** |
| 19.52 | 25.25 |

## 4.3 Test Results of Specimens

As mentioned before one pilot specimen and three groups of specimens are tested to study the structural behavior of Sifcon Vierendeel truss. Results are compared to investigate the significance and effect of experimental variables, which included void shape, void ratio and width. The ultimate load, cracking load and mid-span deflections at ultimate load and cracking load are shown in Table 4-4.

**Table 4-4: Experimental Results of the Tested Specimen**

| Group No. | Specimen designation | Total applied load (KN) | | | Mid-span deflection (mm) | | Max. Crack width (mm) |
|---|---|---|---|---|---|---|---|
| | | $p_{cr}$ | $p_u$ | $p_u/p_{cr}$ | $\Delta_{cr}$ | $\Delta_u$ | |
| Control | VS0.4T60 | 12 | 38 | 3.2 | 1.18 | 6.74 | 0.1 |
| I | VC0.4T60 | 17 | 42 | 2.5 | 1.59 | 5.57 | 0.19 |
| | VT0.4T60 | 19 | 34 | 1.8 | 1.7 | 4.51 | 0.06 |
| II | VS0.6T60 | 5 | 15 | 3 | 1.79 | 11.94 | 0.06 |
| | VS0.2T60 | 22 | 53 | 2.4 | 1.24 | 4.65 | 0.11 |
| | VS0T60 | 29 | 96 | 3.3 | 1.07 | 5.57 | 0.09 |
| III | VS0.4T40 | 10 | 20 | 2 | 1.62 | 6.62 | 0.1 |
| | VS0.4T80 | 14 | 49 | 3.5 | 0.96 | 7.93 | 0.27 |

### 4.3.1 Trial Specimen

This specimen has been tested to verify testing machine, adequacy of instruments, bearing and loading plates as well as to ensure that warping will not occur. The flexure failure occurred finally at load about (16kN).

## 4.4 Effect of Considered Variables on Structural Response

A summary for effect of considered variables (void shape, void ratio and the width) will be discussed and devoted on the main structural response such as the first cracking loads, ultimate load, deflection.

### 4.4.1 Load – Deflection Response and Ultimate Loads

As shown in Figure 4-1 a, at the beginning the deflection curves for VC0.4T60 and VT0.4T60 specimens are similar as control truss, but with increasing the ultimate load and before the ultimate load is achieved, the curves become stiffer than the curve of control truss.

With regard to the opening size, Figure 4-1b shows that the deflection increase with increasing the void ratio with a decrease in ultimate load. Figure 4-1c shows that the deflection increase with decreasing the width .

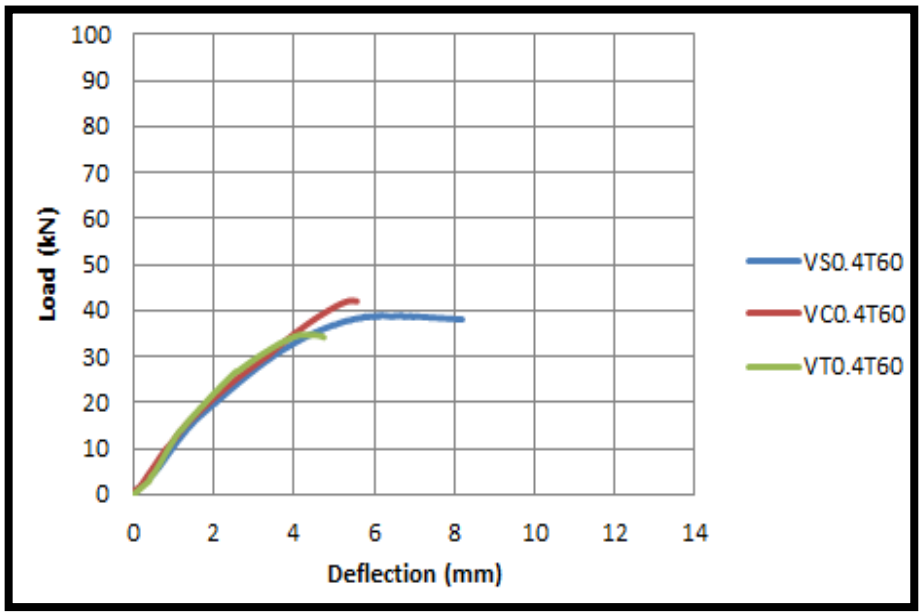


(a) Effect of the opening shape

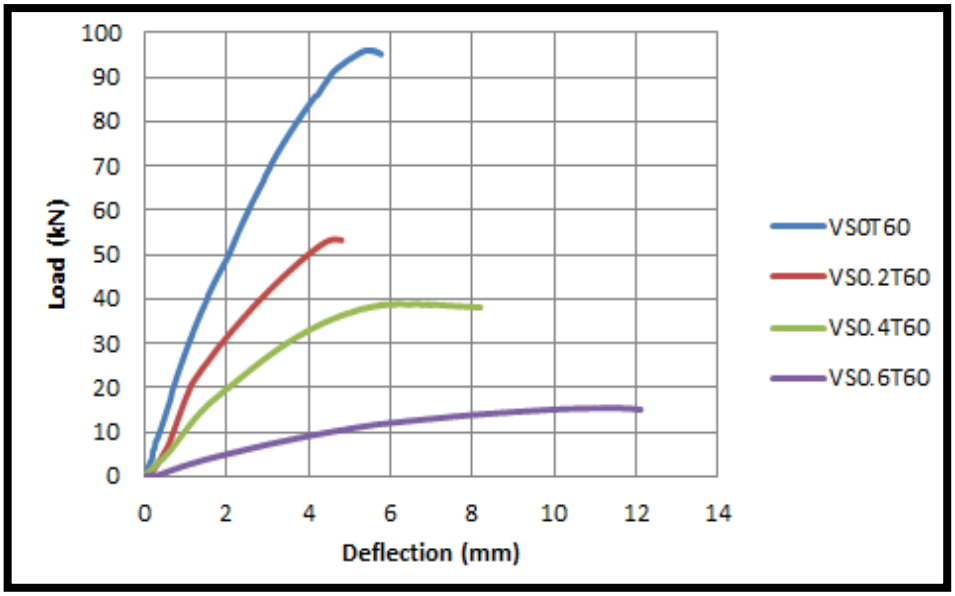


(b) Effect of the opening size

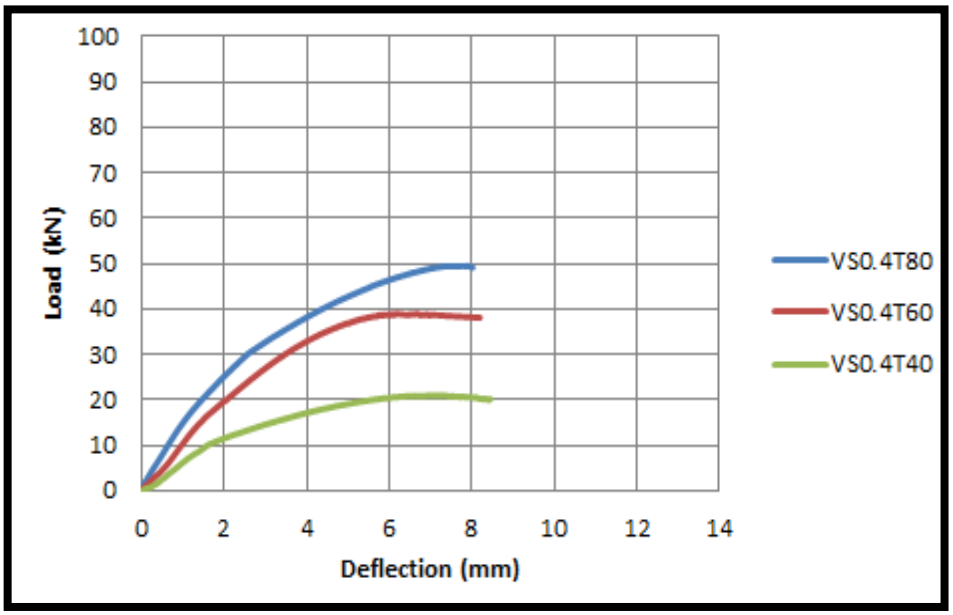


(c) Effect of the width

**Figure 4-1: Experimental Load - Midspan deflection curves**

The ultimate load carrying capacity (Pu), the mid span deflection at cracking load, and the mid span deflection at ultimate loads for Vierendeel trusses are presented in Table 4-4. In general, it is observed that the load capacity of the specimen with circular openings higher than the load capacity of the specimen with square openings in about 8% because these openings haven't corners , while the load capacity of the specimen with

triangular openings decrease in about 10.9% compared with the reference specimen.

With regard to the opening size the load capacity of trusses decreases with increasing the opening size. For (VSO.6T60 specimen), the reduction in the load capacity is 60.5% from the ultimate load of the reference truss. While the increase in the load capacity for (VS0T60, VS0.2T60) is 146.7 and 37.1% respectively.

The ultimate load increases with increasing the width of the truss, for (VS0.4T80) specimen the increasing in the ultimate load is 27%, while the reducing in the ultimate load for (VS0.4T40) is about 46.4% when compared with reference truss.

### 4.4.2 Cracking Behavior

The cracks formation and spread were carefully detected during the tests. The same loading rate, procedure, and under the same conditions were followed in testing for all trusses. All specimens were painted with a white color in order to improve the visibility of the cracks. Results of first cracking load in addition to crack patterns are discussed for all tested trusses mentioned in Table 4-5 and shown in Plate 4-1.

**Table 4-5: First crack loading**

| Group No. | Specimen designation | First crack loading kN | Change in cracking load % | First crack position |
|---|---|---|---|---|
| **Control** | **VS0.4T60** | 12 | --- | Under the right first void |
| **I** | **VC0.4T60** | 17 | 42.6 | Under the left point load |
| | **VT0.4T60** | 19 | 56.6 | Under the left point load |
| **II** | **VS0.6T60** | 5 | -58 | Under the left first void |
| | **VS0.2T60** | 22 | 80.9 | Under the left second void |
| | **VS0T60** | 29 | 143.5 | Under the right point load |
| **III** | **VS0.4T40** | 10 | -17.2 | Under the left first void |
| | **VS0.4T80** | 14 | 16 | Under the right second void |


(a)VS0.4T60 specimen


(b)VC0.4T60 specimen


(c)VT0.4T60 specimen


(d)VS0.6T60 specimen


(e)VS0.2T60 specimen

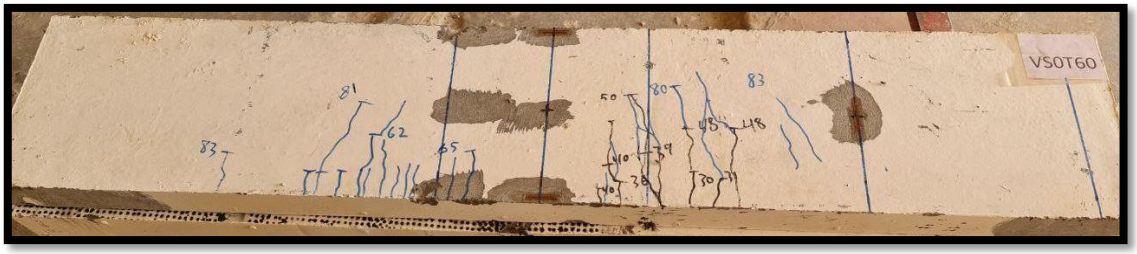


(f)VS0T60 specimen


(g)VS0.4T40 specimen


(h)VS0.4T80 specimen

**Plate 4-1:Crack patterns at failure for Vierendeel trusses**

From above plates, it can be concluded that:

- In general, it is observed that the cracks formed at corners of the openings due to the high-stress concentration.
- As shown in Plate 4-1, because of the lower load capacity for VS0.6T60, VS0.4T40 specimens, they have the least number of cracks.
- VC0.4T60, VT0.4T60, VS0.4T60, VS0.4T80, VS0.2T60,VS0T60 failed by flexure at mid span.
- The failure of (VS0.6T60, VS0.6T40) were at joint between lower chord and the second column.

## 4.4.3 Load-Strain Evolution

In this work strain gauges in different locations is used to indicate the strain of Vierendeel specimens and the process of instillation of these strain are shown in chapter three. It should be known that the strain gauge is fixed on the specimens in horizontal direction at mid-span section in the upper chord (strain1) and at mid-span section in the lower chord (strain2) to measure the flexural strain, but in vertical direction at a mid-height of the second column (strain3).

A typical representation of the experimental load- strain relation is shown in Figure 4-2 to Figure 4-9.

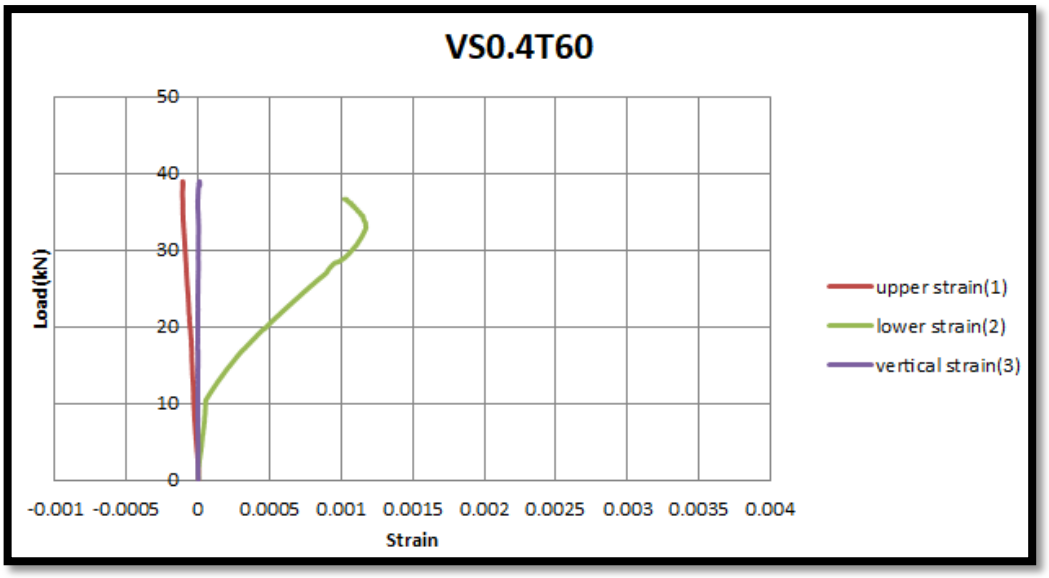


**Figure 4-2: load-strain curve for specimen VS0.4T60**

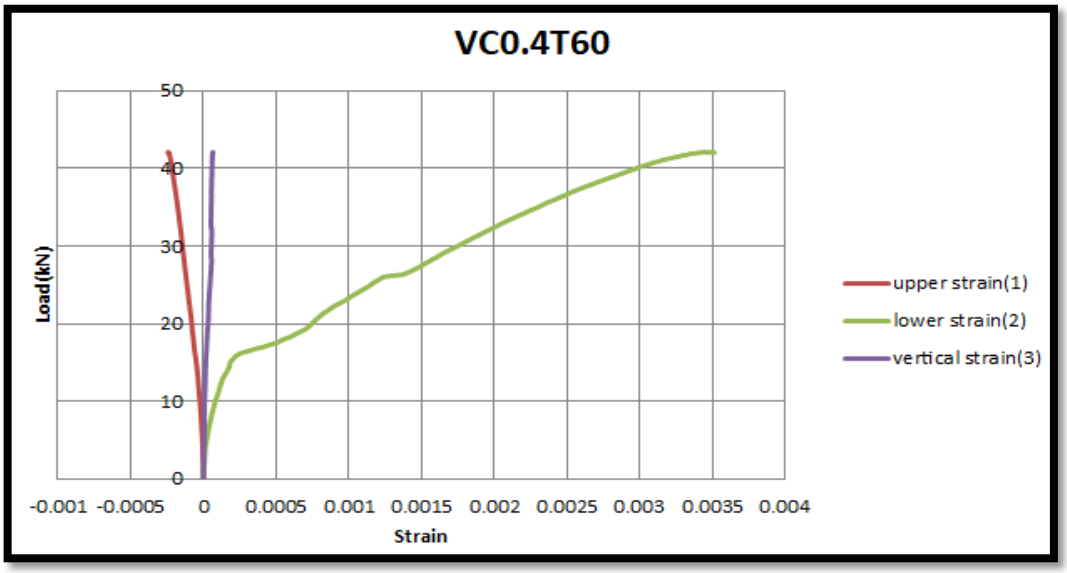


**Figure 4-3: load-strain curve for specimen VC0.4T60**

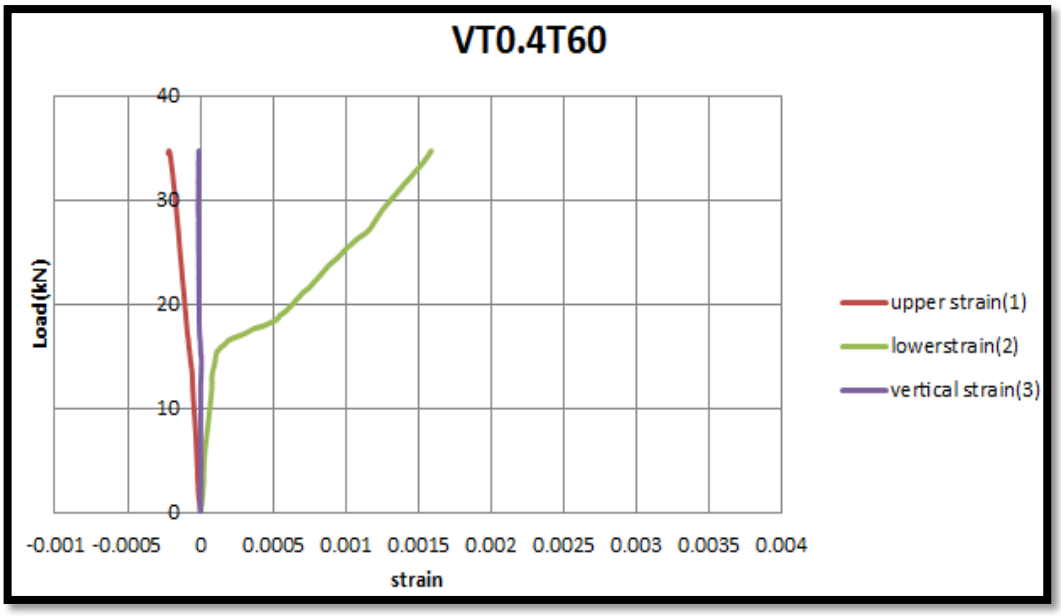


**Figure 4-4: load-strain curve for specimen VT0.4T60**

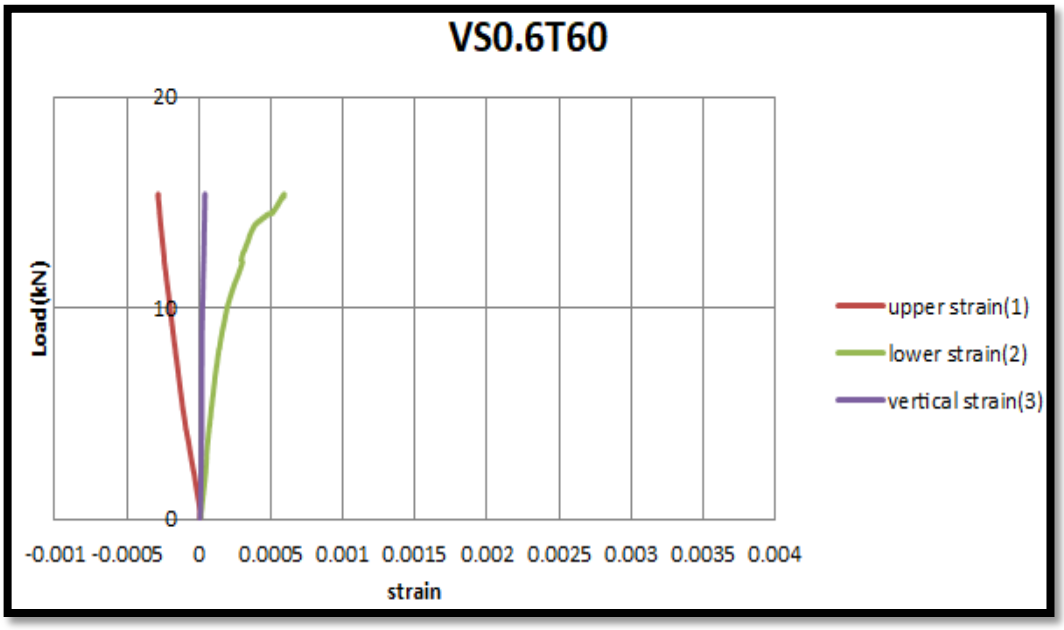


**Figure 4-5: load-strain curve for specimen VS0.6T60**

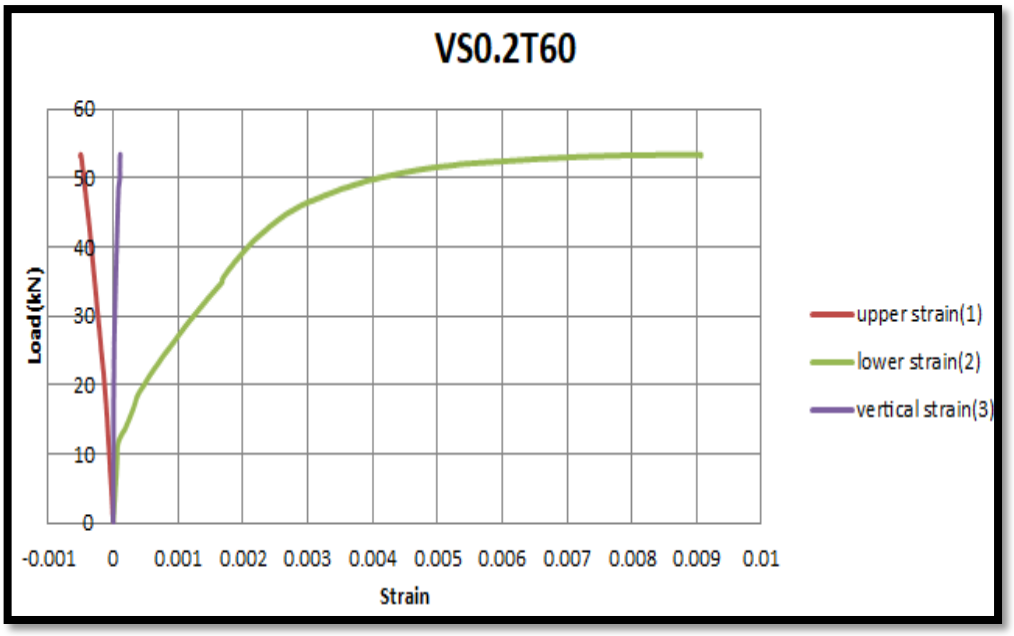


**Figure 4-6: load-strain curve for specimen VS0.2T60**

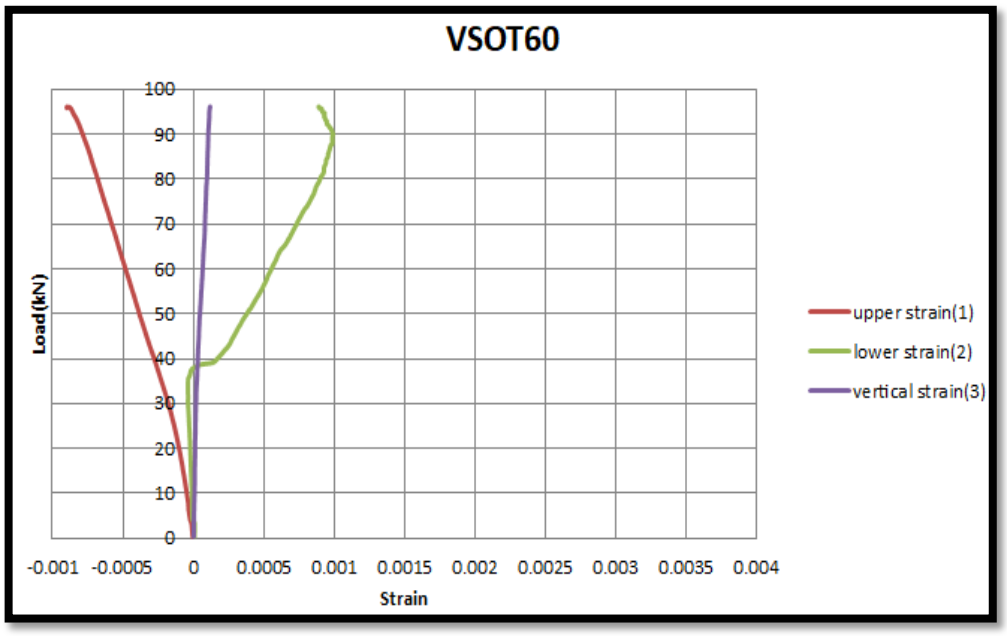


**Figure 4-7: load-strain curve for specimen VS0T60**

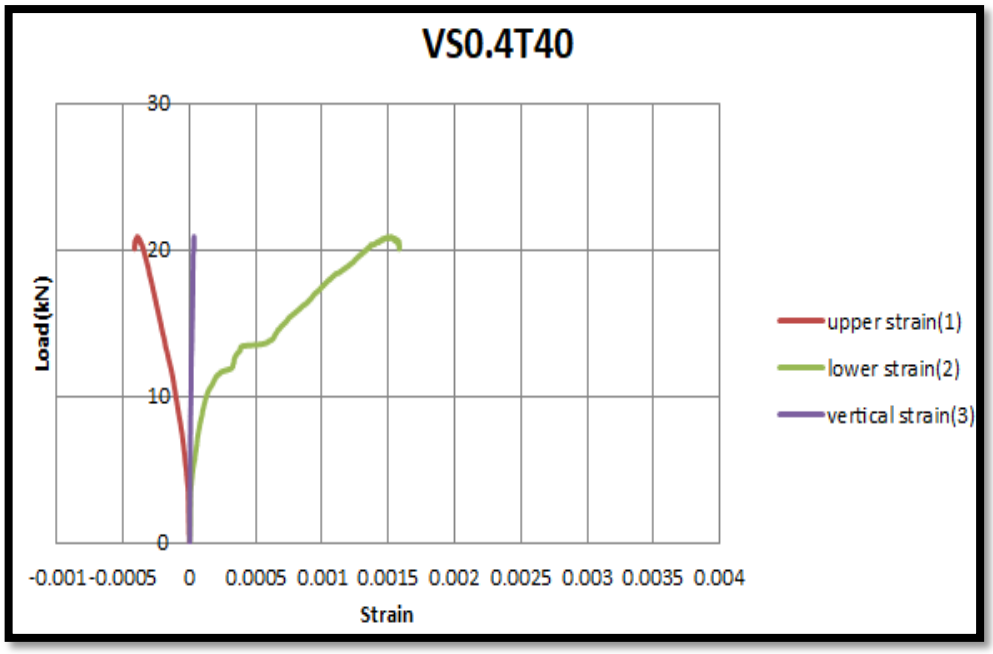


**Figure 4-8: load-strain curve for specimen VS0.4T40**

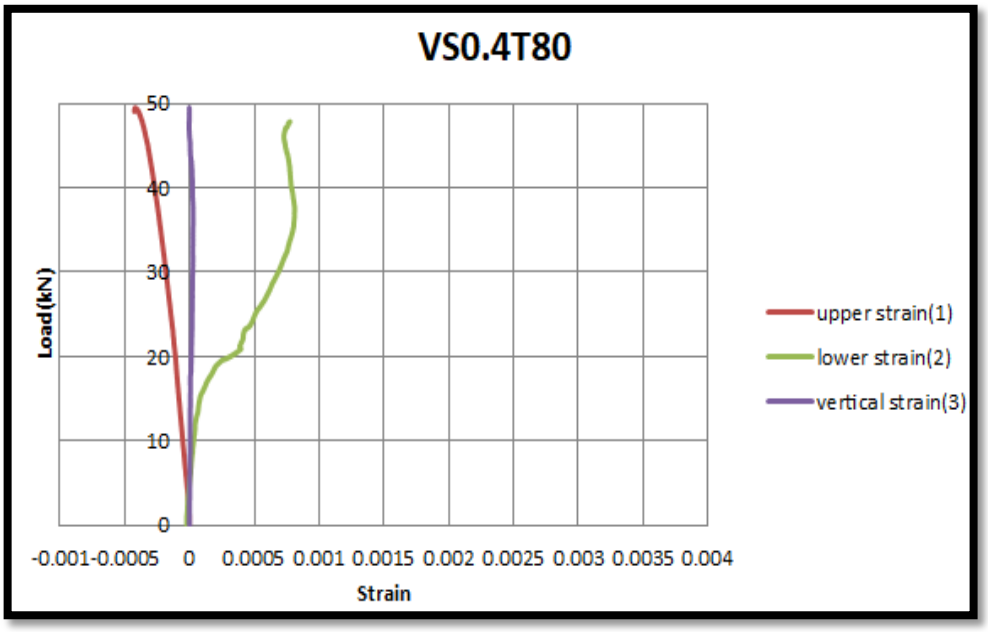


**Figure 4-9: load-strain curve for specimen VS0.4T80**

From the above figures, we can conclude that:

1. The accuracy of the reading is micro-strain which it is small enough to sense any little movement or elongation in concrete.

2. The values of strain in lower chord give positive value which means that the lower chord worked as tension member.
3. The values of strain in upper chord give negative value which means that the upper chord works as compression member.
4. It can be noticed that the concrete strain at the extreme compression fiber behaves linearly with load at early stage of loading, after that it became non-linear with load until failure.

### 4.4.4 Stiffness Criteria

Stiffness is defined as load required for producing unit deformation in the member. The stiffness criteria of any member can be determined as the slope of the secant which drawn in the load deflection curve at 0.75 of the ultimate load[52]. The stiffness criteria of the Vierendeel trusses are given in Table 4-6.

**Table 4-6: Stiffness criteria of the tested Vierendeel trusses**

| Vierendeel beam symbol | 0.75 Pu. (kN) | Deflection at 0.75 Pu. (mm) | Stiffness, K (kN/mm)* |
|---|---|---|---|
| VS0.4T60 | 28.5 | 3.14 | 9.08 |
| VC0.4T60 | 31.5 | 3.42 | 9.21 |
| VT0.4T60 | 25.5 | 2.27 | 11.23 |
| VS0.6T60 | 11.25 | 4.76 | 2.36 |
| VS0.2T60 | 39.75 | 2.63 | 15.11 |
| VS0T60 | 72 | 3.03 | 23.76 |
| VS0.4T40 | 15 | 2.96 | 5.07 |
| VS0.4T80 | 36.75 | 3.48 | 10.56 |

*Stiffness (K)=0.75Pu/0.75 Δu

### 4.4.5 Ductility Factor (μ)

Ductility is defined as its ability to sustain inelastic deformation without any losing of the load-carrying capacity up to failure. In other words, the ductility can be considered as the ratio between the deformations at ultimate stage to yield deformation. The deformation can be strains, curvatures, or deflections[53]. In this study, ductility index is taken as the ratio of the deflection at ultimate load to the yield deflection as presented in Figure 4-10, the notional yield displacement (Δy) is defined as the intersection of the two straight tangent lines associated with the load-displacement curves at the elastic and post elastic stages respectively.

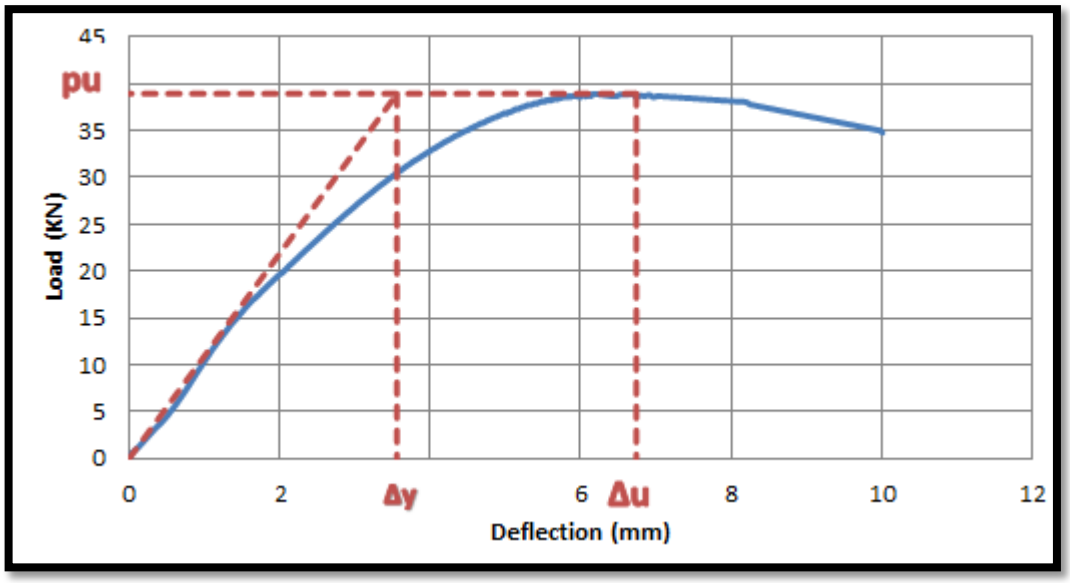


**Figure 4-10: Ductility calculation**

**Table 4-7: Ductility factor (μ) for the tested Vierendeel trusses.**

| Vierendeel truss symbol | Yield deflection Δy (mm) | Ultimate deflection Δu (mm) | Ductility (μ)* |
|---|---|---|---|
| VS0.4T60 | 4 | 6.74 | 1.69 |
| VC0.4T60 | 3.6 | 5.57 | 1.55 |
| VT0.4T60 | 2.93 | 4.51 | 1.54 |
| VS0.6T60 | 5.2 | 10.82 | 2.08 |
| VS0.2T60 | 3.09 | 4.65 | 1.5 |
| VS0T60 | 3.18 | 5.57 | 1.75 |
| VS0.4T40 | 3.4 | 6.62 | 1.95 |
| VS0.4T80 | 3.4 | 7.93 | 2.33 |

* Ductility index (μ) = Δu / Δy

# 5 CHAPTER FIVE: FINITE ELEMENT ANALYSIS

## 5.1 Introduction

Finite element analysis (FEA) is an effective and economic method to study the complex behavior of any construction members, especially for those having complicated non-linear structural behavior. ABAQUS is one of the most commonly used commercial finite element analysis software for understanding the structural mechanism and conducting parametric studies. In the current research, ABAQUS/CAE 2019 is used to simulate numerically the behavior of Vierendeel specimens using the practical parameters.

In this chapter, the validity of the FE model will be verified by comparing the numerical simulation results with the experimental ones for all specimens . The details of the developed FE model will be presented first, which includes the element types, the constitutive model, the mesh size, and the boundary conditions of each component.

## 5.2 Element Type and Material Properties

In order to model the real behavior of specimens, it is recommended that concrete be modeled with eight-nodded linear 3D brick solid element with reduced integration (C3D8R)[54] as shown in Figure 5-1. This element type provides reliable solution to most applications. Each 3D solid element has eight nodes with three degree of freedom per node. It can be used for both linear and complex non-linear analysis involving contact, plasticity, and large deformations. Similar to Vierendeel truss, the three-dimensional solid element (C3D8R) was chosen to model the steel plates in both loading and supporting positions.

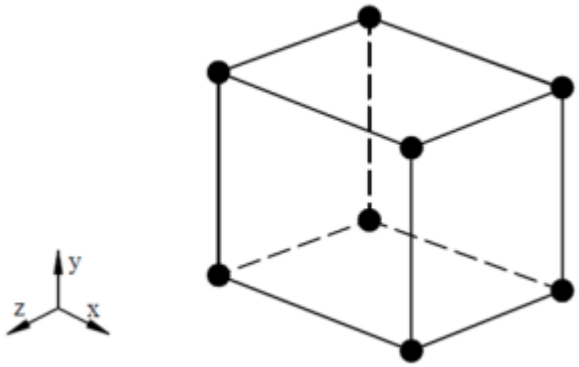


Figure 5-1: C3D8R element used in in ABAQUS[55].

Among the constitutive models for simulating the behavior of concrete, the concrete damaged plasticity model (CDP) that ABAQUS offers was chosen. Details of the CDP model, including the behavior and properties of the concrete and the other material used in this study are shown in Appendix (C).

## 5.3 Model Geometry and Boundary Conditions

3D simulations were performed to get an accurate approximation of the overall behavior and failure mode for SIFCON Vierendeel specimens. By considering symmetry of the specimens, only one quarter of the specimens was used for the simulations. Figure 5-2 gives a 3D view of the geometry of the FE model developed for the control truss. The X-axis is along the longitudinal direction of the truss, and the Y-Z plane represents the cross section of the truss.

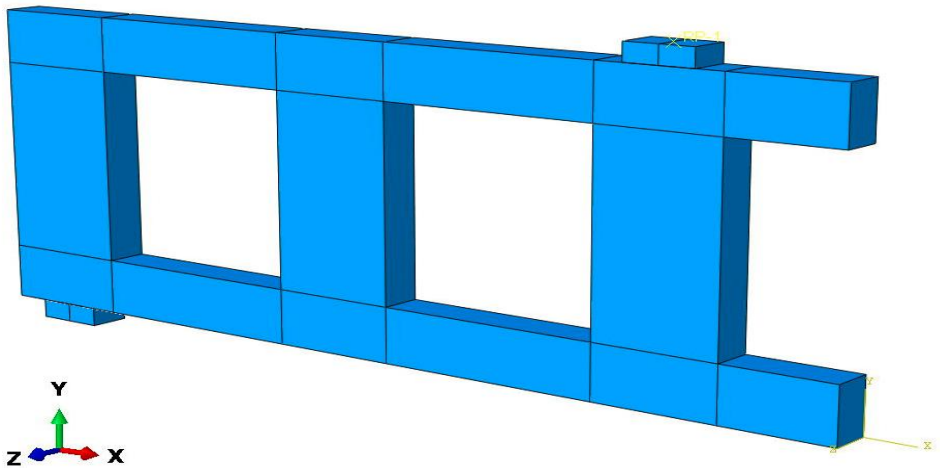


**Figure 5-2: 3D view of the Vierendeel truss FE model**

Steel plates in both loading and supporting positions are connected to the beam specimen using the ‘‘mechanical fraction ’’ option, with a frictional coefficient of 0.3[56].

As stated in Chapter 3 the specimen is simply supported, thus, in one of its ends the specimen has a hinge which constraints translations on x- and y-directions. Moreover, in the other end, a simple support restraining translation in the y-directions is imposed. The actual constraints are inserted along the width of the specimen on a line placed on the middle of the steel plates.

Since FE commercial software can be highly demanding in computational time, two symmetry planes are taken into consideration. The first one is placed in the center of the specimen along its width. For this symmetry plane a constraint along the x-axis is considered. Moreover, a second plane is considered along the length and here the translation along the z-axis is constrained.

The Vierendeel truss has been analyzed using static analysis in ABAQUS/Standard. Figure 5-3 gives details regarding the typical boundary conditions of the specimens used for the simulations.

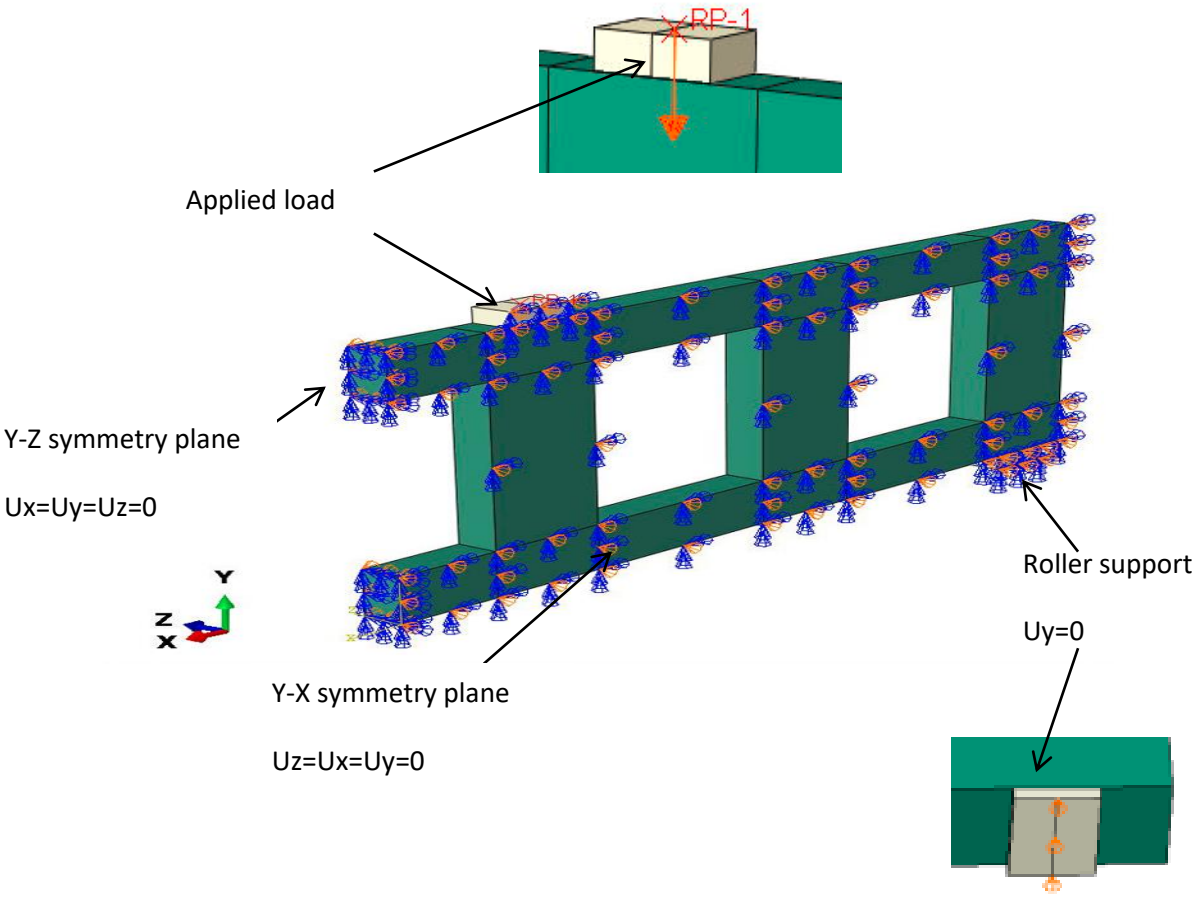


**Figure 5-3 : Typical applied load and boundary conditions of modeled trusses**

## 5.4 Meshing and Convergence Analysis

The main aim of the convergence study is to select the proper mesh size of the model with a minimum number of elements and maximum convergence with the results of the experimental test. This is practically achieved when the decreasing in the mesh size has a negligible effect on the results by using the reference truss (VS0.4T60) with the same material properties were modeled with a decrease in the element sides 12.5, 10, 7.5, 5, 2.5, and 1 mm. The mid-span deflection for the mentioned specimen with different mesh size was observed at the same applied load level of 20kN. As shown in Figure 5-4 convergence study, showed that the difference can be ignored when the mesh size increased from 7.5 mm to 1

mm, therefore; the 5 mm model is adopted for all tested specimens as shown in Figure 5-4.

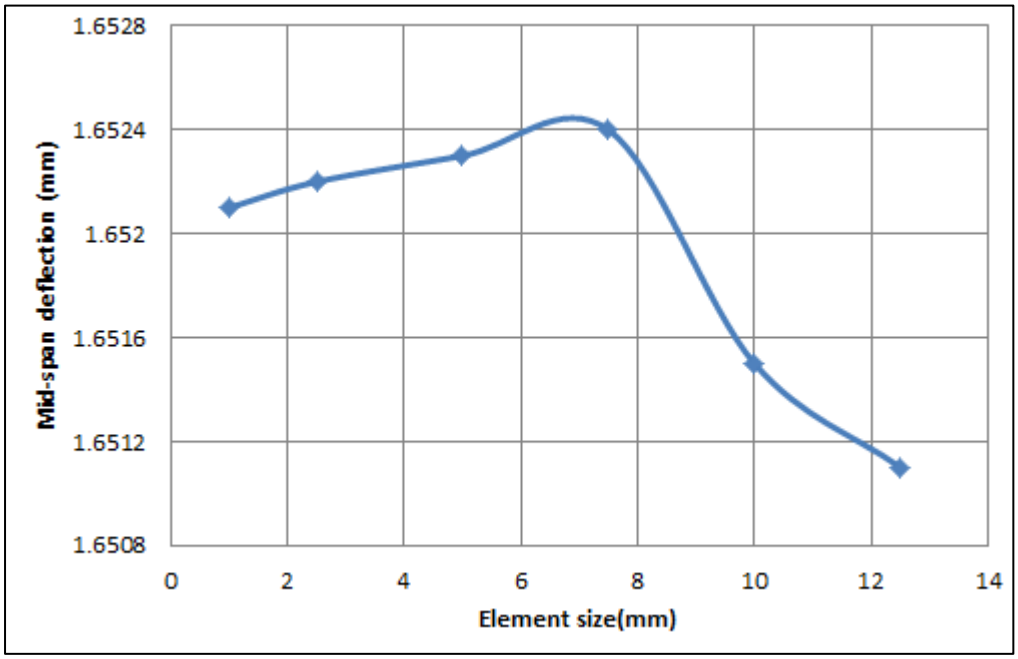


**Figure 5-4: The Results of Convergence Study.**

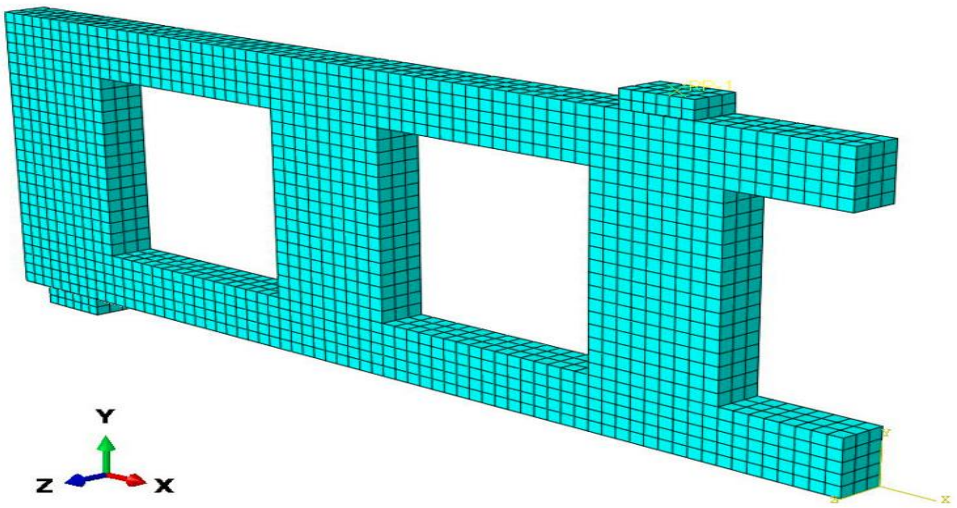


**Figure 5-5: Typical mesh applied for the specimens**

## 5.5 Finite Element Analysis Results and Discussion

The results of finite element analysis using the ABAQUS program were compared with the experimental results for all tested specimens. The validation of the numerical model was established based on this

comparison which includes load-deflection response, ultimate load-bearing capacity and cracking pattern. Table 5-1 includes numerical results, of ultimate load and ultimate deflection.

**Table 5-1: Experimental and Numerical Results for all specimens**

| Specimens | Ultimate load (KN) | | $\frac{P_{u)Num}-P_{u)EXP}}{P_{u)EXP}}$ % | Max. Deflection(mm) | | $\frac{\Delta_{u)Num}-\Delta_{u)EXP}}{\Delta_{u)EXP}}$ % |
|---|---|---|---|---|---|---|
| | $P_{u)EXP}$ | $P_{u)Num}$ | | $\Delta_{u)EXP}$ | $\Delta_{u)Num}$ | |
| **VS0.4T60** | 38 | 38 | 0 | 6.74 | 6.82 | 1.2 |
| **VC0.4T60** | 42 | 41 | -2 | 5.57 | 4.4 | -21 |
| **VT0.4T60** | 34 | 36 | 5.88 | 4.51 | 3.52 | -21.9 |
| **VS0.6T60** | 15 | 15 | 0 | 10.82 | 7.81 | -27.8 |
| **VS0.2T60** | 53 | 54 | 1.89 | 4.65 | 3.57 | -23.2 |
| **VS0T60** | 95 | 101 | 6.32 | 5.57 | 6.4 | 14.9 |
| **VS0.4T40** | 20 | 22 | 10 | 6.62 | 6.81 | 2.8 |
| **VS0.4T80** | 49 | 52 | 6.12 | 7.93 | 7.15 | -9.8 |
| **Average** | | | +3.5% | | | -10.6% |

## 5.5.1 Load - Deflection Response

The load-deflection relationship reflects the behavior of the studied members during the entire loading history. Therefore, it is an important indication of the validity of the FE model. The load–mid span deflection responses obtained from FEM were compared with the experimental results for all trusses, as shown in Figure 5-6 to Figure 5-13 respectively. The load–mid span deflection predicted by the FEM was generally convergent to the experimental data. However, it exhibited stiffer responses than the corresponding ones obtained from the experiments. There could be many reasons behind higher stiffness in FEM. The most important reasons are convergence criteria, gauss points and the development of micro cracks due

to dry shrinkage, concrete handling, environmental effects, in case of the experiments. FEM does not include such micro cracks in the simulations[57].

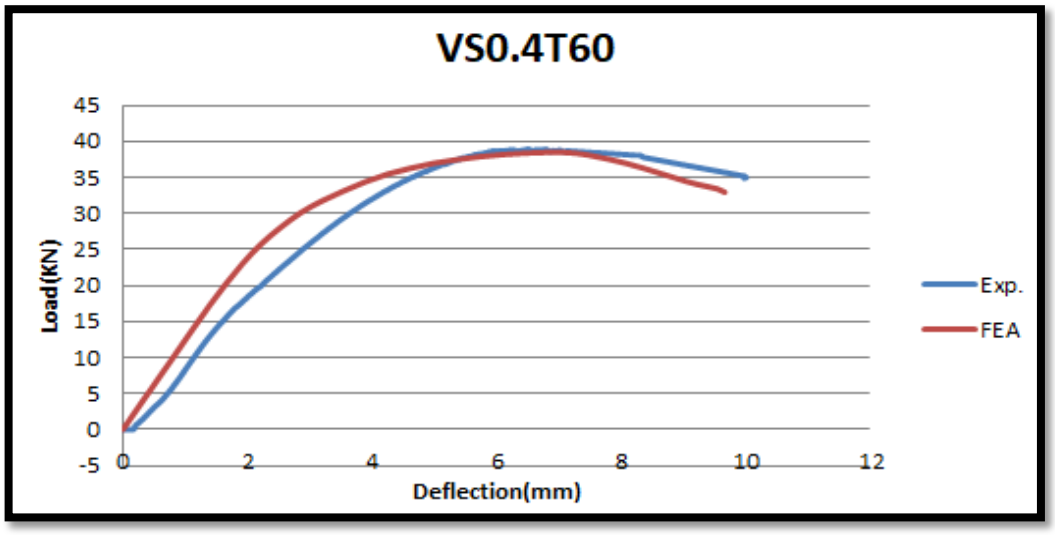


**Figure 5-6: Experimental and numerical load-mid span deflection curves for VS0.4T60**

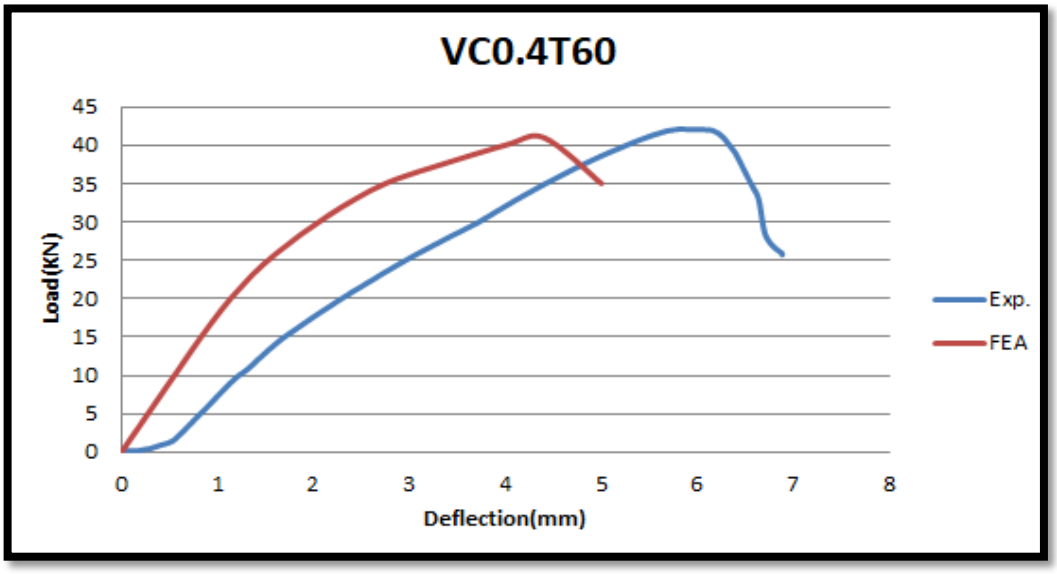


**Figure 5-7: Experimental and numerical load-mid span deflection curves for VC0.4T60**

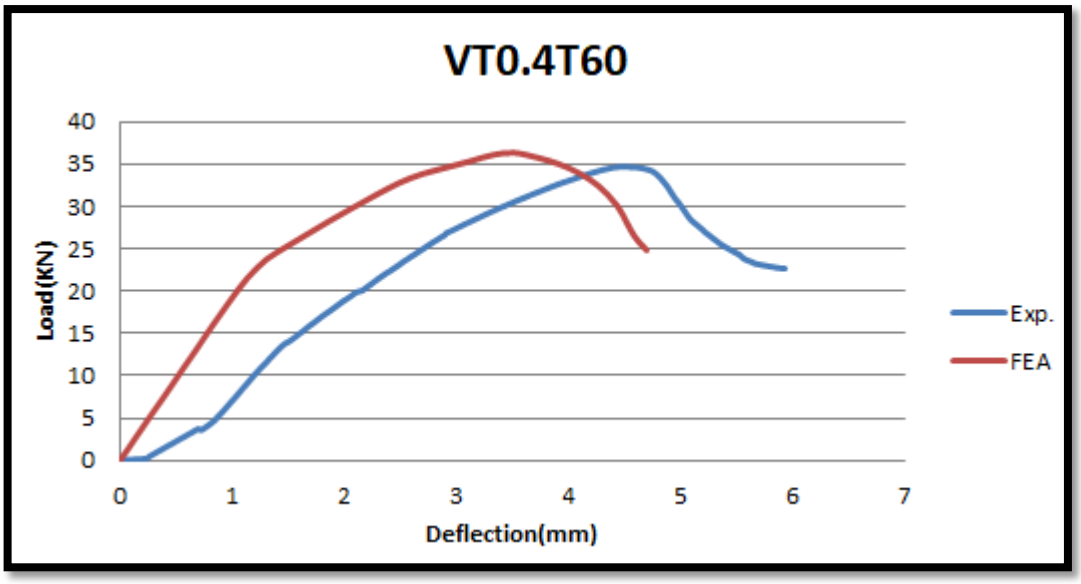


**Figure 5-8: Experimental and numerical load-mid span deflection curves for VT0.4T60**

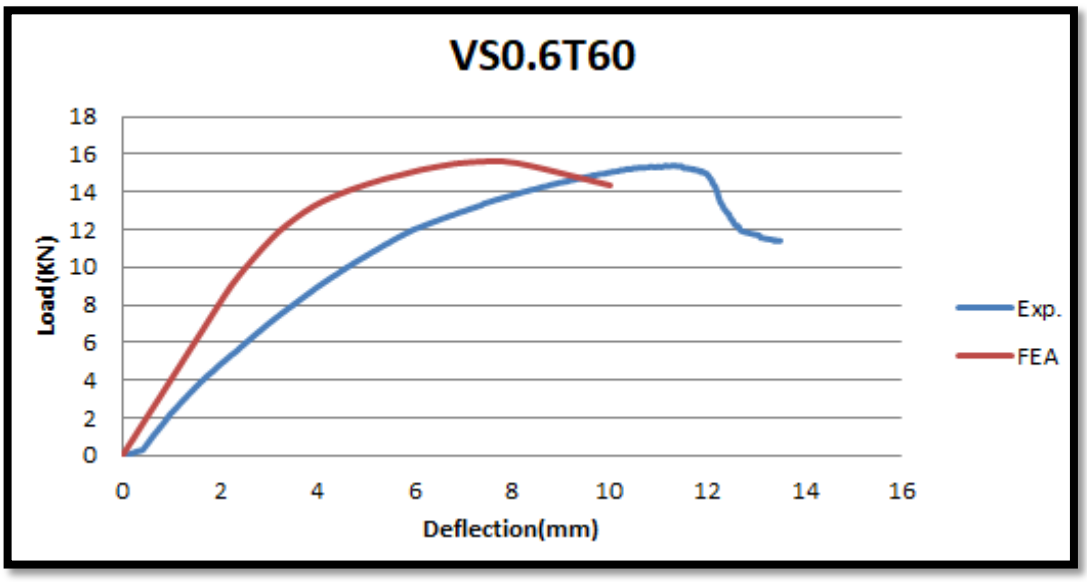


**Figure 5-9: Experimental and numerical load-mid span deflection curves for VS0.6T60**

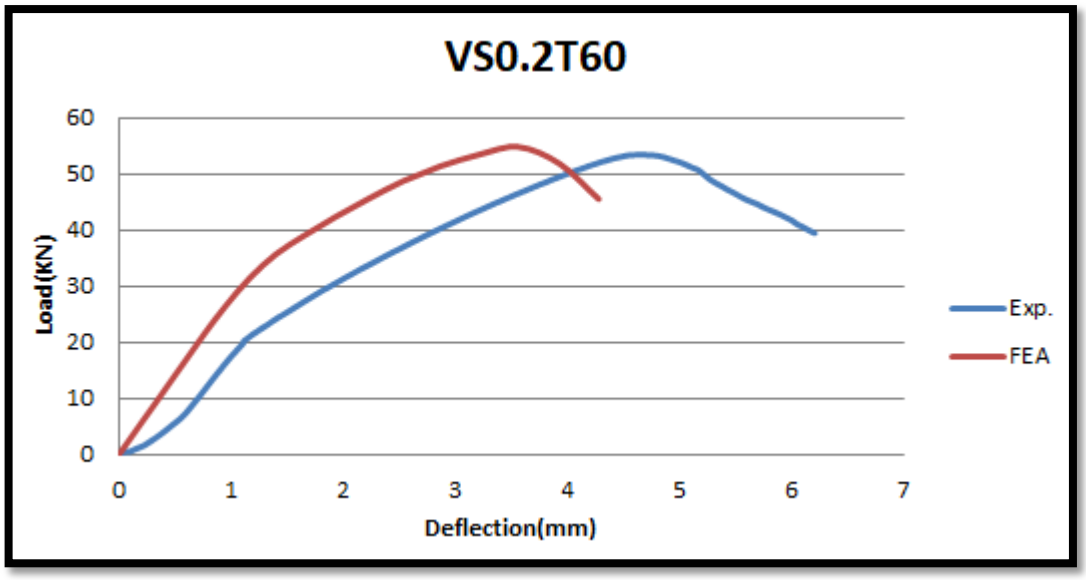


**Figure 5-10: Experimental and numerical load-mid span deflection curves for VS0.2T60**

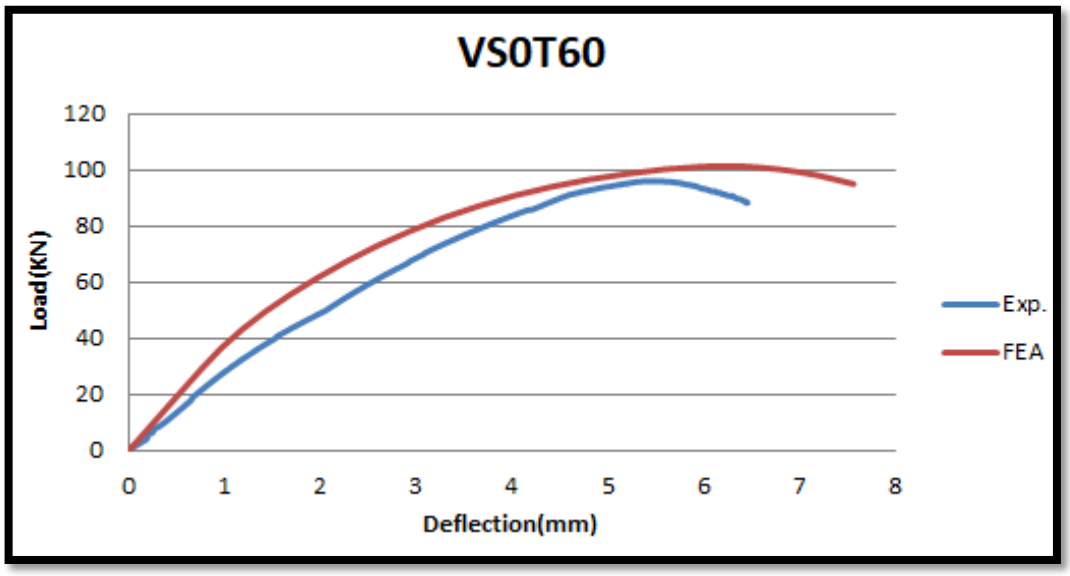


**Figure 5-11: Experimental and numerical load-mid span deflection curves for VS0T60**

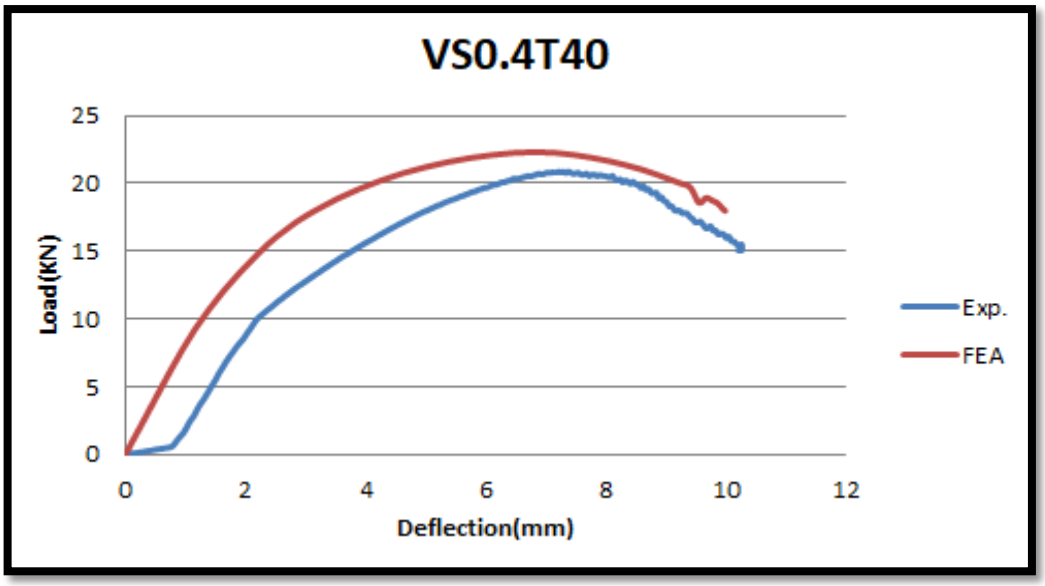


**Figure 5-12: Experimental and numerical load-mid span deflection curves for VS0.4T40**

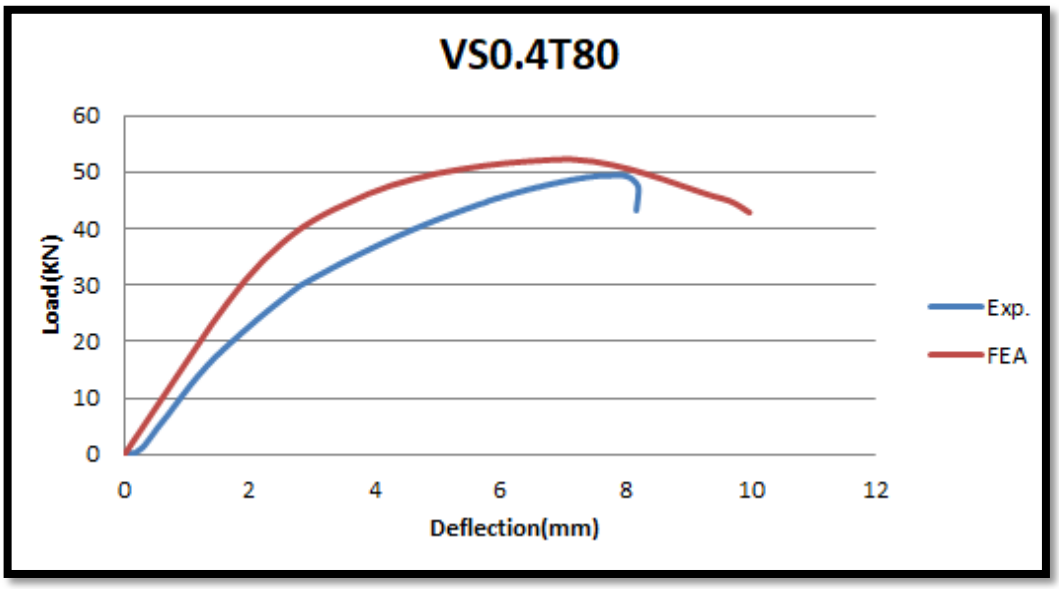


**Figure 5-13: Experimental and numerical load-mid span deflection curves for VS0.4T80**

## 5.5.2 Deflected Shape

As shown in Table 5-1 a comparison between the numerical and experimental mid span deflection at the ultimate load for all the specimens. The ultimate deflection values resulting from the FE analysis gave a

reasonable agreement with the experimental values. Figure 5-14 shows profile of the deflected shape for the tested trusses.

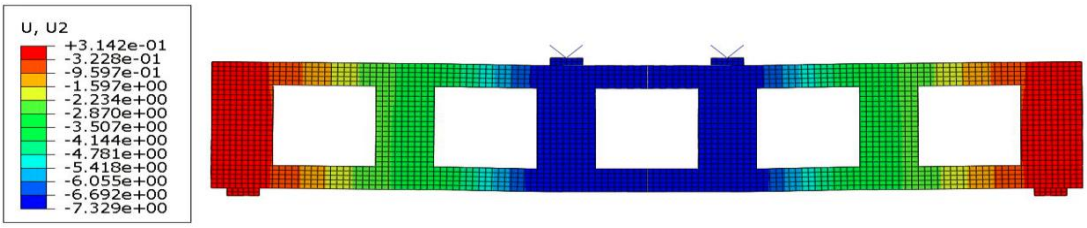


**VS0.4T60**

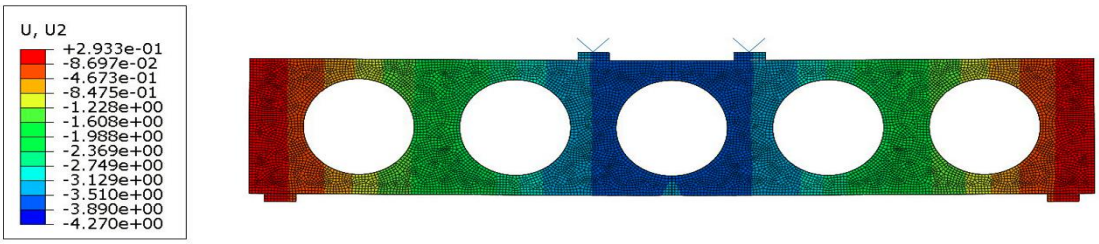


**VC0.4T60**

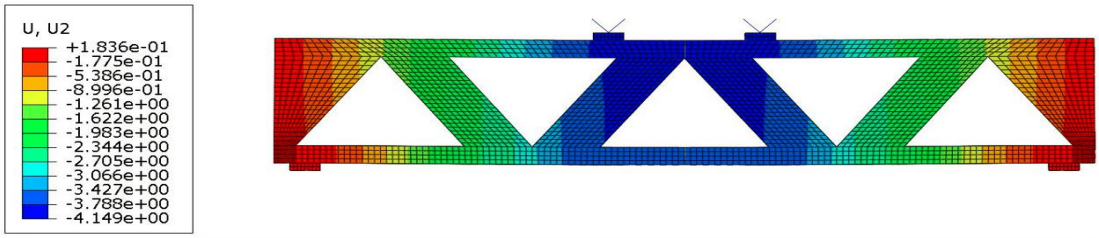


**VT0.4T60**

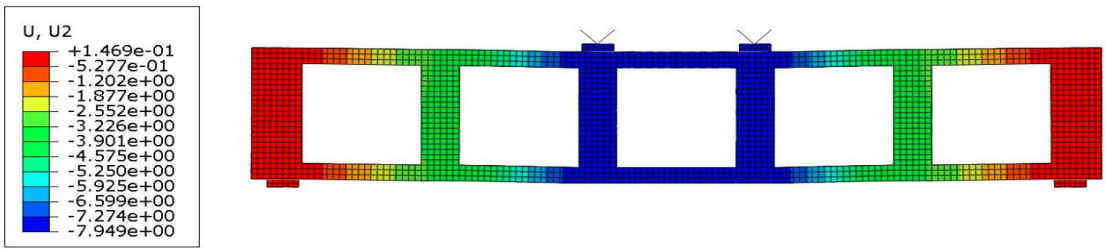


**VS0.6T60**

**Figure 5-14: Profile of deflected shape from ABAQUS program (in mm).**

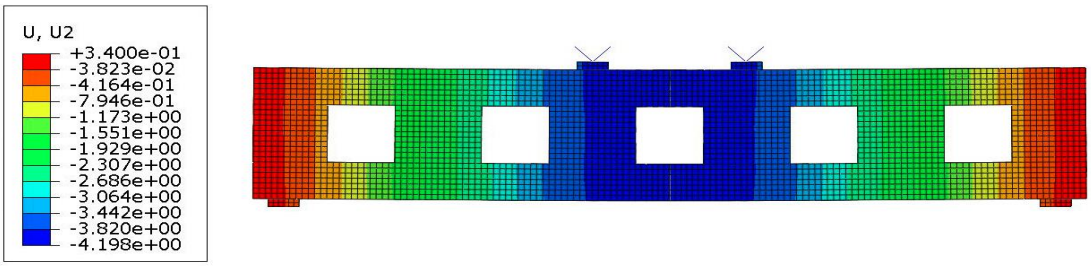


**VS0.2T60**

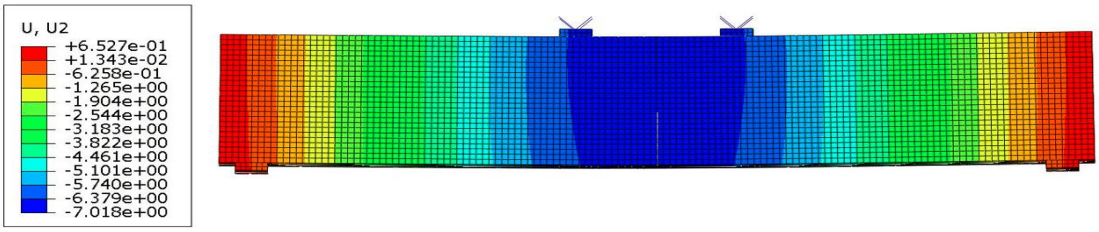


**VS0T60**

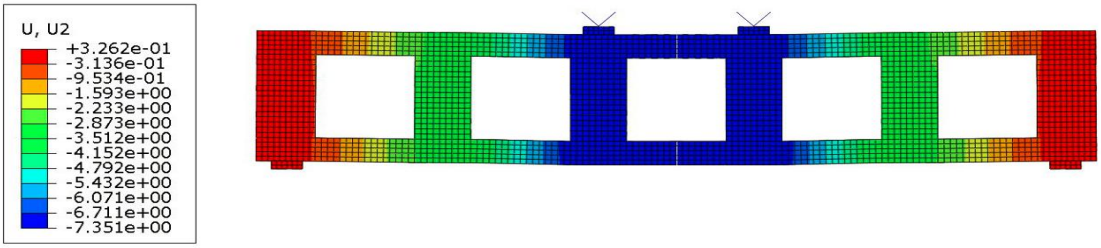


**VS0.4T40**

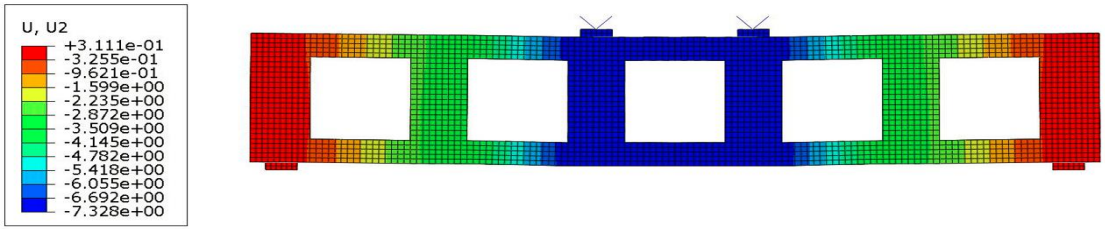


**VS0.4T80**

**Figure 5-14: continued**

## 5.5.3 Stress Behavior at Ultimate Load

Figure 5-15 shows the stress (σ max principal) distribution at ultimate load for the specimens. As shown in Figure, a portion from the compression area was cut off by the presence of the openings and leading to stresses concentrated at its sides. This is the main reason for the reduction in the ultimate load compared with the solid specimen.

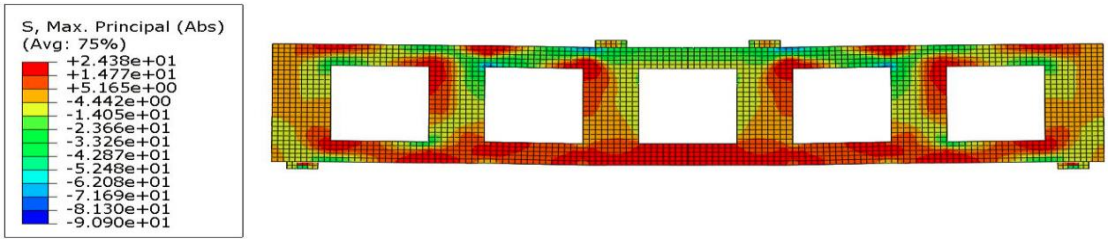


**VS0.4T60**

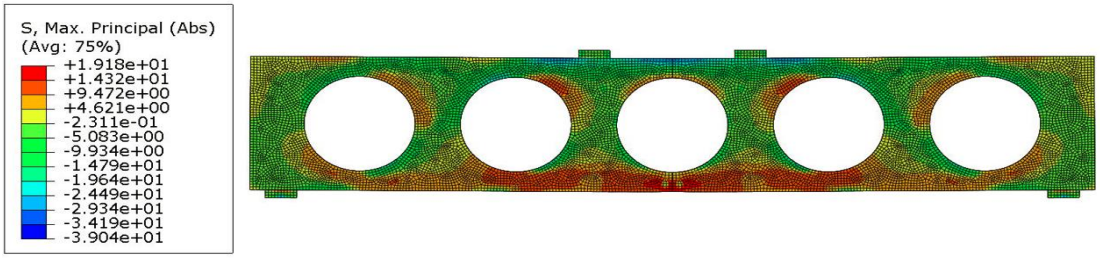


**VC0.4T60**

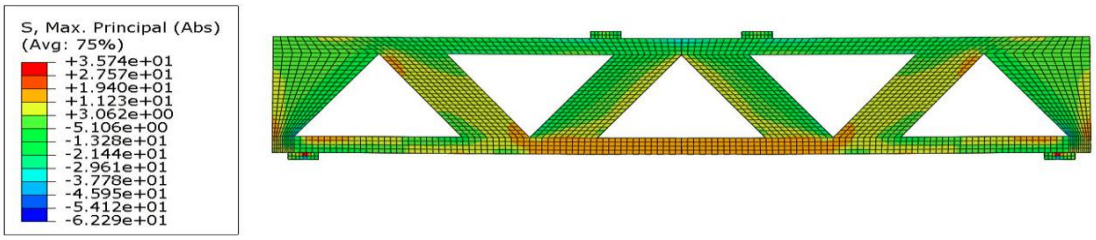


**VT0.4T60**

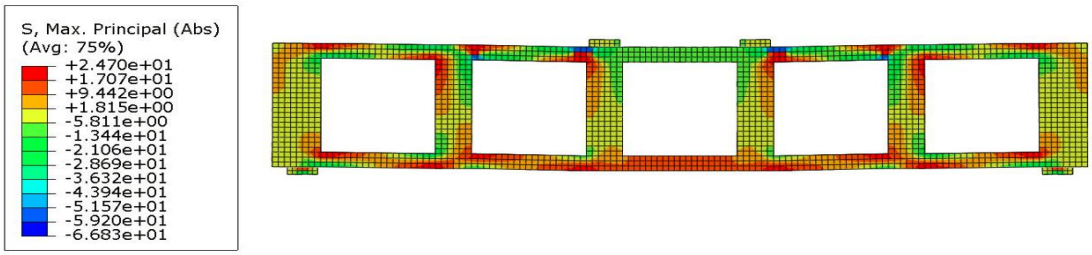


**VS0.6T60**

**Figure 5-15: Stresses (σ max principal) distribution of FEM at ultimate load (in MPa) .**

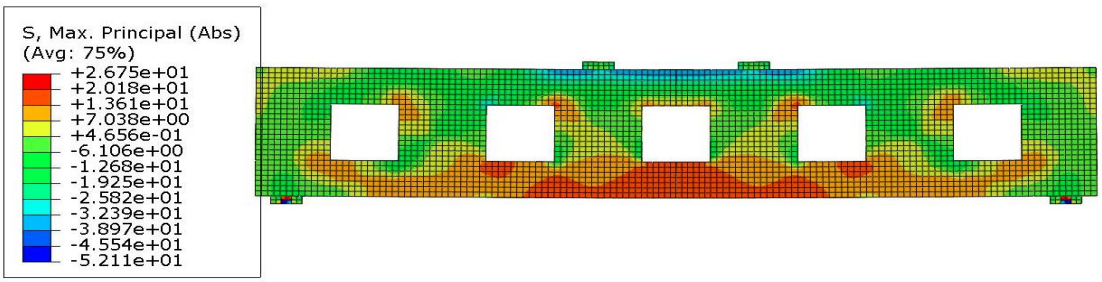


**VS0.2T60**

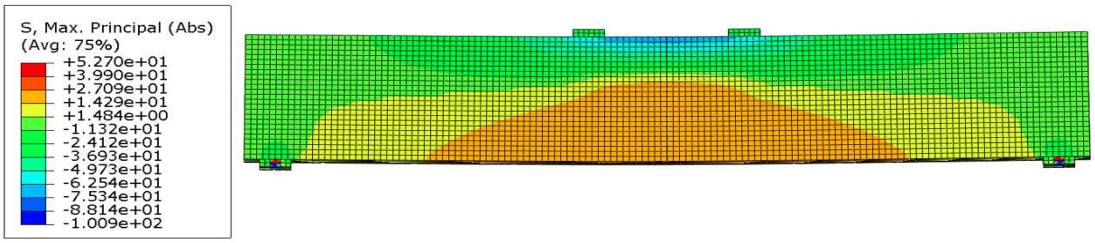


**VS0T60**

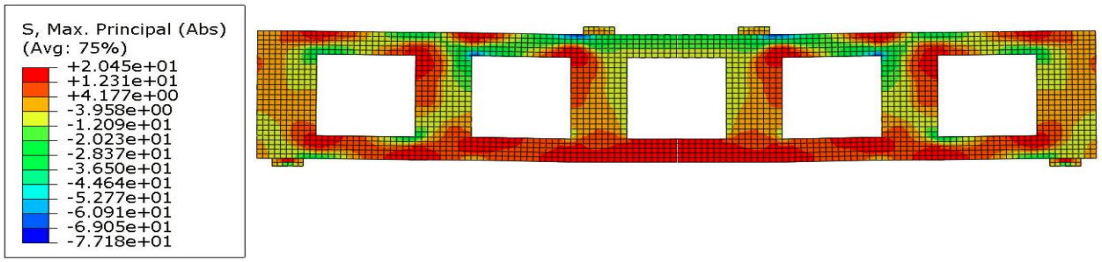


**VS0.4T40**

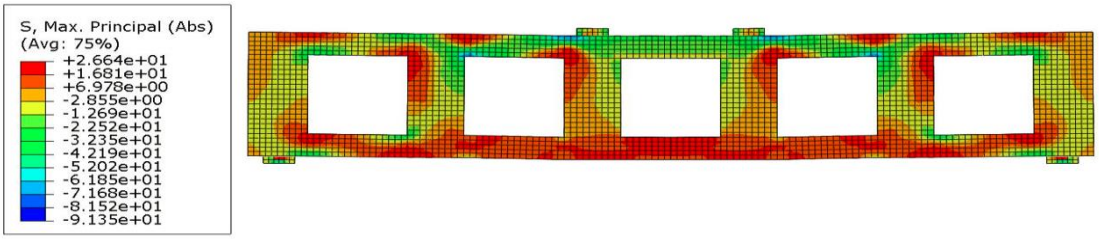


**VS0.4T80**

**Figure 5-15: continuous**

## 5.5.4 Crack Pattern and Modes of Failure

Crack patterns in concrete at failure stages of the tested specimens which obtained by ABAQUS can be shown in Figure 5-16 to Figure 5-23 . By comparing between them, it can be noticed that there is a match between experimental and theoretical results.

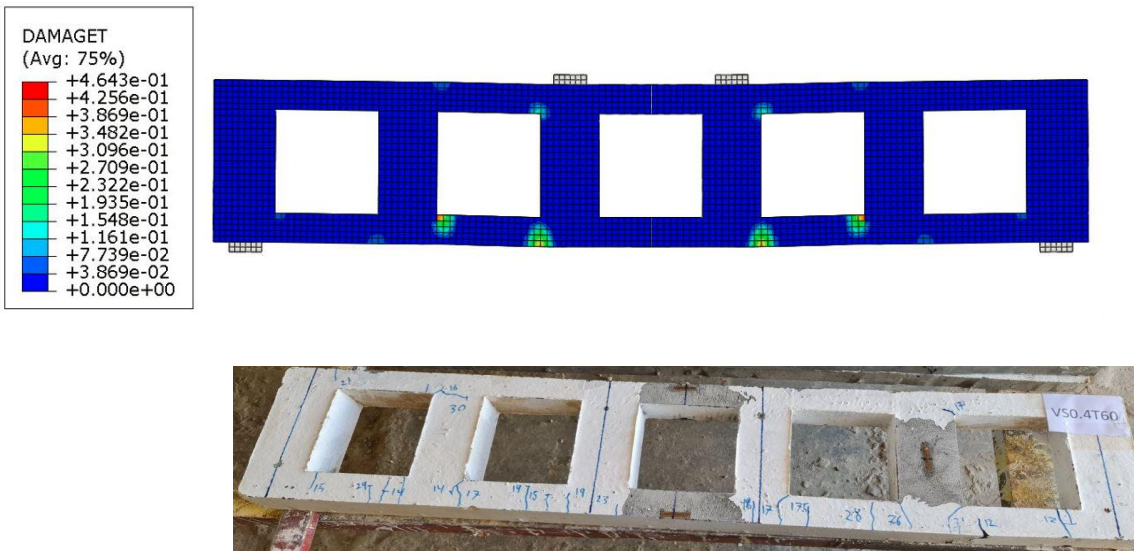


**Figure 5-16: Cracking patterns of FEM versus the experimental study for VS0.4T60**

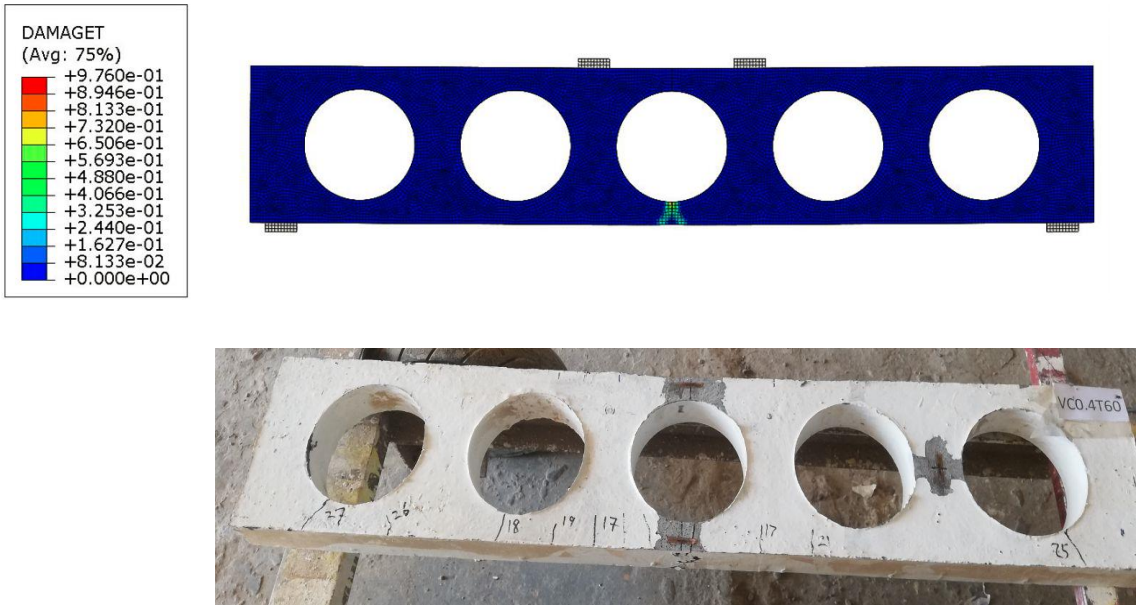


**Figure 5-17: Cracking patterns of FEM versus the experimental study for VC0.4T60**

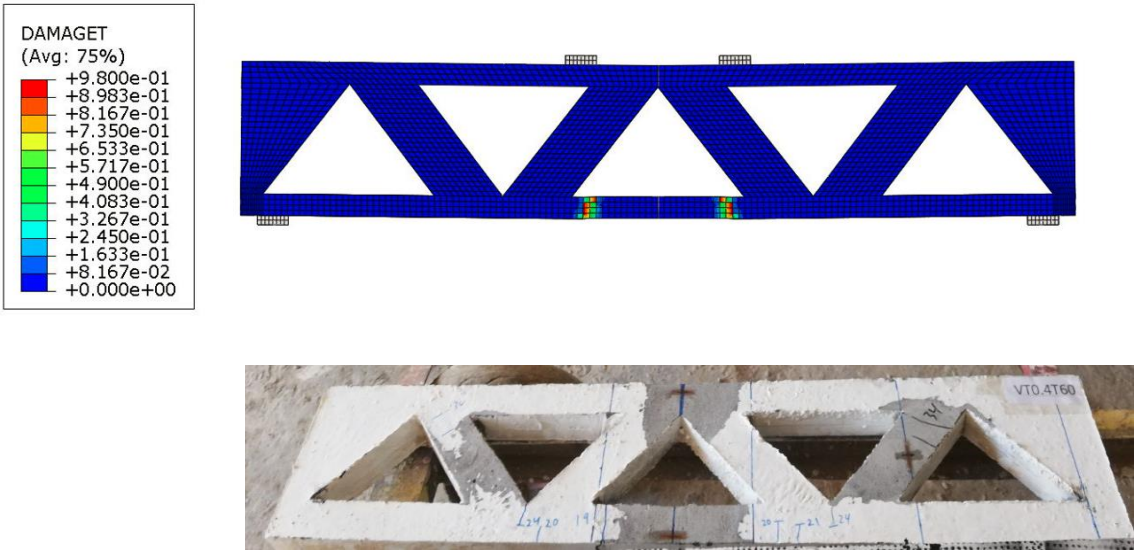


**Figure 5-18: Cracking patterns of FEM versus the experimental study for VT0.4T60**

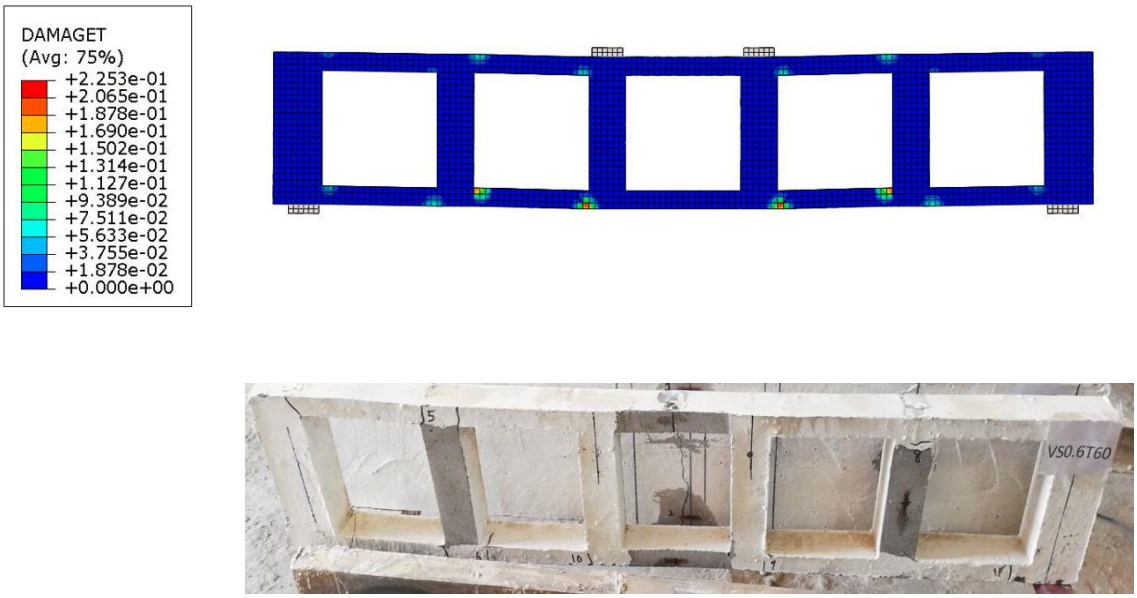


**Figure 5-19: Cracking patterns of FEM versus the experimental study for VS0.6T60**

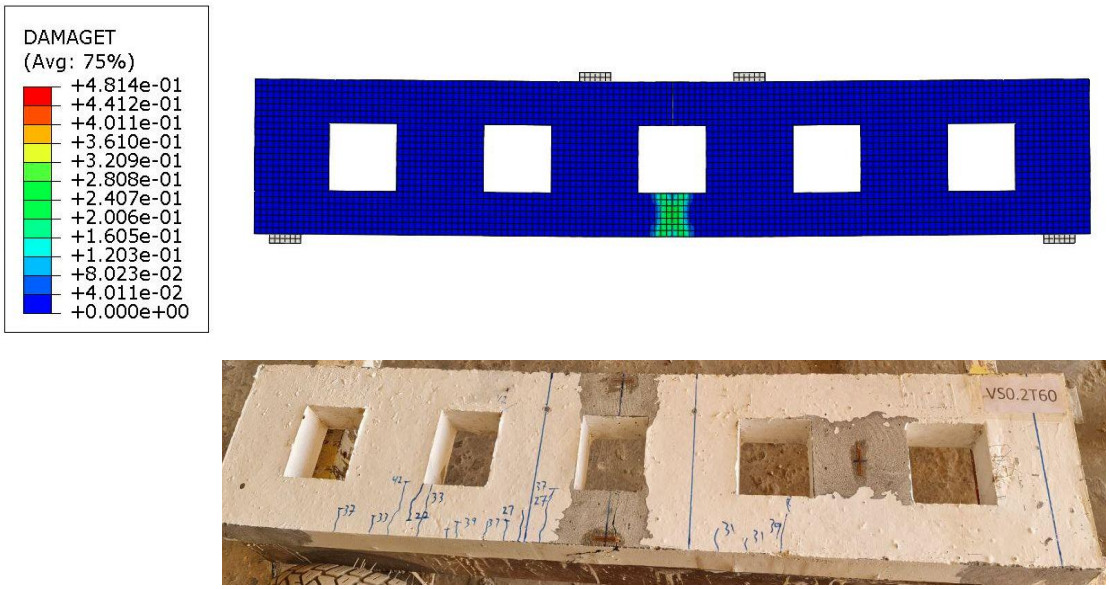


**Figure 5-20: Cracking patterns of FEM versus the experimental study for VS0.2T60**

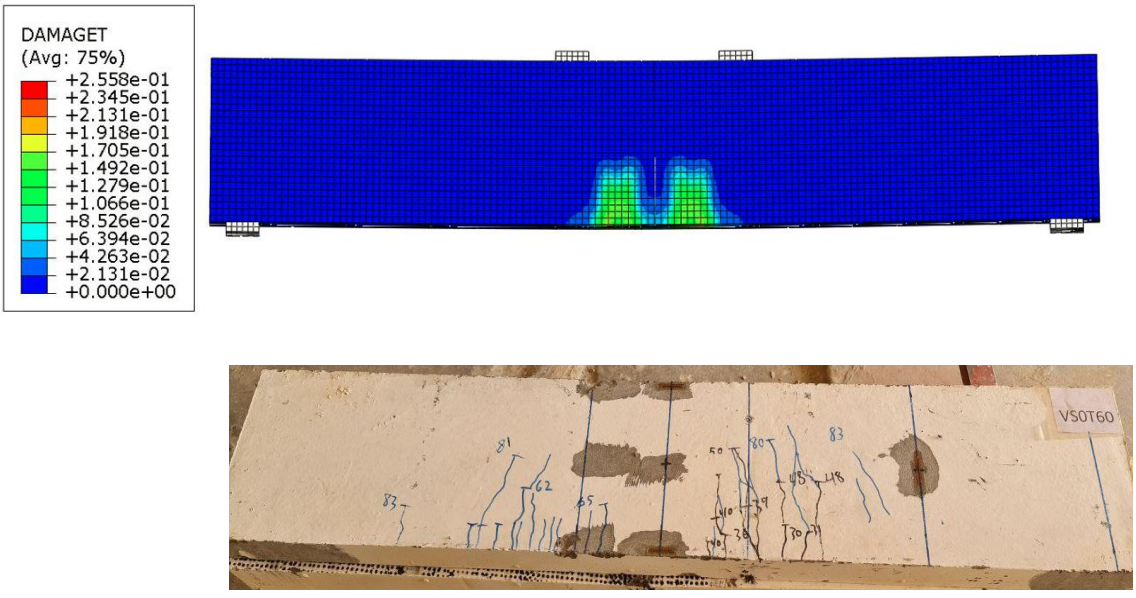


**Figure 5-21:Cracking patterns of FEM versus the experimental study for VS0T60**

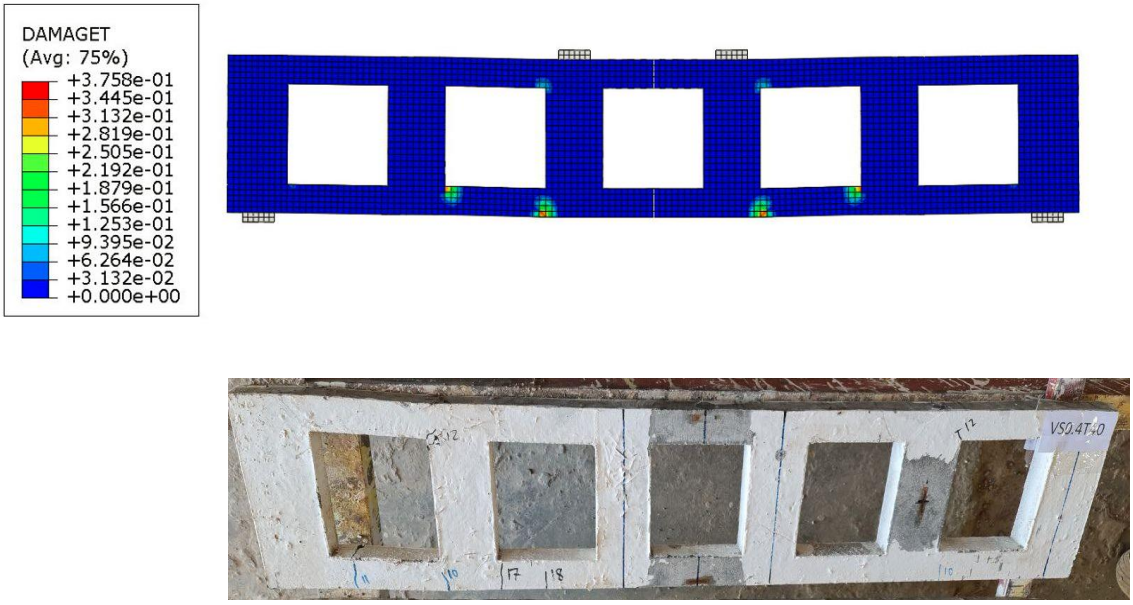


**Figure 5-22:Cracking patterns of FEM versus the experimental study for VS0.4T40**


**Figure 5-23:Cracking patterns of FEM versus the experimental study for VS0.4T80**

# 6 CHAPTER SIX: CONCLUSIONS AND RECOMMENDATIONS

## 6.1 Introduction

In this chapter, conclusions from the experimental and numerical results will be presented, also, some suggestions for future addition works will be offered.

## 6.2 Conclusions

### 6.2.1 The Experimental Work

1. With regard to trusses with square and triangular openings ,it was found that the cracks formed at the edges of the openings due to the high-stress concentration.
2. The strength of the specimen with circular openings higher than the strength of the other openings shapes because these openings haven't corners, It was observed that the ultimate load of the specimen with circular openings is higher than the ultimate load of the specimen with square openings by about 8% , while the ultimate load of the specimen with triangular openings decrease about 10.9% compared with the control specimen.
3. With regard to the opening size, the ultimate load of trusses decreases with increasing the void ratio. For specimen with void ratio 0.6, the reduction in the ultimate load is 60.5% from the ultimate load of the reference truss. While the increase in the ultimate load for solid specimen is 146.7 and 37.1% for specimen with void ratio 0.2.
4. With regard to the width, the results have shown that the ultimate load increases with the increase of width of the specimens, when the width increases to 80 mm, the increase in the ultimate load is about 27%, while when the width reduces to 40 mm, the reduction in the ultimate

load is about 46.4% compared with control specimen.

### 6.2.2 The Analytical Work

Based on the finite element analysis results of this thesis, it can be established that:

1. The constructed model by ABAQUS program predicts a good simulation for the real behavior of SIFCON Vierendeel trusses. The general response of load deflection curves, the ultimate load, and the mid span deflection of the studied specimens predicted by FEM were in good agreement with the experimental results. The average difference in results was about 3.5% increase in ultimate loads and a 10.6% decrease in the maximum deflection at ultimate loads.
2. The crack-propagation patterns obtained in FEM were quite similar to those recorded in the experimental study. On the other hand, the specimens failed with a failure mode similar to that recorded in the experimental test.
3. The presence of openings produces discontinuities or disturbances in the normal flow of stresses, thus leading to stress concentration and early cracking around the opening region.

## 6.3 Recommendations for Future Research

Based on the findings of this study, a number of suggestions for future research are listed below:

1. Studying the effect of dynamic and/or lateral load on the specimens.
2. Studying the behavior of the specimens when using different methods for strengthening like carbon fiber .
3. Investigating the behavior of the specimens under combined loading (torsion and bending ).

# References:

[1] D. J. Wickersheimer, "The Vierendeel," *Journal of the Society of Architectural Historians,* vol. 35, no. 1, pp. 54-60, 1976.

[2] N. K. Raju *Advanced Reinforced Concrete Design*, First Edition ed. CBS Publishers &distributers, 1986.

[3] J. M. Pons Poblet, "The vierendeel truss: past and present of an innovative typology," *Arquitetura revista,* vol. 15, no. 1, pp. 193-211, 2019.

[4] M. CARVALHO and G. LATORRACA, "João Filgueiras Lima Lelé: Arquitetos Brasileiros= Brazilian Architects," ed: Lisboa, Portugal: Editorial Blau, 2000.

[5] H. Yazıcı, S. Aydın, H. Yiğiter, M. Y. Yardımcı, and G. Alptuna, "Improvement on SIFCON performance by fiber orientation and high-volume mineral admixtures," *Journal of materials in civil engineering,* vol. 22, no. 11, pp. 1093-1101, 2010.

[6] M. A. A.-W. Ali, "Properties of slurry infiltrated fiber concrete (SIFCON)," Ph.D thesis, Building and Construction Engineering Department University of Technology, Baghdad, Iraq, 2018.

[7] M. Sonebi, L. Svermova, and P. J. Bartos, "Factorial design of cement slurries containing limestone powder for self-consolidating slurry-infiltrated fiber concrete," *Materials Journal,* vol. 101, no. 2, pp. 136-145, 2004.

[8] K. Azoom and R. M. R. Pannem, "Punching strength and impact resistance study of sifcon with different fibres," *International Journal of Civil Engineering and Technology,* vol. 8, no. 4, pp. 1123-1131, 2017.

[9] "Thamilselvi, P. (2012)." Behaviour of Exterior Beam Column Joints using SIFCON." International Journal of Engineering Research &

Thomas, A. A., & Mathews, J. (2014)." Strength and Behavior of Sifcon with Different Types of Fibers." International Journal of Civil Engineering and Technology (IJCIET)," vol. 5(12), 25-30.

[10] H. G. Alcan and A. F. Bingöl, "Examining SIFCON's mechanical behaviors according to different fiber and matrix phase," *Iranian Journal of Science and Technology, Transactions of Civil Engineering,* vol. 43, no. 3, pp. 501-507, 2019.

[11] M. Elavarasi, "KSR,"Performance of Slurry Infiltrated Fibrous Concrete (Sifcon) with Silica Fume."," *International Journal of Chemical Sciences,* vol. 14, no. 4, pp. 2710-2722, 2016.

[12] J. Newman, & Choo, B. S., *Advanced concrete technology* set. Elsevier, 2003.

[13] A. E. Naaman, "Engineered steel fibers with optimal properties for reinforcement of cement composites," *Journal of advanced concrete technology,* vol. 1, no. 3, pp. 241-252, 2003.

[14] N. Ganesan, P. Indira, and M. Sabeena, "Behaviour of hybrid fibre reinforced concrete beam–column joints under reverse cyclic loads," *Materials & Design (1980-2015),* vol. 54, pp. 686-693, 2014.

[15] F. Olutoge, O. Ofuyatan, O. Olowofoyeku, G. Bamigboye, and A. Busari, "Strength Properties of Slurry Infiltrated Fibrous Concrete (SIFCON) Produced with Discrete Bamboo and Steel Fibres," *ARPN Journal of Engineering and Applied Sciences,* vol. 11, no. 23, pp. 13448-13453, 2016.

[16] L.-K. Chen, "Analysis of Vierendeel Truss by Influence Moments," *Journal of the Structural Division,* vol. 88, no. 4, pp. 33-40, 1962.

[17] P. Varghese, T. Ganesan, and H. Achyutha, "Strength and behaviour of reinforced concrete vierendeel girders," *Building science,* vol. 7, no. 3, pp. 183-195, 1972.

[18] R. M. Korol, A. A. Shehata, and F. A. Mirza, "Inelastic finite element analysis of vierendeel trusses of rectangular hollow sections," in *Computational Methods and Experimental Measurements*: Springer, 1984, pp. 571-581.

[19] Y. Zhilin, "Shear Strength of the Lower Chord of the Reinforced Concrete and Prestressed Concrete Vierendeel Truss (Discussion on Shear Strength of Eccentrical Tension Members)," *Journal of Building Structures,* vol. 1, no. 02, p. 19, 1980.

[20] V. Paramasivam, "Vierendeel Frame Analysis: Slope-Shear Equations," *Journal of the Structural Division,* vol. 106, no. 11, pp. 2333-2339, 1980.

[21] N.A.H.Alwash, "Nonlinear behavior and optimal design of reinforced viereneel trusses," Ph.D. thesis, university of technology, 1995.

[22] I.R.shuber, "Analysis of vierendeel trusses with rigid ended vertical members " M.Sc.thesis, university of technology, 1996.

[23] K. S. Mahmod and A. W. Hameed, "Nonlinear analysis of reinforced fibrous concrete vierendeel truss," *J Eng*, vol. 14, 2008.

[24] Q. S. M. Shaker, H. H. Kamonna, and M. A. Attia, "NONLINEAR ANALYSIS OF REINFORCED CONCRETE VIERENDEEL TRUSSES," *Kufa Journal of Engineering*, vol. 4, no. 1, 2012.

[25] D. R. L. Kar, "Properties, applications: Slurry infiltrated fiber concrete (SIFCON)," *Concrete International*, vol. 6, no. 12, pp. 44-47, 1984.

[26] H. Yazıcı, H. Yiğiter, S. Aydın, and B. Baradan, "Autoclaved SIFCON with high volume Class C fly ash binder phase," *Cement and concrete research*, vol. 36, no. 3, pp. 481-486, 2006.

[27] Y. Wu, D. Oehlers, and M. Griffith, "Partial-interaction analysis of composite beam/column members," *Mechanics of Structures and Machines*, 2007.

[28] B. R. R. S. M. Jayashree, and S. M. Helen, "Flexural Behaviour of SIFCON Beams," *Int. J. Eng. Res. Technol*, vol. 2, pp. 1– 7, 2013, Art no. 2.

[29] M. A. A.-W. Ali, "Properties of slurry infiltrated fiber concrete (SIFCON)," Ph.D thesis, Building and Construction Engineering Department, University of Technology , Baghdad, Iraq, 2018.

[30] A. M. Gilani "Various Durability Aspect of Slurry Infiltrated Fiber Concrete " Ph.d Thesis, Middle East Technical University, 2007.

[31] D. R. Lankard, "Preparation, properties and applications of cement-based composites containing 5 to 20 percent steel fiber," pp. pp. 199–217,

A.(June 1985), 1985. in Steel Fibre Concrete US-Sweden joint seminar, Stockholm.

[32] V. Parameswaran, T. Krishnamoorthy, K. Balasubramanian, and S. Gangadar, "Studies on slurry-infiltrated fibrous concrete (SIFCON)," *Transportation research record*, no. 1382, 1993.

[33] S.-K. Kim and J.-H. Choi, "Compressive and tensile strength properties of slurry infiltrated fiber concrete," *Journal of the Korea Concrete Institute*, vol. 18, no. 5, pp. 703-708, 2006.

[34] M. Abdul Rahim, Z. M. Ghazaly, S. Ragunathan, and S. Shahidan, *The Behaviours Of Steel Fiber As Main Reinfocement In High Performance Slurry Infiltrated Fiber Reinforced Concrete*. Trans Tech Publ, 2014.

[35] R. Giridhar, P. Rama, and M. Rao, "Determination of mechanical properties of slurry infiltrated concrete (SIFCON)," *International Journal for Technological Research in Engineering*, vol. 2, no. 7, pp. 1366-1368, 2015.

[36] *Iraqi specification No. 5; "Portland Cement,"Baghdad,*. (1984).

[37] *Iraqi specification No. 45; "Natural Sources for Gravel that is Used in Concrete and Construction," Baghdad*, . (1984).

[38] *ASTM C1240-05, 2015. "Standard Specification for Silica Fume Used*

*in Cementitious Mixtures". ASTM C1240. ASTM International,*

*West Conshohocken, PA.*

[39] *ASTM C494 / C494M, 2017. "Standard Specification for Chemical*

*Admixtures for Concrete C494/C494M". ASTM International,*

*West Conshohocken, PA.*

[40] *EFNARC. (2005) ,"Specification and guidelines for self-compacting concrete" ,European Federation for Specialist Construction Chemicals and Concrete Systems, 1-32.*

[41] *EFNARC. (2005) ,"Specification and guidelines for self-compacting concrete" ,European Federation for Specialist Construction Chemicals and Concrete Systems, 1-32.*

[42] B. Kondraivendhan and B. Bhattacharjee, "Flow behavior and strength for fly ash blended cement paste and mortar," *International Journal of Sustainable Built Environment,* vol. 4, no. 2, pp. 270-277, 2015.

[43] *ASTM C39/C 39M-05; "Standard Test Method for Compressive Strength of Cylindrical Concrete Specimens," Annual Book of ASTM Standards, American Society for Testing and Materials, pp.1-7.*

[44] *BS 1881: Part 116; "Method for Determination of Compressive Strength of Concrete Cubes," British Standards Institution, 1989.*

[45] *ASTM C78-2002, "Standard Test Method for Flexural Strength of Concrete (Using Simple Beam with Third-Point Loading)". Annual Book of ASTM Standards.*

[46] *ASTM. (2017a). Standard Test Method for Splitting Tensile Strength of Cylindrical Concrete Specimens ASTM C496 / C496M. ASTM*

*International, West Conshohocken, PA.*

[47] S. A. Salih, Q. J. Frayyeh, and M. A. A.-w. Ali, "Flexural Behavior of Slurry Infiltrated Fiber Concrete (SIFCON) Containing Supplementary Cementitiouse Materials," *Journal of Engineering and Sustainable Development*, vol. 22, no. 2, pp. 35-48, 2018.

[48] S. S. Khamees, M. M. Kadhum, and A. A. Nameer, "Effects of steel fibers geometry on the mechanical properties of SIFCON concrete," *Civil Engineering Journal*, vol. 6, no. 1, pp. 21-33, 2020.

[49] A. K. R. T., " Behavior of hybrid fiber reinforced self-consolidating concrete incorporating nanoparticles

" M.Sc thesis, University of Technology, Baghdad, Iraq, 2015.

[50] S. M. D., "Properties Of Polypropylene Fiber Reinforced

High Performance Lightweight Aggregate Concrete " M.Sc thesis University of Technology, Baghdad, Iraq, 2015.

[51] *ASTM Designation C 496-96 "Standard specification for Splitting*

*tensile strength of cylindrical concrete specimens", Annual Book of*

*ASTM Standards, American Society for Testing and Material,*

*Philadelphia, Pennsylvania, section4, Vol. 4.02,* . (1996).

[52] K. Muthuswamy and G. Thirugnanam, "Structural behaviour of hybrid fibre reinforced concrete exterior Beam-Column joint subjected to cyclic loading," *International journal of civil and structural engineering*, vol. 4, no. 3, p. 262, 2014.

[53] R. Park, "Ductility evaluation from laboratory and analytical testing," in *Proceedings of the 9th world conference on earthquake engineering*, 1988, vol. 8: Tokyo-Kyoto Japan, pp. 605-616.

[54] S. Bahij, S. K. Adekunle, M. Al-Osta, S. Ahmad, S. U. Al-Dulaijan, and M. K. Rahman, "Numerical investigation of the shear behavior of reinforced ultra-high-performance concrete beams," *Structural Concrete,* vol. 19, no. 1, pp. 305-317, 2018.

[55] Y. Wu, "Shear strengthening of single web prestressed hollow core slabs using externally bonded FRP sheets," 2015.

[56] A. Jawdhari and I. Harik, "Finite element analysis of RC beams strengthened in flexure with CFRP rod panels," *Construction and Building Materials,* vol. 163, pp. 751-766, 2018.

[57] I. M. Metwally, "Nonlinear analysis of concrete deep beam reinforced with gfrp bars using finite element method," *Malaysian Journal of Civil Engineering,* vol. 26, no. 2, 2014.

# APPENDIX A
# TRAIL SPECIMEN

Characteristics of trail specimen:

- N.C.
- Reinforcement (150*150 mm) Ø6
- Solid (without openings).
- Width 40mm.
- No strain gauge used.
- First crack load=10 KN.
- Ultimate load=16 KN.

**Plate(A-1):** form-work of trail specimen

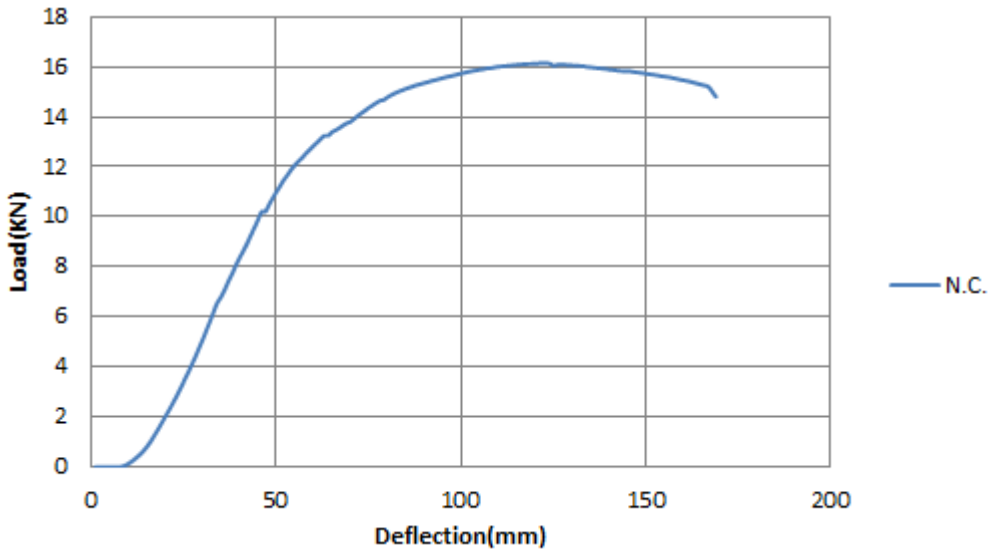


**Figure(A-1):** Load-Deflection curve for trial specimen

# APPENDIX-B
# MATERIAL DATASHEETS

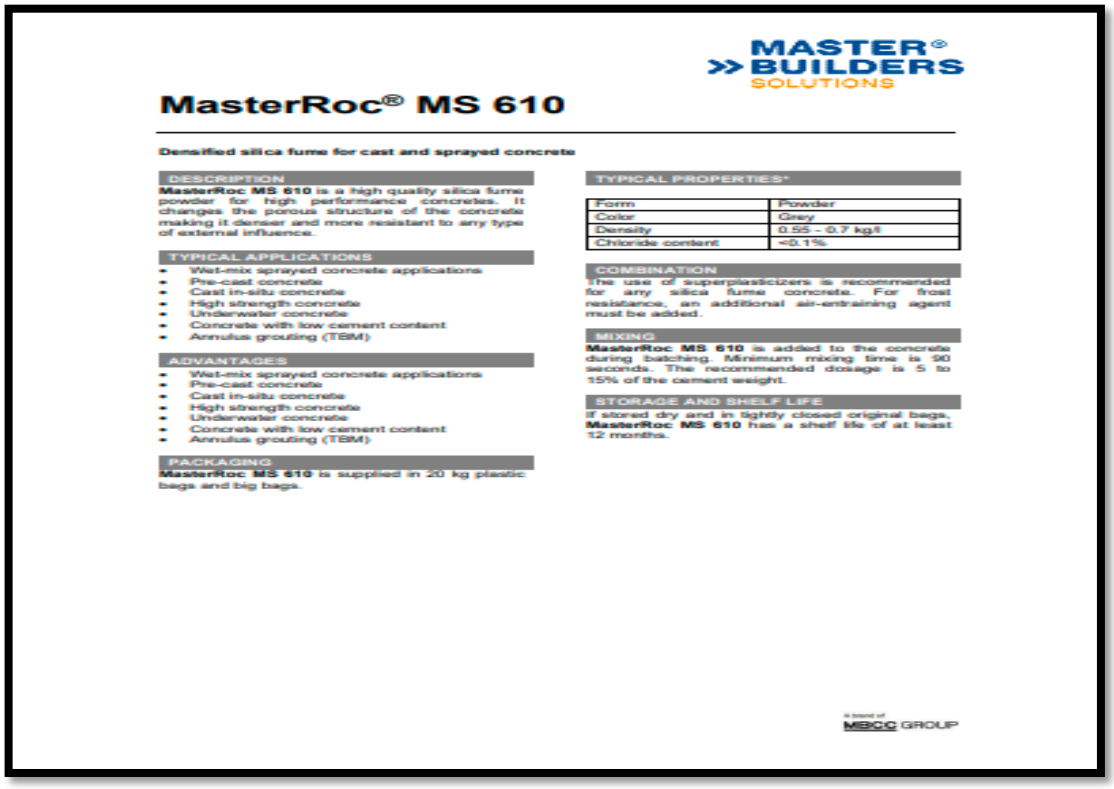

MASTER® BUILDERS SOLUTIONS

## MasterRoc® MS 610

**Densified silica fume for cast and sprayed concrete**

**DESCRIPTION**

**MasterRoc MS 610** is a high quality silica fume powder for high performance concretes. It changes the porous structure of the concrete making it denser and more resistant to any type of external influence.

**TYPICAL APPLICATIONS**

- Wet-mix sprayed concrete applications
- Pre-cast concrete
- Cast in-situ concrete
- High strength concrete
- Underwater concrete
- Concrete with low cement content
- Annulus grouting (TBM)

**ADVANTAGES**

- Wet-mix sprayed concrete applications
- Pre-cast concrete
- Cast in-situ concrete
- High strength concrete
- Underwater concrete
- Concrete with low cement content
- Annulus grouting (TBM)

**PACKAGING**

**MasterRoc MS 610** is supplied in 20 kg plastic bags and big bags.

**TYPICAL PROPERTIES***

| | |
|---|---|
| Form | Powder |
| Color | Grey |
| Density | 0.55 - 0.7 kg/l |
| Chloride content | <0.1% |

**COMBINATION**

The use of superplasticizers is recommended for any silica fume concrete. For frost resistance, an additional air-entraining agent must be added.

**MIXING**

**MasterRoc MS 610** is added to the concrete during batching. Minimum mixing time is 90 seconds. The recommended dosage is 5 to 15% of the cement weight.

**STORAGE AND SHELF LIFE**

If stored dry and in tightly closed original bags, **MasterRoc MS 610** has a shelf life of at least 12 months.

MBCC GROUP

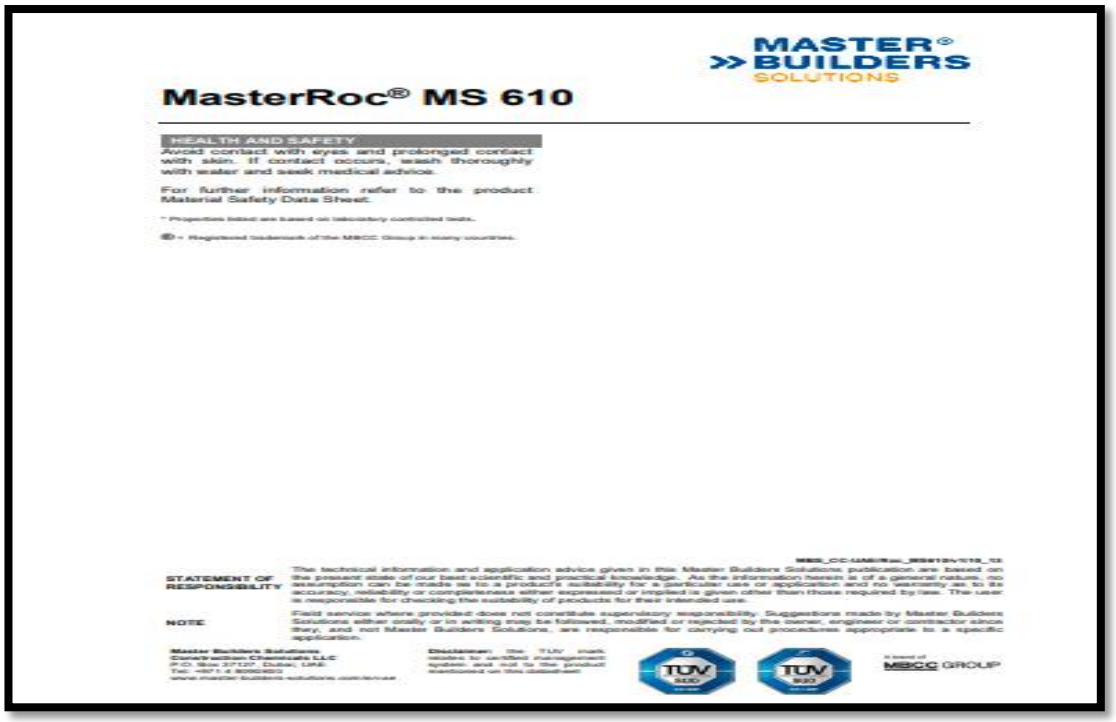

MASTER® BUILDERS SOLUTIONS

## MasterRoc® MS 610

**HEALTH AND SAFETY**

Avoid contact with eyes and prolonged contact with skin. If contact occurs, wash thoroughly with water and seek medical advice.

For further information refer to the product Material Safety Data Sheet.

* Properties listed are based on laboratory controlled tests.

® - Registered trademark of the MBCC Group in many countries.

**STATEMENT OF RESPONSIBILITY**

The technical information and application advice given in this Master Builders Solutions publication are based on the present state of our best scientific and practical knowledge. As the information herein is of a general nature, no assumption can be made as to a product's suitability for a particular use or application and no warranty as to its accuracy, reliability or completeness either expressed or implied is given other than those required by law. The user is responsible for checking the suitability of products for their intended use.

**NOTE**

Field service where provided does not constitute supervisory responsibility. Suggestions made by Master Builders Solutions either orally or in writing may be followed, modified or rejected by the owner, engineer or contractor since they, and not Master Builders Solutions, are responsible for carrying out procedures appropriate to a specific application.

**Master Builders Solutions Construction Chemicals LLC**
P.O. Box 37127, Dubai, UAE
Tel: +971 4 8090800
www.master-builders-solutions.com/en-ae

**Disclaimer:** the TUV mark relates to certified management system and not to the product mentioned on this datasheet

TÜV SÜD TÜV SÜD

MBCC GROUP

**B.1 Data sheet of silica fume provided by the manufacturer**

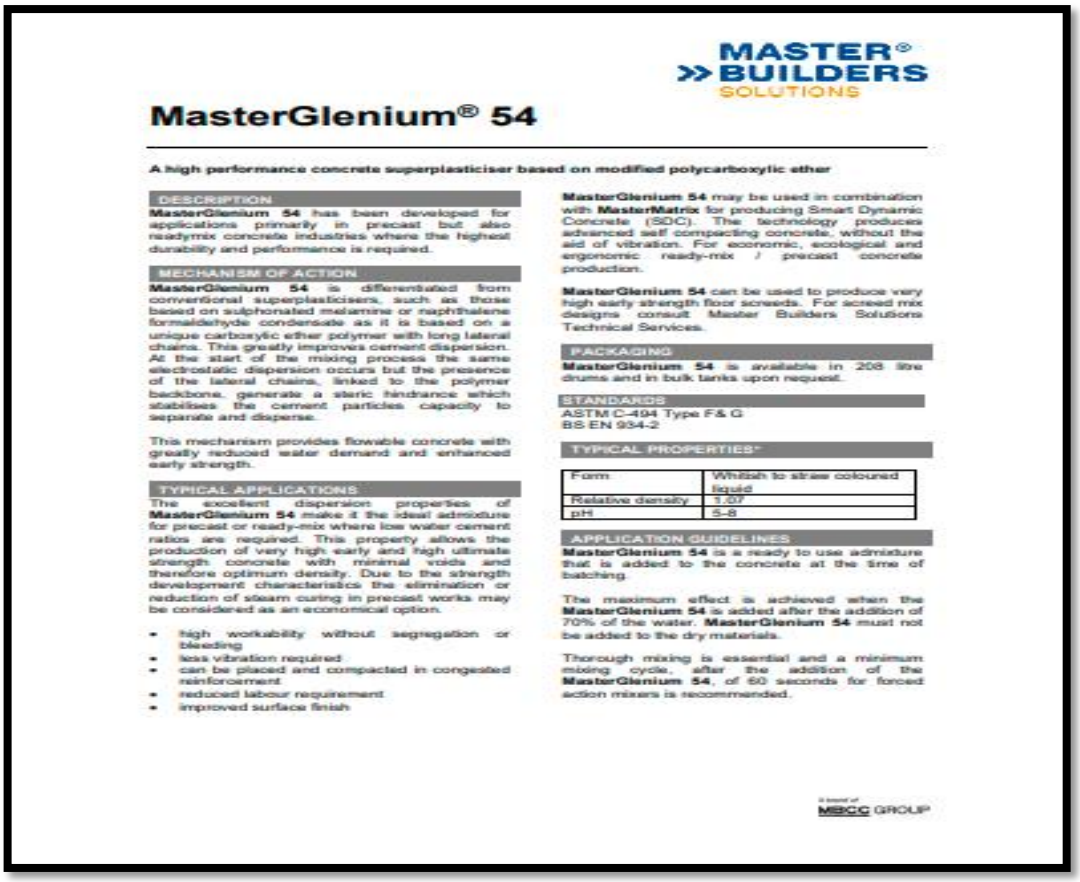

MASTER® BUILDERS SOLUTIONS

# MasterGlenium® 54

**A high performance concrete superplasticiser based on modified polycarboxylic ether**

## DESCRIPTION

**MasterGlenium 54** has been developed for applications primarily in precast but also readymix concrete industries where the highest durability and performance is required.

## MECHANISM OF ACTION

**MasterGlenium 54** is differentiated from conventional superplasticisers, such as those based on sulphonated melamine or naphthalene formaldehyde condensate as it is based on a unique carboxylic ether polymer with long lateral chains. This greatly improves cement dispersion. At the start of the mixing process the same electrostatic dispersion occurs but the presence of the lateral chains, linked to the polymer backbone, generate a steric hindrance which stabilises the cement particles capacity to separate and disperse.

This mechanism provides flowable concrete with greatly reduced water demand and enhanced early strength.

## TYPICAL APPLICATIONS

The excellent dispersion properties of **MasterGlenium 54** make it the ideal admixture for precast or ready-mix where low water cement ratios are required. This property allows the production of very high early and high ultimate strength concrete with minimal voids and therefore optimum density. Due to the strength development characteristics the elimination or reduction of steam curing in precast works may be considered as an economical option.

- high workability without segregation or bleeding
- less vibration required
- can be placed and compacted in congested reinforcement
- reduced labour requirement
- improved surface finish

**MasterGlenium 54** may be used in combination with **MasterMatrix** for producing Smart Dynamic Concrete (SDC). The technology produces advanced self compacting concrete, without the aid of vibration. For economic, ecological and ergonomic ready-mix / precast concrete production.

**MasterGlenium 54** can be used to produce very high early strength floor screeds. For screed mix designs consult Master Builders Solutions Technical Services.

## PACKAGING

**MasterGlenium 54** is available in 208 litre drums and in bulk tanks upon request.

## STANDARDS

ASTM C-494 Type F& G
BS EN 934-2

## TYPICAL PROPERTIES*

| | |
|---|---|
| Form | Whitish to straw coloured liquid |
| Relative density | 1.07 |
| pH | 5-8 |

## APPLICATION GUIDELINES

**MasterGlenium 54** is a ready to use admixture that is added to the concrete at the time of batching.

The maximum effect is achieved when the **MasterGlenium 54** is added after the addition of 70% of the water. **MasterGlenium 54** must not be added to the dry materials.

Thorough mixing is essential and a minimum mixing cycle, after the addition of the **MasterGlenium 54**, of 60 seconds for forced action mixers is recommended.

a brand of MBCC GROUP

MASTER® BUILDERS SOLUTIONS

# MasterGlenium® 54

## DOSAGE

The normal dosage for **MasterGlenium 54** is between 0.50 and 1.75 litres per 100kg of cement (cementitious material). Dosages outside this range are permissible subject to trial mixes.

## COMPATIBILITY

**MasterGlenium 54** is not compatible with **MasterRheobuild** superplasticizers.
**MasterGlenium 54** is suitable for mixes containing all types of Portland cement and cementious materials as follows:

- microsilica
- fly ash (PFA)
- ground granulated blast furnace slag GGBS

## EFFECT ON HARDENED CONCRETE

- increased early and ultimate compressive strengths
- increased flexural strength
- better resistance to carbonation
- lower permeability
- better resistance to aggressive atmospheric conditions
- reduced shrinkage and creep
- increased durability

## STORAGE AND SHELF LIFE

**MasterGlenium 54** should be stored above 5°C in closed containers or storage tanks to protect from evaporation and extreme temperatures. The shelf life is 12 months when stored as above.

The occurrence of a surface layer with **MasterGlenium 54** is normal and will have no effect on the performance of the product.

## HEALTH AND SAFETY

**MasterGlenium 54** contains no hazardous substances requiring labelling. For further information refer to the Material Safety Data Sheet.

## QUALITY AND CARE

All products originating from Master Builders Solutions Dubai, UAE facility are manufactured under a management system independently certified to conform to the requirements of the quality, environmental and occupational health & safety standards ISO 9001 and ISO 14001.

* Properties listed are based on laboratory controlled tests.

® = Registered Trademark of The MBCC Group in many countries.



**B.2 Data sheet of super plasticizer provided by the manufacturer**

# APPENDIX C
# C MODELLING OF MATERIAL PROPERTIES IN FINITE ELEMENT ANALYSIS

## C.1 Introduction

There are three material models for analyzing concrete in ABAQUS: (1) Smeared crack concrete model, (2) Brittle crack concrete model, and (3) Concrete damaged plasticity model. Out of the three concrete models, the concrete damaged plasticity model is selected in the present study. Details of the CDP model used in ABAQUS, including the behavior and properties of the concrete and the other material used in this study are described below.

## C.2 Concrete Damaged Plasticity in ABAQUS

Concrete damaged plasticity is capable of modeling all structural types of reinforced or unreinforced concrete or other quasi-brittle materials subjected to monotonic, cyclic, or dynamic loads. This model is based on a coupled damage plasticity theory and the multi-axial behavior of concrete in damaged plasticity model governs by a yield surface, which proposed by (Lubliner et al.) [58]. Tensile cracking and compressive crushing of concrete are two assumed main failure mechanisms in this model. Furthermore, the degradation of material for both tension and compression behavior have been considered in this model. Degradation of concrete in cyclic and dynamic loadings is taken into account by defining two scalar parameters; tensile damage parameter (dt) and compressive damage parameter (dc).

## C.2.1 Uniaxial Behavior of Concrete

### C.2.1 .1 Stress Strain Curve of SIFCON in Compression

The following model developed by ( Homrich and Naaman) [59]was successfully used in obtaining the behavior of SIFCON in direct uniaxial compression.

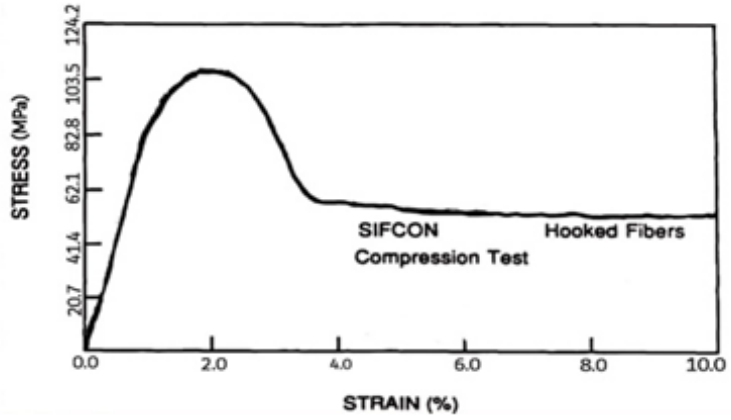


Figure C.1: Stress Strain Curve for Compression[59]

- **Ascending Branch**

To model the ascending branch of SIFCON's stress-strain compression curve, an equation of following form was used:

$$f = f_\circ \left[1 - \left(1 - \frac{\varepsilon}{\varepsilon_\circ}\right)^A\right]$$

Where:

f = compressive stress (MPa)

$f_\circ$ = maximum compressive stress (MPa)

$\varepsilon$ = strain

$\varepsilon_\circ$ = strain at maximum stress

$A = E\,\varepsilon_\circ / f_\circ$

E, the initial tangent modulus, may be calculated from the law of mixtures:

$E = \gamma_1 V_f E_{fibers} + (1 - V_f) E_{slurry}$

$V_f$ = volume fraction of fibers

$\gamma_1$= factor generally assumed equal to 1 for compressive loading

$E_{fibers}$= 206842 MPa

$E_{slurry}$= 6894 MPa

the strain at peak stress, $\varepsilon_\circ$,can be determined:

$\varepsilon_\circ = \varepsilon_{initial} + K_1 V_f l / \emptyset$

Where:

$\varepsilon_{initial}$ =0.005

$K_1$=0.00138

$l$ = fiber length(mm)

$\emptyset$ = fiber diameter(mm)

- **Descending Branch**

To model the descending branch of SIFCON's stress-strain compression curve, an equation of following form was used:

$f = (f_\circ - f_{pl}) Exp[-b(\varepsilon - \varepsilon_\circ)^m] + f_{pl}$

$m = [1 + \ln[\frac{f_i - f_{pl}}{f_\circ - f_{pl}}]^{-1}$

$$b = [\frac{m-1}{m}](\varepsilon_i - \varepsilon_\circ)^{-m}$$

$f_{pl}$ =post peak plateau stress (MPa)

$f_\circ$ = peak stress (MPa)

$f_i$ =stress at post peak inflection point (MPa)

$\varepsilon_\circ$ =strain at peak stress

$\varepsilon_i$ =strain at post peak inflection point

b, m= controlling parameters to be determined

$$f_{pl} = V_f l/\emptyset(K_{31} + K_{32}\sqrt{f_\circ})$$

$K_{31}$=1.38 MPa for hooked fibers

$K_{32}$=0.055 MPa for all types of fiber

### C.2.1 .2 Stress-Displacement Curve of SIFCON in Tension

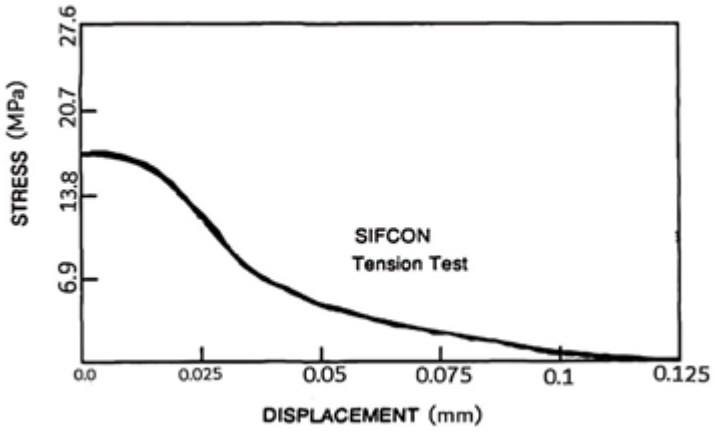


Figure C.2: Stress Displacement Curve for Tension[59]

$$f = f_{\circ t}[\mathrm{Exp}(-b(\delta)^m) - c(\delta)]$$

$$c = 2\mathrm{Exp}\left[-b\left(\frac{l}{2}\right)^m\right]/l$$

$$b = \frac{m-1}{[m(\delta_{it})^m]}$$

$$m = \frac{1}{1+ln\left[\frac{f_{it}}{f_{\circ t}}+c\delta_{it}\right]}$$

Where:

f= tensile stress(MPa)

$f_{\circ t}$= maximum tensile stress= $f_{pl}/3$(MPa)

$f_{it}$ =tensile stress at inflection point = $0.6f_{\circ t}$(MPa)

$\delta$= tensile crack displacement (mm)

$\delta_{it}$=crack displacement at inflection point =$0.01V_f\, l^2/\emptyset$ (mm)

### C.2.2 Concrete Damaged Plasticity Parameters in Triaxial Loading State

In order to describe strength with the equation for triaxial stress as input to the finite element program ABAQUS, a set of five parameters are required to completely describe the plastic behavior of concrete;

Ψ, Dilation angle: The angle of inclination of the failure surface toward the hydrostatic axis, measured in the meridional plane. Physically, dilation angle Ψ is interpreted as a concrete internal friction angle. Maximum value of it equal ($56.3^o$) and minimum value is close to (zero)[60]. Through many trials of geometry with the aim of achieving proper failure to be compatible with the observed experimental failure mechanism, the value of dilation angle was taken as ($40^o$) for all specimens.

ϵ: Plastic potential eccentricity, it is a small positive value which expresses the rate of approach of the plastic potential hyperbola to its asymptote. It

can be calculated as a ratio of tensile strength to compressive strength. It is recommended to assume $\epsilon = 0.1$ in the CDP model [60] .

$Fb_0/fc_0$: is the proportion of initial equiaxial compressive yield stress and initial uniaxial compressive yield stress [60]. The default value in ABAQUS is (1.16).

K: is the ratio of the second stress invariant in the tensile meridian to compressive meridian for any defined value of the pressure invariant at initial yield. It is used to define the multi-axial behavior of concrete and is ($0.5<Kc\leq1$)[60]. The default value in ABAQUS is (0.667).

μ: is the viscosity parameter. It does not affect the ABAQUS/Explicit analysis but contribute to converge in an ABAQUS/Standard analysis. According to (Malm) [61] $\mu=10^{-7}$ is recommended because in comparison with characteristic time increment it should be small.

## C.3 Steel Plate Model Properties

The steel plates were modeled using an isotropic linear elastic material model by the equation below with solid elements for all models. The assumption for the material of loading and supporting plates is to avoid problems in solution due to the large deformations that will be developed or stress singularity in the plates.

$$fs = E_s\varepsilon_s\,(MPa),\ \ \varepsilon s \leq \varepsilon$$

# References:

[1] J. Lubliner, J. Oliver, S. Oller, and E. Oñate, "A plastic-damage model for concrete," *International Journal of solids and structures,* vol. 25, no. 3, pp. 299-326, 1989.

[2] J. R. Homrich and A. E. Naaman, "Stress-strain properties of SIFCON in uniaxial compression and tension," MICHIGAN UNIV ANN ARBOR DEPT OF CIVIL ENGINEERING, 1988.

[3] P. Kmiecik and M. Kamiński, "Modelling of reinforced concrete structures and composite structures with concrete strength degradation taken into consideration," *Archives of civil and mechanical engineering,* vol. 11, no. 3, pp. 623-636, 2011.

[4] R. Malm, "Shear cracks in concrete structures subjected to in-plane stresses," KTH, 2006.

النتائج النظرية تمت مقارنتها مع النتائج العملية التي تم الحصول عليها من حيث منحني الحمل – الهطول ونمط التشققات للعينات .

لقد اظهرت النتائج ان تحليل العناصر المحددة تنبأ بسلوك النماذج الفرنديلية بتوافق جيد مع البيانات العملية وكذلك اظهر استجابة النماذج مع التباين في مختلف المتغيرات بدقة جيدة.

## الخلاصة

هذا البحث يقدم دراسة عملية ونظرية للسلوك الانشائي للنظام الفرنديلي المصنوع من الملاط الخرساني المقوى بألياف الحديد (السفكون).

البرنامج العملي يتضمن صب وفحص ثمان نماذج فرنديلية ابعاد النماذج (1350*250)ملم التي تمثل الطول و العرض على التوالي.

في هذه الدراسة المتغيرات الرئيسية هي شكل الفجوات، حجم الفجوات وسمك النموذج. جميع النماذج مصنوعة من الملاط الخرساني المتخلل بالألياف الحديدية وكانت نسبة الياف الحديد 7%. النموذج المرجعي ذو فجوات مربعة وحجم فجواته 0.4 وسمكه 60 ملم. النماذج الفرنديلية مقسمة الى ثلاث مجاميع، متغير المجموعة الاولى هو شكل الفجوات (مربع، دائري، مثلث) ، متغير المجموعة الثانية هو حجم الفجوات (0.6 ،0.2،0) ومتغير المجموعة الثالثة هو سمك النموذج (80،40 ) ملم .

النتائج العملية اظهرت بأن الحمل الاقصى يقل بزيادة حجم الفجوات ، النموذج ذو حجم الفجوات 0.6 يكون النقصان في الحمل الاقصى 60.5% ، بينما الزيادة في الحمل الاقصى للنموذج المصمت هي 146.7% و 37.1% للنموذج ذي حجم الفجوات 0.2.

من جهة اخرى وجد بأن الحمل الاعظم للنموذج ذي الفجوات الدائرية اعلى من الحمل الاعظم للنموذج ذي الفجوات المربعة بحوالي 8% بينما الحمل الاعظم للنموذج ذي الفجوات المثلثة يقل بحوالي 10.9% مقارنة مع النموذج ذو الفجوات المربعة.

بالنسبة للسمك النتائج اظهرت بأن الحمل الاقصى يزيد بزيادة سمك النموذج ، فعندما يزيد السمك الى 80 ملم فالزيادة في الحمل الاقصى هي 27% ، بينما عندما يقل السمك الى 40 ملم فالنقصان في الحمل الاقصى حوالي 46.4% بالمقارنة مع النموذج المرجعي.

في الجزء الثاني من هذه الدراسة أجري تحليلا لا خطيا بالاعتماد على العناصر المحددة ثلاثية الابعاد باستخدام انموذج اللدونة للخرسانة المتضررة( concrete damaged plasticity) و خصائص المواد التي تم الحصول عليها من الفحوصات العملية لمحاكاة النماذج الفرنديلية المصنوعة من الملاط الخرساني المقوى بالألياف باستخدام البرنامج الحاسوبي ABAQUS/Standard نسخة(2017) . هذه الدراسة تتضمن تأثير متغيرات مختلفة : حجم الفجوات ، شكل الفجوات وسمك النموذج .

جمهورية العراق

وزارة التعليم العالي والبحث العلمي

جامعة بابل

كلية الهندسة

قسم الهندسة المدنية

# السلوك الانشائي للنظام الفرنديلي من الخرسانة المتخللة بالألياف

رسالة مقدمة الى كلية الهندسة – جامعة بابل

وهي جزء من متطلبات نيل درجة الماجستير في الهندسة /الهندسة المدنية/انشاءات

من قبل

**رغده علي ناصر عبد الحسين**

اشراف

**الاستاذ المساعد الدكتور: خالد كريم شدهان**

**1444 A.H** **2023 A.D**